MONASH University

The Cardioprotective and Anti-Remodelling Effects of VCP746, a Novel A_1/A_{2B} Adenosine Receptor Agonist

by

Chung Hui Chuo
BPharm (Hons), BPharmSci (Hons)

Thesis submitted in fulfilment of the requirement for the degree of Doctor of Philosophy

Drug Discovery Biology
Monash Institute of Pharmaceutical Sciences
Monash University, 2016

Summary

Ischaemic heart disease, in particular myocardial infarction and resultant heart failure, places a significant burden on society. The adenosine receptor is a potent mediator of cardioprotection. Adenosine receptor signalling within cardiomyocytes during ischaemia and reperfusion injury reduces infarct size and improves post-ischemic heart function. However, the transition of adenosine receptor agonists into the clinic as a cardioprotective therapy has been hampered by significant on-target side effects such as bradycardia, atrioventricular block and hypotension. As such, while higher adenosine receptor agonist concentrations are likely to be more therapeutically effective, they cannot be trialled due to the likelihood of detrimental effects in patients with acute coronary occlusion. The failure of cardioprotective therapies in the clinic is also likely due to the relative inability of most drug candidates to control the remodelling process following myocardial infarction which leads to heart failure. VCP746, a novel A_1/A_{2B} adenosine receptor agonist, was previously shown to display biased agonism in Chinese hamster ovary cells stably expressing A_1 adenosine receptors and furthermore, cytoprotection without bradycardia in native systems. A strong body of evidence also supports a role for adenosine receptor agonists in regulating cardiac remodelling processes such as cardiac hypertrophy and fibrosis. This project therefore aims to further explore the ability of VCP746 to confer cardioprotection in the absence of haemodynamic adverse effects in more physiologically relevant systems. In addition, the potential for VCP746 to reduce cardiac remodelling will also be investigated for the first time in cell-based and whole animal studies.

Copyright Notice

General Declaration

Monash University

Declaration for thesis based or partially based on conjointly published or unpublished work

In accordance with Monash University Doctorate Regulation 17.2 Doctor of Philosophy and Research Master's regulations the following declarations are made:

I hereby declare that this thesis contains no material which has been accepted for the award of any other degree or diploma at any university or equivalent institution and that, to the best of my knowledge and belief, this thesis contains no material previously published or written by another person, except where due reference is made in the text of the thesis.

This thesis adopts from two original papers published in peer-reviewed journals and one unpublished paper. The core theme of the thesis is 'adenosine receptor agonist-mediated cardioprotective and anti-remodelling effects'. The ideas, development and writing up of all the papers in the thesis were the principal responsibility of myself, the candidate, working within the Drug Discovery Biology theme under the supervision of Associate Professors Paul White and Bing Wang, and Drs. Lauren May and Andrew Kompa.

The inclusion of co-authors reflects the fact that the work came from active collaboration between researchers and acknowledges input into team-based research.

In the case of chapter 5, my contribution to the work involved the following:

Thesis chapter	Publication title	Publication status*	Nature and extent (%) of candidate's contribution
5	VCP746, a novel A_1 adenosine receptor biased agonist, reduces hypertrophy in a rat neonatal cardiac myocyte model	Published	First author (85%). Development of ideas, participation in research design, conduction of experiments, data analysis, writing and editing of the manuscript
5	The hybrid molecule, VCP746, is a potent adenosine A_{2B} receptor agonist that stimulates anti-fibrotic signalling	Published	Co-first author (45%). Development of ideas, participation in research design, conduction of experiments, data analysis, writing and editing of the manuscript

Student signature:  **Date:** 24/11/16

The undersigned hereby certify that the above declaration correctly reflects the nature and extent of the student's and co-authors' contributions to this work. In instances where I am not the responsible author I have consulted with the responsible author to agree on the respective contributions of the authors.

Main Supervisor signature:  **Date:** 24/11/16

Acknowledgments

Firstly, I would like to thank my supervisors for all the support and guidance that they have given me throughout this PhD. To Associate Professor Paul White, I am grateful for the counsel, advice, patience and accessibility which you generously afforded me in spite of your busy schedule. To Dr. Lauren May, I thank you for your invaluable insight, knowledge and wisdom, without which this project would not have proceeded as envisioned. To Associate Professor Bing Wang, I am thankful for your mentorship both inside and outside of the laboratory – I have learned so much from you over the years. To Dr. Andrew Kompa, your expertise, skills and experience was indispensible in this project – thank you for patiently guiding me through various surgical and analytical techniques, many of which were challenging yet fascinating.

I am also grateful for the support shown to me by the staff and students of the Drug Discovery Biology Lab, the many visiting academics and students who have come and gone in the Clinical Pharmacology lab at the Alfred Hospital and talented animal technicians in the Kelly Lab at St. Vincent's Hospital. I would like to especially thank my friends and colleagues in the Adenosine Group for being an integral part of my growth as a scientist from day one.

I also would like to acknowledge the Victorian government and Monash University for providing financial support during my study in the form of scholarships and travel grants.

Last but certainly not least, I would like to offer my heartfelt thanks to my family and friends for their unceasing support, encouragement and love. To you, I dedicate this thesis.

Publications, Awards, Conference Communications

Publications

Valant C, May LT, Aurelio L, **Chuo CH**, White PJ, Baltos J, Sexton PM, Scammells PJ, Christopoulos A. Separation of on-target efficacy from adverse effects through rational design of a bitopic adenosine receptor agonist. (2013) *Proceedings of the National Academy of Sciences of the United States of America* 111(12):4614-4619

Chuo CH, Devine SM, Scammells PJ, Krum H, Christopoulos A, May LT, White PJ, Wang BH. VCP746, a novel A_1 adenosine receptor biased agonist, reduces hypertrophy in a rat neonatal cardiac myocyte model. (2016) *Clinical and Experimental Pharmacology and Physiology* 43:976-982

Vecchio EA*, **Chuo CH***, Baltos J, Ford L, Scammells PJ, Wang BH, Christopoulos A, White PJ, May LT. The hybrid molecule, VCP746, is a potent adenosine A_{2B} receptor agonist that stimulates anti-fibrotic signalling. (2016) *Biochemical Pharmacology* 117:46-56

*Co-first author

Awards

Victorian International Research Scholarship, 2013

ASCEPT Cardiovascular Special Interest Group Prize at the ASCEPT-MPGPCR Joint Scientific Meeting, Melbourne, Australia, 2014

Postgraduate Travel Grant Award to attend the European Society of Cardiology Congress, London, UK, 2015

Second Prize Poster Presentation at the 11th Annual Postgraduate Research Symposium, Monash University, Melbourne, Australia, 2016

Conference communications

VCP746, a novel A_1/A_2 adenosine receptor agonist, confers anti-remodelling effects in cardiomyocytes, cardiac fibroblasts and renal mesangial cells. Drug Discovery Biology 1st Annual Student Symposium, Monash University, Melbourne, Australia (2013).

VCP746, a novel A_1/A_2 adenosine receptor agonist, reduces hypertrophy in cardiac myocytes and collagen synthesis in cardiac fibroblasts and renal mesangial cells. World Congress of Cardiology, Melbourne, Australia (2014).

VCP746: a cardioprotective adenosine receptor agonist with minimal haemodynamic effects. Drug Discovery Biology 2nd Annual Student Symposium, Monash University, Melbourne, Australia (2014).

VCP746: a cardioprotective adenosine receptor agonist with minimal haemodynamic effects. ASCEPT-MPGPCR Joint Scientific Meeting, Melbourne, Australia (2014).

VCP746 is cardioprotective in a rat myocardial infarction model with no effect on heart rate or blood pressure. Drug Discovery Biology 3rd Annual Student Symposium, Monash University, Melbourne, Australia (2015).

VCP746: a cardioprotective adenosine receptor agonist with minimal haemodynamic effects. European Society of Cardiology Congress, London, UK (2015).

VCP746: a cardioprotective adenosine receptor agonist with minimal haemodynamic effects. 11th Annual Postgraduate Research Symposium, Monash University, Melbourne, Australia (2016).

Abbreviations List

AMI	Acute myocardial infarction
Ang II	Angiotensin II
ANP	Atrial natriuretic peptide
AR	Adenosine receptor
BP	Blood pressure
BrDu	5-bromo-deoxyuridine
BSA	Bovine serum albumin
BW	Body weight
cDNA	Complementary deoxyribonucleic acid
CTGF	Connective tissue growth factor
CrCl	Creatinine clearance
DAB	Diaminobenzidine
dH_2O	Distilled water
DMEM	Dulbecco's modified eagle medium
DMSO	Dimethyl sulfoxide
EDPVR	End diastolic pressure-volume relationship
EF	Ejection fraction

ESPVR	End systolic pressure-volume relationship
FBS	Foetal bovine serum
FS	Fractional shortening
GAPDH	Glyceraldehyde 3-phosphate dehydrogenase
GFR	Glomerular filtration rate
HCl	Hydrochloric acid
HF	Heart failure
i.p.	intraperitoneal
i.v.	intravenous
IgG	Immunoglobulin G
IL-1β	Interleukin-1 beta
IVRT	Isovolumic relaxation time
LAD	Left anterior descending
LV	Left ventricle/ventricular
LVEDP	Left ventricular end diastolic pressure
LVEF	Left ventricular ejection fraction
LVESP	Left ventricular end systolic pressure
LVPWd	Left ventricular posterior wall end diastole
MAP	Mean arterial pressure

MEM	Minimal essential media
MI	Myocardial infarction
MQ	Milli Q (Millipore)
mRNA	Messenger ribonucleic acid
MTT	3-(4,5-dimethylthiazol-2-yl)-2,5-diphenyltetrazolium bromide
NaOH	Sodium hydroxide
NBCS	Newborn calf serum
NBF	Neutral buffered formalin
NCF	Neonatal rat cardiac fibroblast
NCM	Neonatal rat cardiac myocyte
NFκB	Nuclear factor-kappa B
PBS	Phosphate buffered saline
PCR	Polymerase chain reaction
PRSW	Preload recruitable stroke work
RAS	Renin-angiotensin system
RAAS	Renin-angiotensin-aldosterone system
ROS	Reactive oxygen species
RPM	Revolutions per minute

RT-PCR	Real-time polymerase chain reaction
s.c.	Subcutaneous
SD	Sprague-Dawley
SDS	Sodium dodecyl sulphate
SEM	Standard error of the mean
SNS	Sympathetic nervous system
TBS	Tris-buffered saline
TBS-T	Tris-buffered saline-Tween 20
TCA	Trichloroacetic acid
TGF-β1	Transforming growth factor-beta 1
TNF-α	Tumour necrosis factor-alpha
v/v	Volume by volume
w/v	Weight by volume
α-SKA	alpha-skeletal actin
β-MHC	Beta-myosin heavy chain

Chapter 1 Literature Review

1.1 Acute myocardial infarction

1.1.1 Pathophysiology

Acute myocardial infarction (AMI) is commonly defined as the death of cardiac myocytes due to prolonged ischaemia as a result of an imbalance in oxygen supply and demand (1). The most frequent underlying condition for myocardial infarction (MI) is the rupture of a coronary atherosclerotic plaque and the formation of a thrombus which obstructs the supply of blood and oxygen to the myocardium (1). After the onset of MI, cell death is not immediate – it may take 6 hours or longer for the death of cardiac cells at risk depending on various factors including the presence of collateral blood flow, preconditioning and sensitivity of the cardiac myocytes (2).

The most prominent form of cell death that occurs during MI is necrosis, whereby myocardial cells characteristically develop leaky membranes, rupture and disintegrate. As a result, different proteins are released into the circulation from these damaged cells. MI can be diagnosed when plasma levels of specific biomarkers such as cardiac troponin, creatine kinase MB isozyme (CK-MB) are found to be raised. However, increased levels of these biomarkers only indicate myocardial damage (and necrosis) but are not specific to MI (2). A second form of cell death that occurs during MI is apoptosis (programmed cell death), characterised by chromatin condensation, cell shrinkage and nuclear and cellular fragmentation. Apoptosis is also defined by the preserved integrity of the plasma membrane of apoptotic cells even after fragmentation into apoptotic bodies (3). Apoptotic cells do not release any intracellular proteins into the circulation, unlike necrotic cells. Therefore, the use of biomarkers alone to diagnose MI inevitably leads to an underestimation of myocardial damage because only necrotic cells are accounted for but not the variable but substantial volume of apoptotic cells (4).

A third type of cell injury and death in MI is oncosis, which involves cell swelling and membrane permeability defects (in contrast to apoptosis) (5).

The relative contribution of each of the three types of cell death after the onset of MI is variable, dependent on timing and severity of the insult, and remains debatable (3, 4). While some have found apoptosis to be the dominant form of cell death especially in the early stages of MI (4, 6), other studies have found instead a greater role for oncosis (7). Necrosis is generally thought to be more prominent when cardiac injury is more severe and is also the fate of all oncocytic cells and apoptotic cells that are not removed by phagocytosis. Oncosis and apoptosis have thus been considered precursors of necrosis (4).

1.1.2 Current treatments and therapies

The immediate intervention given to patients suffering from AMI aims to reperfuse the ischaemic myocardium to reduce infarct size and prevent complications. Percutaneous Coronary Intervention (PCI) is currently accepted as the gold standard treatment for AMI when it can be performed in a timely fashion (ideally < 12 hours from the onset of symptoms) by experienced operators (8). A $P2Y_{12}$ receptor inhibitor such as clopidogrel, prasugrel or ticagrelor, and aspirin (maintained indefinitely) are given as adjunctive antiplatelet therapy for PCI and are usually started before the procedure (8-10). In most cases, placement of a stent (bare metal stent or drug eluting stent) at the time of PCI decreases restenosis and possibly reinfarction rates (11). Compared with fibrinolytic therapy, PCI leads to higher rates of infarct artery patency, lower rates of reinfarction, intracranial haemorrhage and death (12). Potential complications of PCI include adverse reactions to contrast medium, technical complications and the 'no-

reflow' phenomenon which refers to suboptimal myocardial reperfusion despite restoration of epicardial flow in the infarct artery (8, 13).

Fibrinolytic therapy becomes the reperfusion strategy of choice when PCI cannot be performed within 2 hours of first medical contact. Fibrin-specific agents such as tenectaplase, reteplase or alteplase are preferred and are ideally given within 12 hours of the onset of symptoms along with adjunctive antiplatelet therapy (as with PCI). While not a first-choice therapy, the benefits of fibrinolytic therapy in patients with AMI are well established, with a time-dependent reduction in both mortality and morbidity rates. Fibrinolytic therapy, however, should not be given to patients with absolute contraindications including but not limited to: prior intracranial haemorrhage, active bleeding (except menses), severe uncontrolled hypertension and ischaemic stroke (within 3 months) (8, 14).

Coronary artery bypass graft (CABG) has a limited role as a method for reperfusion but may be indicated over PCI or fibrinolytic therapy under specific circumstances including failed PCI or coronary anatomy not suitable for PCI. CABG was previously associated with a significant mortality risk when performed early after MI; this was related to worsening myocardial injury from cardiopulmonary bypass, aortic cross-clamping and cardioplegic arrest. However, modern modifications to the standard operative approach, such as on-pump beating-heart surgery and mechanical circulatory support devices, may lead to reduced mortality rates after CABG in the acute phase (8).

On top of strategies for reperfusion, patients are also placed on routine medical therapies to reduce rates of recurrent MI, rehospitalisation and mortality. Beta blockers such as metoprolol and mixed alpha/beta blocker carvedilol are recommended for all patients without contraindications within 24 hours of MI (8, 15). Early intervention

with beta blockers was shown to reduce rates of recurrent MI and ventricular fibrillation while beta blockers were also shown to be beneficial for secondary prevention in numerous trials, especially for patients with MI complicated by heart failure (HF), left ventricular (LV) dysfunction or arrhythmias (16). Oral angiotensin-converting enzyme (ACE) inhibitors been shown to reduce cardiovascular events in patients with AMI and are thus considered crucial medical therapy during and after AMI (17-19). ACE inhibitors have been shown to be protective independent of other medical therapies (such as aspirin and beta blockers) and provide an early benefit, supporting prompt use of these agents (within 24 hours) in patients with no contraindications such as hypotension, shock, renal failure or allergy (8). Angiotensin receptor blockers (ARB), particularly valsartan – found to be similarly efficacious as captopril in the VALIANT trial – can be used in patients with ACE inhibitor intolerance (20). High intensity statin therapy has been shown to lower the risk of recurrent MI, stroke, coronary revascularisation and other non-fatal clinical endpoints and should therefore be initiated or continued in patients with AMI when no contradictions to its use exists (21, 22). In addition, evidence suggests that statin therapy after AMI in patients with baseline low-density lipoprotein (LDL) levels below the therapeutic goal of 70 mg/dl remains beneficial (23). While the mechanism by which statins confer protection independent of its lipid-lowering effect is not fully understood, it can be partly explained by the fact that statins display a number of biological effects that may be relevant in the setting of myocardial ischaemia. Various studies have found that statins do indeed improve vascular endothelial function, stabilise plaques, reduce vascular inflammation and even regulate myocardial protection and remodelling (23-25).

1.1.3 Ischaemia and reperfusion injury

Reperfusion therapy is undoubtedly crucial for the treatment of AMI as evidenced by improved outcomes in patients with AMI. However, while reperfusion therapy aims to salvage viable ischaemic myocardial tissue by restoring blood flow and oxygen supply, it also causes harmful effects collectively known as ischaemia/reperfusion (IR) injury. Various studies in animal models have shown that IR injury may account for up to 50% of the final infarct size (IS) (26, 27). IR injury therefore attenuates and undermines the full benefits of infarct artery reperfusion in terms of IS reduction. The major contributory factors to IR injury include but are not limited to oxidative stress, calcium overload and mitochondrial permeability transition pore (MPTP) opening (28, 29).

Laboratory measurements of free radical formation indicates that reactive oxygen species (ROS) are produced in the greatest amount in the first minute of reperfusion and this overproduction can last up to tens of minutes (30, 31). Activated neutrophils have been reported to be the main source of ROS during reperfusion. Neutrophils, upon stimulation by pro-inflammatory mediators, are activated and recruited to the site of injury and produce superoxide anions (29, 32). Another significant source of ROS is the cardiac myocytes, and myoyte-derived ROS is thought to originate from the mitochondrial electron transporting system. Although the exact mechanism is unclear, inhibition at the level of NADH dehydrogenase (early step of the mitochondrial respiratory chain) significantly attenuates the level of ROS release during reperfusion (33, 34). The release of ROS exerts many harmful effects on the myocardial tissue including but not limited to the oxidation and destruction of proteins important for homeostasis, destruction of nucleic acid (especially mitochondrial DNA due to proximity) and peroxidation of membrane lipids (29, 35, 36).

Intracellular and mitochondrial calcium overload begins during acute myocardial ischaemia and is exacerbated during reperfusion when oxidative stress further damages the plasma membrane and sarcoplasmic reticulum. Entry of Ca^{2+} into the mitochondria induces the opening of the MPTP, resulting in a chain of events that ultimately lead to cell death (28). Animal studies have shown that pharmacological blockade of the sarcolemmal Ca^{2+} channel (26) or mitochondrial Ca^{2+} uniporter (37) at the onset of reperfusion can reduce the final infarct size by up to 50%. Unfortunately, this success is yet to be replicated in the clinical setting. The CASTEMI study had previously examined the safety and efficacy of intravenous (i.v.) caldaret, an intracellular Ca^{2+} handling modulator that was shown to inhibit calcium overload in animal models, in patients with AMI undergoing PCI. While the study found that caldaret was well-tolerated (unlike reports of calcium channel blockers in this setting) even at high doses, no evidence of efficacy was found (38).

Many of the factors that promote IR injury appear to converge on a common point: the MPTP (28). In response to oxidative stress, mitochondrial Ca^{2+} and rapid pH correction that occurs during reperfusion, the MPTP, which is located in the inner mitochondrial membrane, opens, leading to uncoupling of oxidative phosphorylation, ATP depletion and ultimately cell death (28, 39). As such, the MPTP provides an important therapeutic target for preventing IR injury. A number of small and large mammal MI models have reported a reduction in infarct size of up to 50% of area at risk (AAR) upon administration of MPTP inhibitors (such as cyclosporin A) at the onset of reperfusion (40-42). Clinical studies of pharmacologic agents that are known to attenuate MPTP opening have produced mixed outcomes with possibly the most promising candidate being cyclosporin A (28). In a pilot trial conducted by Piot et al., cyclosporin A treatment in patients with AMI undergoing PCI led to a significant

reduction in creatine kinase levels and infarct size, warranting further investigation in a larger clinical trial (43).

1.1.4 Pre-clinical Models

A variety of experimental models of MI has been developed ranging from *in vitro* simulated-ischaemia models to *in vivo* left anterior descending coronary artery (LAD) ligation models in small and large animals. Table 1.1 provides a brief description of various cell-based, isolated heart and *in vivo* models of myocardial infarction and ischaemia/reperfusion injury. These well-established models may not mirror exactly what is observed in clinic, however, they are crucial for replicating features of the phenotype of myocardial ischaemia and reperfusion injury which do occur clinically.

Reference	Ischaemia/Reperfusion Injury Model	Experimental Details
In Vitro Models		
Germack, Dickenson (2005) (44)	Simulated ischaemia/reperfusion model using neonatal rat cardiac myocytes. Duration: 4 hr ischaemia, 18 hr reperfusion	Cells were serum-starved overnight before experiments. The medium was then changed to glucose and serum free DMEM and subjected to hypoxia in a hypoxic incubator (5% CO_2/0.5% O_2 at 37°C). Cells were preconditioned with agonists for 15 minutes prior hypoxia exposure. Following hypoxia, cells were reoxygenated in normoxic atmosphere
Urmaliya et al. (2010) (45)	Simulated ischaemia model using H9c2(2-1) embryonic rat atrial cell line. Duration: 12 hr ischaemia	Cells were incubated in simulated ischaemia (SI) medium at pH 6.4 plus 2% foetal bovine serum (FBS). Cells were subjected to a 100% N_2 gas atmosphere at 37°C. Cells were treated with adenosine receptor agonists at the start of SI and when antagonists were used, they were added 20 minutes prior to the addition of agonists.
O'Brien, Ferguson, Howlett	Simulated ischaemia/reperfusion model using isolated ventricular	Ventricular myocytes were isolated by enzymatic dissociation from either young or aged rats. Isolated

(2008) (46)	myocytes from young adult or aged rats. Duration: 30 min ischaemia, 30 min reperfusion	myocytes were superfused with an SI solution (pH 6.8; gassed with 90% N_2-10% CO_2) and then reperfused with Tyrode solution.
Isolated Heart Models		
Hausenloy et al. (2013) (47)	Ischaemia/reperfusion model using Langendorff-perfused isolated rat hearts. Duration: 35 min ischaemia, 120 min reperfusion	Excised hearts were mounted on a constant pressure Langendorff-perfusion apparatus and perfused with Krebs-Hanseleit buffer gassed with 95% O_2/5% O_2 at pH 7.35-7.45 at 37˚C. Regional myocardial ischaemia was induced by tightening a suture placed around the LAD to and reperfusion by releasing the snare.
Urmaliya et al. (2010) (48)	Ischaemia/reperfusion model using Langedorff-perfused isolated mouse hearts. 30 min ischaemia, 60 min reperfusion	Excised hearts were perfused through the aorta at a constant pressure with modified Krebs-Henseleit buffer. After 30 min stabilisation, hearts were subjected to no-flow normothermic global ischaemia and followed by reperfusion. Ischaemia was attained by stopping perfusate inflow and immersing the heart in perfusate buffer saturated with 95% N_2/5% O_2. Reperfusion was achieved by restarting perfusate flow.
Solenkova et al. (2006)	Ischaemia/reperfusion model using Langendorff-perfused isolated rabbit hearts. Duration: 30 min ischaemia, 120 min reperfusion	All hearts were exposed to ischaemia (using a snare around the left coronary artery) followed by reperfusion. Hearts given ischaemic preconditioning treatment received 5 minutes of global ischaemia followed by 10 minutes of reperfusion before lethal 30-minute regional ischaemia. Antagonists and/or signalling pathway inhibitors were perfused 5 minutes before or 10, 30, 60 minutes after reperfusion for 20 minutes.
In Vivo Models		
Lasley et al. (2001) (49)	Porcine ischaemia/reperfusion injury model. 60 min ischaemia, 180 min reperfusion	Animal preparation was allowed to stabilise for 30 minutes. Ischaemia was initiated by LAD occlusion with a vascular occluding clamp followed by reperfusion. Treated pigs received intracoronary agonist for 60 minutes at the start of reperfusion followed by 120

		minutes of PBS for the remainder of reperfusion. Control pigs were infused with PBS for the entire 3 hours of reperfusion.
Lankford et al. (2006) (50)	Murine ischaemia/reperfusion injury model. 45 min ischaemia, 60 min reperfusion	All mice subjected to ischaemia by LAD occlusion followed by reperfusion. LAD occlusion and reperfusion was achieved by inflating or deflating a "balloon occluder". The ischaemic preconditioning mice were given three cycles of 5-minute ischaemia and 5-minute reperfusion before lethal ischaemia. Reperfusion in the third cycle was for 10 minutes.
Morel et al. (2014) (51)	Murine ischaemia/reperfusion injury model. 30 min ischaemia, 24 hr reperfusion	Left thoracotomy was performed to gain access to the heart whereby an 8-0 prolene suture was passed around the LAD and a small piece of polyethylene catheter was used to form a snare. Ischaemia was induced by pulling on the snare followed by reperfusion by releasing the snare.

Table 1.1 Models of myocardial infarction and ischaemia/reperfusion injury in the *in vitro*, *ex vivo* and *in vivo* setting

1.2 Post-myocardial infarction cardiac remodelling

Improved standard of care for patients suffering MI has led to a steady decline in in-hospital mortality (11.2% to 9.4% from 1990 to 1999) (52). The decrease in in-hospital fatality can be attributed to the increasing use of established treatment protocols like PCI, thrombolysis, aspirin and beta blockers. However, in spite of our success in lowering AMI case-fatality rates, heart failure secondary to MI remains a major source of patient morbidity and mortality (52, 53).

1.2.1 Pathophysiology

The acute loss of myocardium from MI results in a sudden increase in loading conditions that triggers a cascade of intracellular signalling pathways, initiating what would be the reparative process which includes chamber dilatation, hypertrophy and the formation of a collagen scar (54). Infarct size (IS) largely determines the extent of post-MI left ventricular (LV) function, remodelling and survival. In an animal study conducted by Watzinger and colleagues (55), IS as determined by contrast-enhanced magnetic resonance imaging (MRI) in rats correlated closely with end-systolic volumes (denoting LV chamber enlargement) and was inversely correlated with ejection fraction. Similarly, a clinical study on long-term survivors of MI (> 4 years) concluded that a strong linear relation exists between IS (but not infarct location or transmurality) and ejection fraction and LV volumes (56).

The early phase of post-MI remodelling involves the expansion of the infarct zone, a biomechanism aptly called ‘infarct expansion’. Infarct expansion occurs as a result of the degradation of intermyocyte collagen struts by matrix metalloproteinases (MMPs) released by inflammatory cells like macrophages and polymorphonuclear leukocytes (57). Due to this increase in fibrillar collagen degradation, there is a loss of structural integrity leading to myocyte slippage, wall thinning, ventricular dilation and subsequently an elevation of diastolic and systolic wall stresses (54). Alterations in wall stress serves as a strong stimulus for hypertrophy mediated by myocardial stretch, neurohormonal activation and activation of the local renin-angiotensin system (RAS). LV remodelling post-MI is usually a state of volume overload and therefore leads to primarily a lengthening of myocytes (eccentric hypertrophy), as opposed to concentric hypertrophy, which is a thickening of myocytes elicited by pressure overload (58). In addition to hypertrophy, the initial inflammatory response post-MI characterised by

elevated levels of cytokines promotes the activation and proliferation of myofibroblasts (59). Myofibroblasts are responsible for the deposition of extracellular matrix necessary for scar formation and wound-healing in the infarct zone (60).

1.2.2 Cardiac myocytes and hypertrophy

Cardiac remodelling post-MI involves myocyte hypertrophy and changes in ventricular architecture (along with the formation of a collagen scar) to distribute increased wall stresses more evenly and prevent further deformation. Myocardial stretch, neurohormones, inflammatory factors and activation of the local RAS all work in tandem to initiate cardiac myocyte hypertrophy (54).

Haemodynamic disturbances serve as a potent activator of the sympathetic nervous system (SNS) which leads to enhanced noradrenaline release at the injury site and into the circulation (61). Increased SNS activity is a doubled-edged sword – on one hand, it helps to support cardiovascular function and thus preserve flow to vital organs, while on the other hand, increased catecholamine levels resulting from upregulated SNS activity will contribute to the development and severity of ventricular arrhythmias (62). Prolonged SNS activation and elevated plasma catecholamine levels also lead to alterations in cardiac structure and function through the remodelling process. Stimulation of alpha-1 adrenoceptors (α1AR) on cardiac myocytes by noradrenaline leads to hypertrophy via a $G_{\alpha q}$-dependent signalling pathway. In addition, the increased release of noradrenaline leads to enhanced activation of beta-1 adrenoceptors (β1AR) on renin-releasing juxtaglomerular cells in the kidney. β1AR stimulation on juxtaglomerular cells increases renin secretion and subsequently the production of angiotensin II (Ang II), which is a key peptide involved in pathological cardiac remodelling and heart failure (54, 61).

Increased release of Ang II has been shown experimentally to promote hypertrophy either directly via the activation of Ang II type 1 receptor (AT_1R) on cardiac myocytes or indirectly via a paracrine mechanism mediated by cells such as cardiac fibroblasts (63). A study by Liu et al. found that in adult rat ventricular myocytes, Ang II exposure induced hypertrophy and this effect was inhibited by the AT_1R blocker losartan but not PD123319, an AT_2R antagonist. In the same study, post-infarcted myocytes were also shown to have a higher expression level of AT_1R than in control cells, further implicating the critical role of AT_1R in cardiac myocyte hypertrophy (64). An abundance of Ang II receptors are also found on cardiac fibroblasts and indirectly affect cardiac myocyte hypertrophy. Activation of the AT_1R on cardiac fibroblasts increases the mRNA expression level and secretion of transforming growth factor-β1 (TGF-β1). Numerous reports have shown that TGF-β1 serves as a potent activator of the foetal gene programme and cell growth in cardiac myocytes thus suggesting a paracrine mechanism for Ang II-mediated cardiac myocyte hypertrophy (63, 65, 66).

Cardiac injury also results in the migration of macrophages, monocytes and neutrophils into the myocardium leading to a localised inflammatory response (67). Elevated levels of cytokines such as interleukin (IL)-1β and IL-6 have been observed in post-MI patients (68). Emerging evidence also demonstrates that tumour necrosis factor-α (TNF-α) is associated with myocardial hypertrophy and left ventricular dysfunction and remodelling (69). In a study by Liao et al. (70), a strong positive correlation was found between plasma TNF-α levels and heart weight/body weight ratio. The same study also found that stimulation with TNF-α triggered an increase in protein synthesis in cardiac myocytes further implicating a role for TNF-α in myocyte hypertrophy.

These triggers of hypertrophy are well-known to alter cardiac gene expression in cardiac myocytes (71). The molecular changes seen in cardiac hypertrophy resemble

those observed during foetal cardiac development and is commonly described as the reactivation of the 'foetal gene programme'. The reactivation of the foetal gene programme is thought to play a causative role in adverse cardiac remodelling in both human and animal models (72). Foetal genes like atrial and brain natriuretic peptide (ANP and BNP), β-myosin heavy chain (β-MHC) and α-skeletal actin (α-SKA) are often upregulated in pathological hypertrophy while adult cardiac genes, most prominently the gene encoding the α isoform of myosin heavy chain (α-MHC) are downregulated (71).

1.2.3 Cardiac fibroblasts and fibrosis

Injury to the heart also evokes complex cellular responses in non-muscular cells, of which the majority are cardiac fibroblasts. Reparative deposition of extracellular matrix (ECM) material (fibrosis) in the infarct region occurs in an attempt to maintain the structural integrity of the heart (54). It is critical that a strong, mature scar be formed as early as possible to prevent further infarct expansion and deformation of the heart. Fibrous tissue formation at the infarct site is usually evident within the first month in humans while in rats, the process is accelerated and scar tissue is evident by day seven post-MI (60, 73). While initial reparative fibrosis is crucial as part of the healing process after MI, ongoing, chronic fibrosis has the potential to spill over into the remote regions of the LV (52). The excessive accumulation of collagens in the heart, particularly in viable myocardium, is thought to limit the motion of cardiac myocytes during the contraction/relaxation cycle and also impede the passage of depolarising wave through the myocardium (74, 75).

In the acute stages following MI, fibroblasts at the site of injury undergo phenotypic transformation to myofibroblasts, which are more proliferative and have a greater

capacity for collagen synthesis (76). In a study by Santiago et al., immunofluorescence staining of procollagen revealed that intracellular procollagen levels in cardiac myofibroblasts were significantly greater than in fibroblasts. By measuring procollagen type I N-terminal peptide (P1NP) secretion using enzyme immunoassay, cardiac myofibroblasts were also observed to secrete significantly more mature collagen type 1 compared to fibroblasts (77). Fibroblast activation, proliferation and collagen synthesis are initiated and regulated by signals of local and systemic origin. Signals such as Ang II and TGF-β1 are able to increase fibroblast collagen synthesis partly through the upregulation of genes encoding collagen I and III, which are the predominant collagen isoforms in the heart (75, 78, 79). In the normal heart, fibroblast expression of TGF-β and fibrillar collagen is kept low (60, 80). However, the expression and secretion of TGF-β by fibroblasts increase acutely after cardiac injury, subsequently leading to enhanced expression and deposition of collagen via an autocrine or paracrine mechanism. Ang II and TGF-β are also able to induce connective tissue growth factor (CTGF) expression in cardiac fibroblasts. The work of Dean et al. (81) suggests that TGF-β1 is crucial in the acute induction of total collagen in the early stages of MI, but is less critical in the chronic phase of cardiac remodelling. In a LAD ligation-induced rat MI model, Dean and colleagues observed major increases in TGF-β1 mRNA and protein expression in the border and infarct zone (but not the remote zone) of the myocardium that peaked within the first week of injury before falling to baseline levels. The locality and timing of TGF-β1 mRNA and protein induction indicates that TGF-β1 was involved in initial scar formation and wound healing. Conversely, CTGF mRNA and protein were only found to peak in viable rat myocardium 180 days post-MI, and this was associated with fibrosis. It was posited that CTGF is involved in the ongoing

fibrosis of the remote myocardium, after the acute post-MI inflammatory phase has subsided.

1.2.4 Current treatments and therapies

The anti-remodelling effects of current treatments for chronic heart failure (CHF) secondary to MI, such as ACEIs and beta blockers are postulated to be key mechanisms underlying improvements in parameters of patient morbidity and mortality. The bulk of these therapies target circulating neurohormonal systems; this underscores their importance in influencing LV structure and function.

ACEI are now employed as standard therapy in the treatment of HF post-MI. The benefits of ACEI treatment are well documented in both animal and clinical studies, and include improved survival, improvements in LV function and attenuation of LV dilatation (82, 83). For patients unable to tolerate ACEI, ARB can be used. The importance of AT1R in post-MI LV remodelling is highlighted by findings that AT1R knockout (KO) mice demonstrate attenuated LV remodelling, including reduced fibrosis and better survival rates versus wildtypes (84). However, AT1R blockade has thus far not been shown to be superior to ACEI in the treatment of post-MI HF based on the findings of the VALIANT and OPTIMAAL trials (20, 85). Interestingly, evidence suggests that combined ARB and ACEI therapy may confer greater benefit on post-MI remodelling and ventricular dysfunction than either therapy alone (86, 87). This benefit from combined therapy, however, did not translate into a significant reduction in morbidity or mortality in the VALIANT trial compared to ACEI alone (20).

Following MI, high levels of local aldosterone induce cardiac hypertrophy and fibrosis (88). Spironolactone, an aldosterone receptor blocker, has been shown to reduce

myocardial hypertrophy, fibrosis and dysfunction in pre-clinical models (89). In the RALES (Randomized Aldactone Evaluation Study) trial, spironolactone, in addition to standard ACEI therapy, significantly reduces morbidity and mortality in patients with severe CHF (90). The same study also demonstrated that high levels of peripheral blood collagen markers (surrogates for cardiac fibrosis) such as procollagen type III amino-terminal peptide (PIIINP) were associated with poor outcomes for patients. Subgroup analysis revealed that the addition of spironolactone to standard therapy attenuated the levels of the collagen markers, indicating that the blockade of aldosterone-mediated fibrosis is a key mechanism of action by which spironolactone exerts its cardioprotective effects in CHF patients (91). The outcomes of the RALES trial were also in concurrence with that of the EPHESUS (Eplerenone Post-Acute Myocardial Infarction Heart Failure Efficacy and Survival Study) trial where investigators concluded that the addition of eplerenone to standard therapy was shown to reduce morbidity and mortality in patients with left ventricular dysfunction and heart failure secondary to AMI (92).

One of the most important mechanisms responsible for the progression of heart failure is the activation of the SNS. As such, numerous clinical trials sought to investigate the effects of beta blockers in the setting of heart failure. In the 2647-patient CIBIS-II (Cardiac Insufficiency Bisoprolol Study II) trial, the use of the β1-selective antagonist bisoprolol (target dose of 10 mg/day) led to a 34% reduction in all-cause mortality versus placebo (93). A similar outcome was achieved in the MERIT-HF (Metoprolol CR/XL Randomised Intervention Trial in-Congestive Heart Failure) where all-cause mortality was significantly lower in the metoprolol CR/XL group than in the placebo group (relative risk 0.66, $p = 0.00009$) (94). The Carvedilol Post-Infarct Survival Control in LV Dysfunction (CAPRICORN) trial investigated the effect of the non-

selevtive beta/alpha 1 blocker, carvedilol, in patients with left ventricular dysfunction receiving optimised therapy. All-cause mortality was 23% lower in the carvedilol-assigned group than the placebo-assigned group (p=0.03) (95). Exploratory analyses on arrhythmia frequency revealed that carvedilol treatment resulted in 59% reduction of atrial fibrillation/flutter and 76% reduction of ventricular tachycardia/fibrillation events. While the exact mechanism in operation is unknown, it is thought to be related to the non-selective blockade of beta and alpha-1 receptors and HERG potassium channels by carvedilol (96). The COPERNICUS (Carvedilol Prospective Randomized Cumulative Survival) trial also investigated the beneficial effects of carvedilol, but specifically on the survival of patients with severe heart failure already on optimised therapy. The COPERNICUS trial was warranted as previous trials had shown benefit for the use of beta blockers such as bisoprolol, metoprolol and carvedilol itself in patients with mild-to-moderate HF (97). Furthermore, a separate, large scale study using bucindolol in patients with very advanced HF had failed to demonstrate a favourable effect of treatment on survival (98) – this raised the possibility that the benefits of beta-blockade might diminish with advancing HF. In contrast to the study on bucindolol, the COPERNICUS trial found that the previously reported benefits of carvedilol in terms of morbidity and mortality in patients with mild-to-moderate HF were also seen in patients with severe HF (97). Overall, the results from these trials strongly support the role for beta blocker therapy in patients with heart failure regardless of severity.

1.2.5 Pre-clinical models

Various *in vitro* and *in vivo* experimental models have been developed to better understand the complex nature of cardiac remodelling and dysfunction and are critical to the development of new therapies for the management of heart failure. While these

models do not necessarily mirror what is seen in the clinic, they have proven useful in simulating features and phenotypes of heart failure seen in the clinical setting. Table 1.2 provides a brief summary of the various types of cell- and animal-based models of cardiac remodelling and heart failure.

Reference	Model	Experimental Details
In Vitro		
Wang et al. (2010) (99)	Hypertrophy and fibrosis using rat neonatal cardiac myocytes (NCM) and fibroblasts (NCF)	NCM and NCF were isolated from 1-2-day-old Sprague-Dawley rats using enzymatic digestion. Cardiac myocyte hypertrophy was stimulated with aldosterone or Ang II. Cardiac fibroblast collagen synthesis was stimulated with Ang II. ^{3}H-leucine incorporation was used as a measure of hypertrophy while ^{3}H-proline incorporation was used as a measure of collagen synthesis.
Gan et al. (2004) (100)	Rat neonatal cardiac myocyte hypertrophy	NCM were isolated. NCM were treated for 24 h with 10 μM phenylephrine to stimulate hypertrophy. Cardiac myocyte surface area was determined for 50 randomly selected cells per experiment as a measure of cardiac myocyte hypertrophy.
Tanaka, Honda, Takabatake (2001) (101)	Adult rat cardiac myocyte hypertrophy	Adult rat cardiac myocytes were isolated from 10-week-old Sprague-Dawley rats. Cells were stimulated with endothelin-1 or phenylephrine to induce hypertrophy. For evaluation of hypertrophy, [^{3}H]-phenylalanine incorporation into myocytes were measured.
In Vivo		
Wakeno et al. (2006) (102)	LAD ligation model in rats kept for 4 weeks	Male Wistar rats were subjected to MI induced by permanent ligation of the LAD. The proximal LAD was tied of with a suture. In the sham group, the same surgical procedure was performed except that the suture around the LAD was not tied. Rats were kept for 4 weeks after MI.
Lu et al. (2008) (103)	Transverse aortic constriction (TAC) model in mice kept for	Male C57BL/6 mice were subjected to TAC of moderate (with the use of a 26-gauge needle to calibrate the

	4-5 weeks	degree of constriction) or severe (with the use of a 27-gauge needle) degree. A suture was snugly tied around the needle and the aorta; after ligation the needle was quickly removed. The mice were kept for 4-5 weeks to generate cardiac hypertrophy as a result of pressure overload.
George et al. (2009) (104)	Coronary embolization-induced heart failure model in dogs.	A thin Silastic cannula was inserted into the LAD. CHF was induced by daily intracoronary microembolization with 25,000 polymer beads (90-120 μM in diameter) injected through the implanted LAD cannula for three consecutive weeks. The dogs were observed for 4 weeks after stopping embolization and infusion.

Table 1.2 Models of cardiac remodelling and heart failure in the *in vitro and in vivo* setting.

1.3 Adenosine

Adenosine (Fig. 1.1), an endogenous purine nucleoside, can be found in various tissues intracellularly and extracellularly (105, 106). Under physiological conditions, the concentration of adenosine is estimated to be in the nanomolar range both inside and outside the cell while in extreme physiology or pathophysiology, the concentration of adenosine can rise to micromolar levels (105, 107). Adenosine is predominantly formed from adenine nucleotides (105). The dephosphorylation of adenosine monophosphate (AMP) by intracellular 5'-nucleotidase and the hydrolysis of S-adenosyl homocysteine (SAH) by SAH hydroxylase both contribute to the formation of adenosine inside the cell (108).

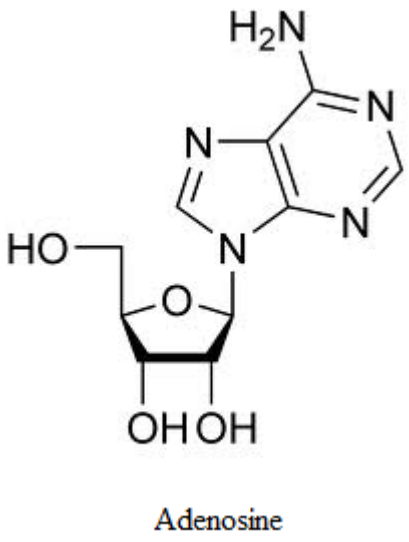

Figure 1.1 The chemical structure of adenosine. Adenosine consists of a ribose sugar ring attached to a purine-furan complex via a β-N9-glycosidic bond.

There is normally a high concentration of adenosine triphosphate (ATP) in cells but ATP can be released outside the cell either by cell-mediated processes or when membrane damage occurs (105). Once outside the cell, ATP is rapidly dephosphorylated by various ectonucleotidases working in tandem (105, 107). Ectonucleoside triphosphate diphosphohydrolases like CD39 can split off phosphate groups in ATP and adenosine diphosphate (ADP) (105, 107, 108). This is followed by hydrolysis by ecto-5'-nucleotidases like CD73, which is the last enzymatic step for the formation of adenosine outside the cell (105, 107, 108). Intracellular adenosine can also be transported out of the cell through the plasma membrane via facilitated diffusion (with bi-directional transporters) – in most tissues, this balances out the levels of adenosine in the extra- and intracellular regions (105, 108). There are two key enzymes that reduce the levels of adenosine: adenosine kinase (ADK) and adenosine deaminase (ADA). ADK phosphorylates adenosine to AMP while ADA (also present extracellularly), degrades adenosine to inosine (105, 108). Both enzymatic processes

are crucial for controlling physiological adenosine levels, ensuring that they are kept low (105, 106).

In pathophysiological conditions such as ischaemia or hypoxia, extracellular adenosine levels are known to rise significantly. This can be due to several reasons, one being the imbalance of ATP synthesis and utilisation (106, 107). In situations where oxygen and glucose supply is decreased, synthesis of ATP is reduced while the amount of breakdown products of ATP increases, leading to a net increase in adenosine levels (106, 107). Other factors leading to increased extracellular adenosine levels include, but are not limited to cell necrosis (with subsequent leakage of adenosine or ATP) and the upregulation of 5'-nucleotidase under stressful conditions (106, 107). Overall, the increased levels of adenosine lead to cytoprotective effects and this is achieved via the interaction of adenosine with adenosine receptors (106). Thus, the use of exogenous adenosine agonists in hypoxic conditions works in the context of high extracellular adenosine concentrations conferring cytoprotection.

1.3.1 Adenosine receptors

The various physiological effects of adenosine are predominantly mediated through adenosine receptors. Adenosine receptors were named as such because their preferred endogenous agonist is the purine nucleoside adenosine (108). Other endogenous agonists known to activate adenosine receptors include inosine (109-111), the breakdown product of adenosine, and AMP, more recently reported by Rittiner et al. (112). Rittiner and colleagues showed in HEK293 cells co-expressing human A_1AR and G_{qi} that AMP and a non-hydrolysable AMP analogue, deoxyadenosine 5'-monophosphonate (ACP) evoked nucleotidase-independent calcium mobilisation

responses that are no different to the response evoked by adenosine in terms of onset and magnitude.

Adenosine receptors are G protein-coupled receptors and can be classified into four different subtypes: A_1, A_{2A}, A_{2B} and A_3 (108). A_1 and A_3 adenosine receptors (AR) are predominantly coupled to the $G_{i/o}$ protein, which inhibits adenylate cyclase (via the α subunit of the G protein), while A_{2A} and A_{2B}ARs are predominantly coupled to the G_s protein which stimulates adenylate cyclase, also through the α subunit (107, 108).

The A_1AR has a high affinity for adenosine and is the most highly conserved subtype of AR across species (113). The A_1AR is widely expressed throughout the body with high expression levels in the central nervous system, eyes, adrenal glands and atria; intermediate expression levels in the skeletal muscles, liver, kidneys and heart; and low expression levels in the lungs and pancreas (113, 114). Within the cardiac region alone, A_1AR expression can vary significantly. For instance, the A_1AR is more highly expressed in the atria compared to the ventricles (115, 116). The A_1AR has also been found in coronary artery smooth muscle in pigs (117) and mice (118), and coronary endothelial cells in guinea pigs (119).

Similar to the A_1AR, the A_{2A}AR also has high affinity for adenosine and is widely expressed around the body. The A_{2A}AR is expressed at a high level in the spleen, thymus and on leukocytes; and intermediate level in the heart, lungs and blood vessels (113). With regards to the cardiac expression of the A_{2A}AR, immunological evidence has shown that the A_{2A}AR is present in the atria and ventricles of both humans and pigs (120). Cardiac fibroblasts are also known to express the A_{2A}AR, which may have a role in regulating cardiac fibrosis (121). A significant number of reports have also confirmed the expression of A_{2A}ARs in coronary vessels. They have been shown to

mediate vasodilation in multiple species through regulation of either endothelial (122, 123) or smooth muscle cells (118).

Unlike the A_1 or A_{2A}AR, the A_{2B}AR has the lowest affinity for adenosine among the AR subtypes. Higher expression of the A_{2B}AR can be found in the caecum, colon and bladder; intermediate expression in the lungs, blood vessels, eyes and mast cells; and low expression in adipose tissue, brain, kidney, liver and ovaries (113). In the heart, studies suggest that A_{2B}ARs are expressed in myocytes (124) and have a cardioprotective role in rats (125) and mice (126). The A_{2B}AR is also the most abundantly expressed AR subtype on cardiac fibroblasts (127) and plays a key role in modulating collagen synthesis and fibrogenic gene expression (102, 128). Although not as prominent as the A_{2A}AR, A_{2B}ARs are also known to mediate vasodilation, mostly via nitric oxide (NO) and K_{ATP} channel dependent mechanisms (129). The vascular A_{2B}ARs are thought to be located on both endothelial (130) and smooth muscle cells (131).

The A_3AR is the newest member of the AR family and was initially identified as an orphan receptor in rat testis (132). High expression levels of the A_3AR can be found in the testes and in mast cells; intermediate expression levels in the lungs and pineal; and low expression levels in the thyroid, adrenal gland, intestine and liver. Cardiac expression of A_3AR is thought to be low as well (113). However, A_3AR-mediated cardioprotection have been reported in multiple studies implicating the importance of the receptor in the heart in spite of its low expression level (133, 134). Some evidence also suggests that the A_3AR may have a functional role in vascular smooth muscle (135) and coronary arterial (136) cells.

1.3.2 Cardiac effects of adenosine

Adenosine plays an important role in the regulation of cardiac functions such as impulse generation and conduction, contractility and coronary tone. Adenosine also influences cardiac function under physiological and diseased conditions by modulating inflammatory cells and the immune system.

1.3.2.1 Rate and conduction control

The A_1AR is most highly expressed in the atrial region of the heart and thus it is unsurprising that it plays an important role in regulating impulse generation. Negative chronotropy or reduction in heart rate has been demonstrated in numerous studies as a result of A_1AR activation (137, 138). This effect of the A_1AR involves the activation of the inwardly rectifying K^+ current (I_{KAdo}), and the inhibition of the inward calcium current (I_{Ca}) and the "funny" current (I_f), also known as the pacemaker current (139). Adenosine can also indirectly modulate I_{Ca} by suppressing cellular responses to adrenergic stimulation, which involves A_1AR-mediated inhibition of catecholamine-induced rise in intracellular cyclic adenosine monophosphate (cAMP) levels (139, 140). The reduction of cAMP levels is also the mechanism by which the A_1AR reduces the rate and extent of the opening of hyperpolarisation-activated cyclic nucleotide-gated (HCN) channels (channels responsible for the conduction of I_f) and thus the firing of pacemaker potentials (141, 142). Indeed, the role of adenosine and the A_1AR in cardiac rate control cannot be understated. Experimental deletion of the A_1AR results in an elevated resting heart rate in mice, as demonstrated by Yang et al. (138), while overexpression of the receptor leads to reduced baseline heart rate, as reported by Headrick and colleagues (143).

On top of rate control, adenosine also has a negative dromotropic effect on the heart. Adenosine, via the activation of A_1AR, is able to delay conduction and even induce atrioventricular (AV) blockade. The entirety of the dromotropic actions of adenosine is confined to the AV node and involves the local activation of I_{Kado} by A_1ARs and the inhibition of catecholamine-induced L-type Ca^{2+} currents ($I_{Ca,L}$) (139). In a study by Rankin and colleagues, action potentials and membrane currents from rabbit AV node myocytes were studied using the whole cell patch clamp technique to investigate the ionic mechanisms underlying the negative dromotropic effect of adenosine. Results from voltage clamp experiments showed that adenosine induced I_{Kado} and this effect was blocked by the A_1AR-selective antagonist, 8-cyclopentyl-1,3-dipropylxanthine (DPCPX), indicating the involvement of the A_1AR. Furthermore, isoprenaline-induced increase in I_{Ca} was also abolished by adenosine treatment. Together, results from the study by Rankin and colleagues indicate that the ionic mechanisms of action of adenosine in the AV node involve the activation of I_{Kado} and an anti-adrenergic effect on I_{Ca} (144). Interestingly, while the dromotropic actions of adenosine are conventionally associated with excitable cells, there is also evidence suggesting that the release of nitric oxide (NO) and prostaglandins from the endothelium as a result of endothelial AR activation may have a role to play as well (145).

1.3.2.2 Inotropic Control

The A_1 and A_2ARs are the main subtypes of adenosine receptors involved in the control of inotropy. As with heart rate, the A_1AR inhibits the inotropic influence of beta (β)-adrenergic activation by means of suppressing cAMP generation and PKA activation (146). Studies have also shown that the inhibitory effect of adenosine on contractility is not necessarily confined to the cAMP-PKA signalling pathway. A study by Fenton and colleagues (147) found that A_1AR activation by 2-chloro-N^6-cyclopentyladenosine

(CCPA; A_1AR-selective agonist) lead to a phospholipase C (PLC)-dependent decrease of sarcomere shortening in isolated rat ventricular myocytes. The same study also showed that A_1AR activation stimulated the colocalisation of protein kinase C (PKC)-ε and receptor for activated C kinase (RACK) 2, leading the authors to propose that A_1AR activation reduces ventricular contractility by a PLC/PKC/RACK2-dependent pathway. Another possible mechanism by which adenosine could inhibit cardiac contractility is via the inhibition of noradrenaline release from cardiac nerve terminals, as reported by Lorbar et al. (148) in a study on rat hearts. In the study, adenosine and CCPA was found to inhibit noradrenaline release by 49% and 54%, respectively, and simultaneous infusion of a non-specific (8-(p-sulfophenyl)theophylline, 8-SPT) and specific A_1AR (8-cyclopentyl-1,3-dipropylxanthine, DPCPX) antagonists reversed the effect, suggesting an important role for the A_1AR. Through these mechanisms collectively, the A_1AR counters β-adrenoceptor-mediated cardiac over-stimulation whether in conditions of reduced energy availability, excess stimulation, or both (132).

While most studies have focused on A_1AR effects on contractility, some work have also shown that the A_2AR, which couple to the G_s protein to stimulate adenylate cyclase, can stimulate a positive inotropic response in cardiac myocytes (149). While the A_{2A}AR is known to stimulate a contractile response via the activation of the cAMP/PKA pathway (similar to β-adrenergic stimulation), the Ca^{2+} transient and contractile response stimulated by the receptor was found to be lower in magnitude than that elicited by β-adrenoceptor activation, as reported by Dobson and colleagues (150). While the PLC/PKC pathway appears to be important for the A_1AR, it does not seem to play a role in A_{2A}AR-mediated contractile events (150). Recent evidence from the use of pharmacological agents and knockout (KO) mice has suggested a role for the A_{2B}AR in stimulating inotropy as well. Chandrasekera and colleagues (151) showed

that the use of BAY 60-6583, an A_{2B}AR-selective agonist, in wildtype (WT) mouse hearts significantly increased contractility while this effect by BAY 60-6583 was absent in A_{2B}AR-KO mouse hearts, implicating a role for the A_{2B}AR in cardiac contractility.

1.3.2.3 Coronary vascular control

Evidence suggests that every AR subtype may be involved in coronary vascular function. However, it is apparent, based on the body of evidence available, that the A_{2A} and A_{2B}ARs are the subtypes that play a main role in coronary vascular control (152-154). The importance of either receptor in vasoregulation is highly species-dependent. In a study utilising Langendorff-perfused isolated hearts, Flood & Headrick (152) compared the vasodilatory effects of A_{2A} and A_{2B}AR activation in both mice and rats using a pharmacological approach. Results from the study suggest a predominant role for the A_{2A}AR in regulating vasodilation in mice compared to the A_{2B}AR in rats. In mice, it was also shown that adenosine-mediated coronary dilation was NO- and K_{ATP} channel-dependent. Further demonstrating the species dependence of adenosine-mediated vascular control, Gurden et al. (153) showed that vascular control in canine coronary vessels is mainly A_{2A}AR-mediated while in guinea pig aorta, the more important receptor is the A_{2B}AR.

There is also evidence for a role in vasoconstriction for the A_1AR. Using human coronary arterioles, Sato et al. (154) showed that CGS21680, an A_{2A}AR agonist, dose-dependently caused vasodilation but when vessels were treated with (2S)-N^6-(2-endo-norbornyl)adenosine (ENBA), an A_1AR agonist, CGS21680-mediated dilation was significantly attenuated. Furthermore, adenosine-mediated dilation was also shown to be significantly reduced by SQ22536, an inhibitor of AC. These findings suggest the

A_1AR and the A_{2A}AR have opposing effects on vasoregulation as the former inhibits AC while the latter activates AC.

The role of the A_3AR remains very obscure. While there is evidence for A_3AR expression on vascular smooth muscle, the role of the A_3AR is thought to be mostly indirect, that is via the modulation of mast cells (135, 155). Shepherd and colleagues (155) found, in a hamster cheek pouch model, that application of N^6-(3-iodo-4-aminobenzyl)adenosine (I-ABA), an A_1/A_3AR agonist, lead to vasoconstriction, an effect that was not blocked by 8-SPT, an A_1/A_2AR antagonist. This suggested that the A_1AR had no role in I-ABA-mediated vasoconstriction, and that the effect was A_3AR-mediated. Applications of I-ABA to arterioles lead to mast cell activation (as assessed by ruthenium red uptake) and also arteriolar constriction. When both diphenhydramine (histamine antagonist) and SQ29548 (thromboxane antagonist) were added, the incidence of I-ABA-mediated constriction was reduced from 91% to 19% and the magnitude from 50.4% to 1.5%. This outcome suggests that the A_3AR is able to cause vasoconstriction through the activation of mast cells and the release of mast cell mediators, histamine and thromboxane.

1.4 Cardioprotection

It is well-accepted that the optimisation of reperfusion and adjunctive medical therapy has improved outcomes of patients suffering from AMI. However, further effort in improving these techniques is likely to lead to diminishing returns. For several decades, a significant amount of research effort has been focused on finding a method or agent that would confer protection to myocardial cells exposed to ischaemia followed by reperfusion. Cardioprotection involves the manipulation of cellular events by the use of

pharmacological agents or other methods at different stages of ischaemia and reperfusion to reduce cell death (156).

Pre-conditioning involves activating endogenous protective mechanisms by inducing repeated sub-lethal bouts of ischaemia and reperfusion prior to a prolonged period of ischaemia. Because pre-conditioning is applied before an ischaemic event, it cannot be used in a typical setting of AMI. However, it remains practical in situations where ischaemia is predicted or anticipated, for example, during elective PCI or cardiac surgery (156). The cellular and molecular mechanisms of pre-conditioning have been the focus of many studies. Hausenloy and colleagues (157) showed in a study that pre-conditioning confers cardioprotection via the activation of pro-survival kinases at reperfusion. The study, which utilised isolated rat hearts, found that pre-conditioning in the form of two 5-minute periods of ischaemia and two 10-minute periods of reperfusion led to an increase in Akt and extracellular signal-regulated kinase (ERK)1/2 activation during reperfusion and a significant reduction in infarct size. The protective effect of pre-conditioning was abolished when LY-294002 (a PI3K/Akt pathway inhibitor) or PD-98059 (a MEK/ERK1/2 pathway inhibitor) was added for the first 15 minutes of reperfusion, suggesting that the cardioprotective effect of pre-conditioning was mediated by Akt and ERK1/2. Pharmacological agents can also be used to mimic the effects of classical ischaemic pre-conditioning, an approach called pharmacological pre-conditioning. In a study using rabbit hearts, the administration of adenosine and A_1AR-selective agonist N^6-R-phenylisopropyladenosine (R-PIA) prior to ischaemia produced a similar decrease in infarct size as ischaemic pre-conditioning (5- minute occlusion followed by 10-min reperfusion) in rabbits subjected to 30-minute ischaemia followed by 180 minutes of reperfusion. Infusion of 8-SPT or PD115199 (A_1/A_2AR blockers) was also enough abolish the infarct-sparing effect of ischaemic pre-

conditioning. Together, these results showed that the infusion of adenosine receptor agonists can mimic the cardioprotective effect of pre-conditioning and that cardioprotection conferred by pre-conditioning is, in part, mediated through adenosine receptor activation (158).

While a large body of evidence has shown that pre-conditioning is cardioprotective, its application in the clinical setting is too limited. Post-conditioning on the other hand, is a technique that applies the principles of pre-conditioning after ischaemia and is thus more clinically relevant, especially in terms of treating AMI (156). Zhao et al. (27) were among the first to investigate if short, repeated bouts of ischaemia and reperfusion post-lethal-ischaemia were enough to attenuate reperfusion injury. The study, conducted on anaesthetised open-chest dogs, found that post-conditioning (three cycles of 30 s LAD occlusion and 30 s reperfusion) was equally effective as pre-conditioning (5 min occlusion followed by 10 min reperfusion) in reducing infarct size. Much like pre-conditioning, pharmacological agents can also be used to mimic post-conditioning. A randomised control trial investigating the effect of cyclosporine on reperfusion injury in patients with AMI undergoing PCI found that cyclosporine administered just prior to stenting (reperfusion) led to a significant reduction in serum creatine kinase levels and infarct size (as assessed by magnetic resonance imaging, MRI). The authors of the study speculated that the inhibition of mitochondrial permeability transition by cyclosporine may be partly responsible for the observed infarct-sparing effect (43), a notion supported by data from various pre-clinical studies (42, 159, 160).

1.4.1 Adenosine receptor-mediated cardioprotection

Adenosine has long been studied as a cardioprotectant in the setting of IR injury. Under pathophysiological conditions like myocardial ischaemia, the endogenous level of

adenosine is elevated and this is thought to activate AR-dependent cytoprotective signialling in the myocardium to limit cellular injury. Each of the four AR subtypes has been implicated in cardioprotection, some with more direct involvement than others.

The A_1 adenosine receptor (A_1AR) is the most extensively studied of the four receptor subtypes, and was the first receptor subtype to be associated with cardioprotection. The first evidence of A_1 receptor-mediated cardioprotection came from Lasley et al. who showed that R-N6-(phenyl-2R-isopropyl)-adenosine (R-PIA), a selective A_1AR agonist, delayed the onset of ischaemic contracture in globally ischaemic isolated rat heart, an effect that was blocked by pharmacological A_1AR antagonism (161). Following this study, others have also shown in either isolated hearts or animals that A_1AR agonists can reduce infarct size and improve post-ischaemic function (45, 162, 163). Investigations in isolated cardiomyocytes and cardiac cell lines have also demonstrated protection conferred by A_1AR agonists in simulated ischaemia assays (45, 164). The mechanisms underlying A_1AR-mediated cardioprotection is yet to be fully uncovered but it is known that it involves various downstream signaling pathways including the MEK1/2-ERK1/2 (165), PI3K-Akt (166), PLC-PKC (167) and the mitoK_{ATP} (168) pathways (Fig. 1.2).

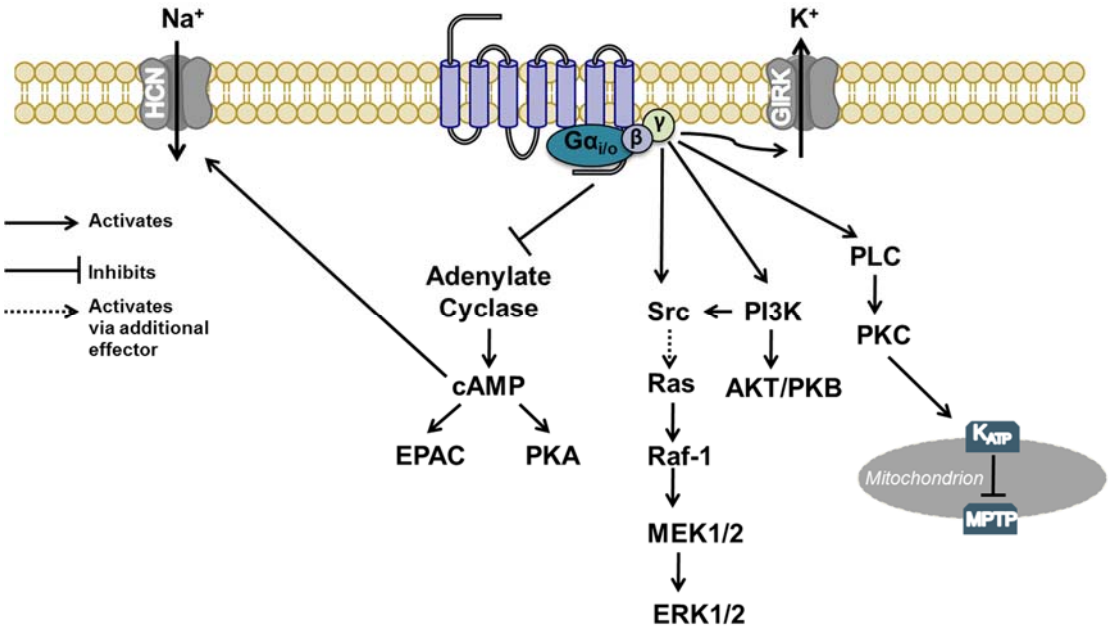

Figure 1.2 A_1AR-mediated signaling pathways. Activation of A_1AR reduces heart rate by directly activating GIRK channels via the Gβγ subunit. G_i-mediated reduction in cAMP also reduces the activity of the HCN channel, thereby inhibiting I_f and decreasing heart rate. A_1AR activation also confers cardioprotection via the activation of pro-survival kinases such as ERK1/2, PI3K-AKT, and PKC. Opening of mitochondrial K_{ATP} channels downstream of PKC inhibits the opening of mitochondrial permeability transition pores (MPTP), thus preserving mitochondrial function and preventing cell death.

A substantial body of work lately has also demonstrated synergistic cardioprotection from A_1 and A_2ARs. Lopes et al. were the first to report evidence of A_1 and A_2AR functional interactions in rat hippocampal and cortical synaptosomes (169). Various studies in isolated heart and *in vivo* models using genetic and pharmacologic intervention have shown that the activation of more than one AR subtype is required for full cardioprotection against ischaemia and reperfusion injury. Lasley and colleagues (170) first showed in *in vivo* rat myocardium that the A_{2A}/A_{2B}AR antagonist ZM241385 abolished A_1AR agonist-mediated infarct size reduction to the same extent as an A_1AR antagonist (DPCPX). Others have also shown in isolated perfused heart

models, this cooperative cardioprotection through the A_1 and A_{2A}/A_{2B}ARs. Urmaliya et al. (48) reported that ZM241385 and MRS1754 (A_{2B}AR antagonist) blocked A_1AR-mediated cardioprotection during reperfusion. This synergistic cardioprotection was also confirmed in hearts of knockout animals where A_1AR-mediated cardioprotection was abolished in A_{2A} (48, 126) and A_{2B} (126) knockout mouse hearts. Interestingly, treatment with A_{2A} and A_{2B}AR agonists alone was not shown to be beneficial in terms of improving postischaemic cardiac function and reducing infarct size in the isolated heart (126). Initially, this appears to contradict with several reports that show the infarct sparing effect of A_{2A} and A_{2B}AR agonism (49, 162, 171). However, these beneficial effects were primarily seen in *in vivo* preparations where A_{2A} and A_{2B}AR are able to modulate the inflammatory component (neutrophil adherence, accumulation and superoxide production) of myocardial infarction. In a study by Koeppen and colleagues (172), it was concluded that A_{2B}AR-mediated cardioprotection occurs predominantly through inflammatory cells and that the activation of these receptors on endothelial cells or cardiomyocytes does not contribute to the cardioprotective effects. In this study, chimeric mice, either A_{2B}KO mice with WT bone marrow (and hence WT haematopoetic cells) or WT mice with A_{2B}KO bone marrow (hence A_{2B}KO haematopoetic cells), were subjected to an ischaemia/reperfusion injury protocol. When A_{2B}ARs were absent on all cells except inflammatory cells, infarct size was shown to be identical to WT controls. However, when A_{2B}ARs were absent on inflammatory cells (but present on other tissue), infarct size was significantly greater than WT controls and was similar to A_{2B}KO controls. Furthermore, BAY60-6583, a selective A_{2B} adenosine receptor agonist reduced infarct size to the same extent as polymorphonuclear leukocyte (PMN) depletion. Combination of PMN depletion along

with BAY60-6583 treatment had no additional protective effect suggesting that A_{2B}ARs are cardioprotective when activated exclusively on PMNs.

Much less is known about A_3AR-mediated cardioprotection. Indeed, A_3AR expression in the heart is very low, with apparent absence of protein expression in mouse myocardium (113, 173). Nevertheless, reports of cytoprotection mediated by A_3AR in cardiac myocytes implicate its expression in the heart. Safran and colleagues (174) showed in isolated rat cardiac myocytes subjected to simulated ischaemia that adenosine-mediated cytoprotection can be abolished with the use of MRS1523, an A_3AR antagonist. Furthermore, CI-IB-MECA (A_3AR agonist)-treated cardiac myocytes showed reduced lactate dehydrogenase (LDH) release compared to untreated cardiac myocytes, an effect blocked by MRS1523. The outcomes of this study suggest a direct role for the A_3AR in reducing cardiac myocyte injury caused by ischaemia. Others have also shown that the A_3AR may have a less direct mechanism in reducing IR injury, that is by suppressing inflammation and leukocyte-mediated myocardial injury during reperfusion. Ge and colleagues (175) found that the infarct-sparing effect of CI-IB-MECA (A_3AR agonist) in wild-type (WT) mice was abolished in A_3AR-KO mice or chimeric mice lacking A_3ARs in bone marrow-derived cells. Leukocyte accumulation and infiltration was also markedly reduced in WT mice treated with CI-IB-MECA compared to A_3AR-KO or chimeric mice. Collectively, the results of this study suggest that CI-IB-MECA treatment reduces cardiac IR injury via the activation of A_3AR in bone marrow-derived cells, potentially by reducing the migration and pro-inflammatory actions of leukocytes.

1.5 Adenosine receptors and post-myocardial infarction cardiac remodeling

The prognosis of AMI survivors is associated with not only the initial infarct size but also the maladaptive remodeling that takes place after. Various studies have implicated ARs in the roles of regulating cardiac hypertrophy and fibrosis.

1.5.1 Cardiac hypertrophy

A_1AR activation has been consistently found to attenuate hypertrophy in cardiac myocytes (70, 100, 176) and animal models (102, 177). This is perhaps unsurprising given that cardiac myocytes have a far greater expression of the A_1AR relative to the other subtypes of ARs. In a report by Liao et al., treatment of rat cardiac myocytes with either adenosine or CPA (A_1AR-selective agonist) led to a significant reduction in phenylephrine (PE)-induced ^{3}H-leucine incorporation (a measure of total protein synthesis and cell hypertrophy). In the same report, the role of the A_1AR in cardiac hypertrophy and function was further investigated in a TAC mouse model. The treatment of TAC mice with adenosine or CPA led to a significant reduction in heart weight/body weight ratio and myocyte cross section area, reflecting an anti-hypertrophic effect. TAC mice treated with adenosine or CPA were also found to have significantly improved left ventricular fractional shortening and contractility (dP/dt_{max}) compared to untreated mice subjected to TAC. The beneficial effects of adenosine and CPA on cardiac function were completely abolished with the addition of 8-SPT (non-selective AR antagonist) and DPCPX (A_1AR-selective antagonist), confirming the involvement of the A_1AR. Together, these results suggest that A_1AR activation attenuates cardiac hypertrophy and improves cardiac function in heart failure, if only in a left ventricular pressure-overload TAC model (177). In support of the findings of

Liao et al., Wakeno and colleagues (102) also confirmed the anti-hypertrophic role of the A_1AR, albeit in a rat MI model. In rats subjected to LAD ligation-induced MI, adenosine treatment was enough to significantly reduce post-MI increases in heart weight/body weight ratio and myocyte cross-sectional area, similar to what was found by Liao et al.. The effects of adenosine were also significantly blunted by the addition of 8-SPT and DPCPX, confirming the involvement of the A_1AR in reducing hypertrophy. Collectively, the outcomes of the two studies suggest that the anti-hypertrophic role of the A_1AR is not only relevant across different species but also applicable in different models of heart failure.

The roles of the other AR subtypes in cardiac hypertrophy remain unclear. While some have shown A_{2A} and A_3AR activation to be anti-hypertrophic (100, 176), others were unable to reproduce this outcome (70, 177). In a recently published report, Sassi et al. (121) found that extracellular cAMP (subsequently converted to adenosine by enzymes such as ectonucleotide 5'-nucleotidase) was able to reduce isoprenaline/phenylephrine-induced hypertrophy in mice and NCMs, an effect abolished by pharmacological antagonism of the A_1AR but not the A_{2A}, A_{2B} or A_3AR. Liao and colleagues showed in two separate reports that neither CGS21680 (A_{2A}AR agonist) nor IB-MECA (A_3AR agonist) had anti-hypertrophic effects on cardiomyocytes stimulated with pro-hypertrophic agents TNF-α (70) or phenylephrine (177).

Interestingly, Lu et al. (178) demonstrated that A_3AR deficiency (A_3AR KO) in mice attenuated transverse aortic constriction (TAC) –induced left ventricular hypertrophy. The same group also showed in NCMs that A_3AR antagonism could enhance the anti-hypertrophic effects of 2-chloroadenosine, a non-selective adenosine analogue (178). The results of this study by Lu and colleagues suggest that rather than having no

bearing on cardiac myocyte hypertrophy, the deletion or pharmacological blockade of A_3AR is in fact beneficial in attenuating left ventricular hypertrophy.

This was in contrast to findings by both Gan et al. (100) and Xia et al. (176), where CGS21680 (A_{2A}AR agonist) and IB-MECA (A_3AR agonist) were shown to reverse hypertrophy in cardiac myocytes stimulated with phenylephrine. The discrepancy in findings in these studies may be due to differences in methods for triggering hypertrophy (cytokines, TAC, catecholamine), detecting hypertrophy (cell surface area, ^{3}H-leucine incorporation, ^{3}H-phenylalanine incorporation), the pharmacological tools used and their concentrations. More studies utilizing animals or cardiac myocytes with A_{2A} or A_3AR knockout/knockdown may be useful to confirm the role of these receptors in cardiac myocyte hypertrophy.

1.5.2 Cardiac fibrosis

With respect to cardiac fibrosis, a variety of genetic and pharmacological evidence suggest that A_{2B} adenosine receptor (A_{2B}AR) activation reduces fibroblast collagen synthesis. Chen and colleagues (179) showed that silencing the A_{2B}AR on adult rat cardiac fibroblasts resulted in an increase in collagen synthesis compared to control levels in the absence or presence of 2-chloroadenosine or NECA (a non-selective, potent A_{2B}AR agonist). Others have confirmed pharmacologically, with the use of A_{2B}AR antagonists (102) or selective AR agonists (128), that the A_{2B}AR, but not the other AR subtypes, plays a crucial role in the regulation of cardiac fibroblast collagen synthesis. In *in vivo* models, the role of the A_{2B}AR is less clear. Wakeno and colleagues (102) showed in a rat model of heart failure induced by LAD (left anterior descending coronary artery) ligation that increases in cardiac collagen volume fraction initiated by MI could be attenuated by the administration of adenosine. Treatment with MRS1754

(A_{2B}AR antagonist), but not antagonists for the A_1, A_{2A} or A_3AR subtypes, abolished the effect of adenosine on collagen volume fraction. The improvement in cardiac function by adenosine treatment (as assessed by echocardiography) was also blunted by MRS1754 only. More recently, the anti-fibrotic effect of adenosine (metabolized from extracellular cAMP) was also shown in a mouse model of cardiac pressure overload (121). This effect was shown to be blocked by pharmacological antagonism of the A_2R.

On the other hand, Toldo and colleagues (180) found in a mouse model that GS6201, an A_{2B}AR antagonist, was able to dose-dependently attenuate left ventricular enlargement and dysfunction and preserve cardiac function. It was suggested that blockade of the A_{2B}AR could reduce caspase-1 activation (resulting from ischaemic injury), IL-1β release and subsequent inflammatory response by other cytokines, thus limiting cardiac remodeling. Whether A_{2B}AR activation is beneficial or detrimental in post-MI cardiac remodeling remains unelucidated and more investigations, perhaps in A_{2B}AR-KO or transgenic mice, are warranted. The other AR subtypes do not appear to play a significant role in cardiac fibrosis, especially the A_1 and A_3AR, given their low expression levels in cardiac fibroblasts.

1.6 Impact of age and disease on efficacy

The impact of age and disease on the efficacy of cardioprotective and anti-remodeling therapeutics (adenosine included) cannot be understated. While many interventions have shown efficacy on the bench, they produce only modest benefits in the clinic (181). Evidence suggests this failure to translate in the clinic may be due to impairments in cardioprotective responses caused by ageing (182) and/or co-morbidities (183) that often accompany IHD such as hypercholesterolaemia and

diabetes. IHD and MI primarily affect those over the age of 55 but paradoxically, very little basic research into I/R injury and subsequent management goes to older hearts.

A substantial body of evidence has demonstrated the effect of ageing on ischaemic tolerance and adenosinergic cardioprotection. In a study by Schulman and colleagues where isolated rat hearts were subjected to ischaemic (IP) or pharmacological preconditioning prior to lethal IR injury, young hearts (aged 3 months) pre-treated with IP or either CCPA (selective A_1AR agonist), DOG (PKC activator) or diazoxide (mitoK_{ATP} channel opener) were shown to have significantly reduced infarct size compared to control hearts (184). In contrast, aged hearts (aged 18-20 months) subjected to the same pre-treatment protocol infarct sizes that were no different to control hearts post-IR injury. This outcome suggests that A_1AR, PKC and mitoK_{ATP} signaling may be impaired in aged hearts.

Interestingly, previous reports have shown that cardiac adenosine production is increased with age (185, 186). Thus, the age-induced reduction in A_1AR function, thought to be caused by the uncoupling of the receptor from the G protein, may be an adaptive response to A_1AR overstimulation. On the other hand, the increased adenosine production may be a compensatory response to declining A_1AR function. Either way, the reduction in A_1AR coupling to G proteins and thus function is likely to undermine the efficacy of A_1AR agonists, endogenous or exogenous. Age-related changes in PKC, a pro-survival kinase downstream of AR and other GPCR activation, have also been identified. These changes include altered expression of PKC isoforms and its translocation, and have been identified in rats (187, 188) and rabbits (189). As such, age-dependent dysfunction in cardiac PKC signaling appears to be conserved across species. Importantly, these changes may – at least in part – explain the failure of preconditioning and DOG in reducing infarct size in Schulman and colleagues' aged rat

model. MitoK_{ATP} channels are widely thought to be end effectors of cardioprotective signaling although little is known about how age affects its function. However, it is likely that the observed lack of efficacy of diazoxide in reducing infarct size is related to age-induced decreases in mitochondrial dynamics and functionality, and changes in mitochondrial membrane make-up (189).

Certain diseases also appear to sensitise the myocardium to IR injury while diminishing cardioprotection. Ueda et al. found in a study whereby rabbits with high cholesterol subjected to ischaemic preconditioning followed by lethal IR had similar infarct sizes to rabbits that had not received IP, suggesting that hypercholesterolaemia had abolished the protective effect of IP (190). The group also showed that the IP-induced activity of ecto-5'-nucleotidase, an enzyme responsible for adenosine production, is significantly blunted by hypercholesterolaemia. Since the activation of ecto-5'-nucleotidase is required for the infarct-sparing effect of IP, it is likely that hypercholesterolaemia attenuates the effect of IP via ecto-5'-nucleotidase. The protective effect of preconditioning appears to also be abrogated in the diabetic heart, as demonstrated by Sharma and colleagues in a study that investigated adenosine preconditioning in the diabetic rat heart (191). Not only were diabetic hearts shown to be more susceptible to lethal IR injury (infarct size, creatine kinase (CK) release $p<0.05$ vs. normal IR hearts), they were also shown to be resistant to adenosine preconditioning (infarct size, CK release not significantly different to diabetic IR hearts). One potential explanation for the effect of diabetes on preconditioning is its association with increased interstitial uptake of adenosine by cardiac fibroblasts and myocytes (192). In the same study (191), co-treatment with dipyridamole, an adenosine reuptake inhibitor, was shown to significantly restore the cardioprotective effect of adenosine preconditioning in the diabetic rat heart (as measured by infarct size and CK release). As such, it is reasonable

to suggest that impaired preconditioning and thus cardioprotection in the diabetic heart is, at least in part, caused by reduced myocardial availability of adenosine.

1.7 Clinical trials

Much effort has been invested into the research of adenosine, with strong evidence showing its importance as a modulator various physiological and pathophysiological processes. Thus, a growing number of rationally-designed ligands targeting the AR have been synthesized for use as pharmacological tools in experimental studies. Naturally, this has also resulted in increasing numbers of clinical trials investigating adenosine-based drugs that have shown promise at the pre-clinical stage in all types of diseases and conditions, including ischaemic heart disease and heart failure.

Administration of adenosine has consistently been shown to be cardioprotective against IR injury in animal models. The therapeutic potential of adenosine as a cardioprotective agent has led to studies like the Acute Myocardial Infarction Study of Adenosine (AMISTAD) trial (193). The AMISTAD trial investigated the ability of adenosine to reduce infarct size in patients undergoing thrombolysis. It was found that adenosine (70 μg/kg/min) treatment led to a 67% relative reduction (15% vs. 45.5% of left ventricle in placebo group) in final infarct size in patients with anterior MI. However, this reduction in infarct size did not lead to improved clinical outcomes. A trend towards increased haemodynamic adverse clinical events was also noted in patients treated with adenosine, especially those with non-anterior MI.

A larger follow-up trial (AMISTAD-II) (194) was then designed to evaluate clinical outcomes and infarct size of patients suffering from anterior MI receiving thrombolysis

or PCI. Patients were randomized to receive either a 70 μg/kg/min or a lower 50 μg/kg/min dose of adenosine intravenously. The lower dose was trialed as it was found to be effective in a preclinical study and could possibly reduce the incidence of bradycardia and hypotension reported in the original AMISTAD trial. The 70 μg/kg/min group showed a relative reduction of infarct size of 57% from the placebo group (11% vs. 26% of left ventricle respectively). This result was consistent with what was seen in the previous trial. The lower dose however failed to produce any statistically significant reduction in infarct size. In spite of demonstrating the significant infarct-sparing effect of adenosine, the trial did not show an improvement in patient outcomes and therefore failed to reach its primary endpoints; AMISTAD II was not considered a success. However, post-hoc analysis of the trial did reveal a significant reduction in early and late mortality, and composite clinical endpoint of death or chronic heart failure at 6 months in patients treated with adenosine within 3.17 hours of onset of symptoms compared (195).

In the ADMIRE (AMP579 Delivery for Myocardial Infarction Reduction) study, AMP579, an A_1/A_2 AR agonist was also evaluated in terms of infarct size reduction. In the interest of patient safety, the maximum dose of AMP579 tested in the clinical trial was limited to the lowest dose found to be effective in animals. While AMP579 was well-tolerated in patients, it failed to demonstrate a significant infarct-sparing effect (196).

A number of A_1AR antagonists have also been trialed in patients with HF. In a phase 2 trial, the short term effects of a single 5, 10, and 15 mg dose of SLV320, an A_1AR-selective antagonist, were investigated in patients with heart failure and compared to placebo and furosemide (197). SLV320 was found to have no significant haemodynamic effects and was well-tolerated in patients while furosemide was found

to increase total peripheral resistance (TPR). SLV320 administration was also found to decrease cystatin C plasma concentrations whereas furosemide resulted in a significant increase of cystatin C levels compared to baseline, indicative of worsening kidney function. Sodium excretion and diuresis was also increased significantly in the SLV320 (10 and 15 mg) group compared to the placebo group although the diuretic effect of SLV320 was much weaker compared with furosemide. The outcomes of this study were positive and authors concluded that SLV320 is well-tolerated in patients and increases sodium excretion as well as diuresis without compromising kidney function. Several subgroups of HF patients may benefit from an A_1AR antagonist, including patients with diuretic resistance and patients with chronic HF requiring long-term treatment with diuretics. The success of this trial suggested that A_1AR antagonism might represent a new therapeutic strategy for treating patients with HF.

A year later, the outcomes of the PROTECT study (198), a large, phase III clinical trial were published. In the study, patients with acute heart failure with impaired renal function received daily rolofylline (30 mg), an A_1AR-selective antagonist or placebo for up to 3 days. The primary endpoint of the study was treatment success, treatment failure or no change in patient clinical condition; the secondary endpoints were post-treatment development of persistent renal impairment and the 60-day rate of death or admission for cardiovascular or renal causes. Rolofylline (compared to placebo) was not beneficial with respect to the primary or secondary endpoints. A total of 11 patients (0.8%) in the rolofylline group had seizures while there were none in the placebo group ($P = 0.02$), highlighting the risk of lowering the seizure threshold as a result of A_1AR antagonism. The PROTECT pilot trial had previously shown that patients receiving 30 mg of rolofylline were more like to have improvement in dsypnoea and were less likely to have renal impairment than those receiving placebo, with a trend towards lower 60-

day death or readmission for cardiovascular or renal causes. However, in spite of similarities in study design, inclusion criteria and dose of rolofylline, the phase III PROTECT trial did not reproduce the findings of the pilot trial.

The failure of the PROTECT, AMISTAD and ADMIRE trials further highlights the complexity of managing IR injury and heart failure. Valuable lessons can be learned from the outcome of these trials, including a need for a new approach to adenosine-based drug design and development that aims to minimize on-target adverse effects (such as those found in the PROTECT and AMISTAD trials) while maintaining a high efficacy for desired effects.

1.8 G protein-coupled receptor biased agonism

Classical pharmacology posits that the ability of a ligand to produce a response through its target receptor is governed by two molecular properties: affinity (attraction between ligand and receptor) and efficacy (level of response elicited by the bound ligand) (199). Based on a given system, ligands can be classified as full agonists (generating maximal response), partial agonists (generating sub-maximal response even at the highest doses), neutral antagonists (generating no response or having zero efficacy) or inverse agonists (reducing signalling output below that of basal state or having negative efficacy) (200). Bound agonists are expected to activate all signalling pathways linked to the receptor to the same relative extent while an antagonist was expected to antagonise every signalling pathway to the same degree. Based on this, only the quantity of stimulus conferred to the cell determines ligand characteristic (intrinsic efficacy; e.g. partial vs. full agonism) (201). Recently however, it has emerged that different ligands can mediate varying functional outcomes through a given receptor and

that the characteristic of a ligand at a receptor can be different depending on the signalling pathway investigated (system-dependent). This phenomenon is known as "biased agonism". Biased agonism in G protein-coupled receptors (GPCR) can be described as the ability of GPCR ligands to stabilise different active receptor conformations resulting in differential coupling and activation of downstream signalling pathways (199, 200). Berg et al. were one of the first to rigorously test this phenomenon in a study looking at 5-HT_{2c} signalling whereby ligands were assessed on their ability to activate two independent pathways that lead to either inositol phosphate (IP) accumulation or arachidonic acid (AA) release (202). It was found that some 5-HT_{2C} agonists had a preference for the IP pathway while others had greater relative efficacy towards the AA pathway (202) – an observation that challenges the classical receptor theory. Other receptors like the melanocortin 4 receptor (203), and GPR109A (204) have also been found to display such bias for certain pathways when activated by different ligands. More recently, we identified a biased A_1AR agonist VCP746, which preferentially couples to the ERK1/2 pathway, rather than the cAMP pathway. VCP746 was also found to be cytoprotective, but does not cause bradycardia, unlike the prototypical A_1AR agonist CPA. (205) The discovery of biased agonism opens a new avenue in drug development for the design of drugs that preferentially modulate pathways that are involved in disease and not normal cellular function (200).

1.9 VCP746

VCP746 is a hybrid molecule comprising adenosine and the positive allosteric modulator, VCP171, joined by a 6-carbon linker. The affinity, potency, and maximal agonist effect of VCP746, along with prototypical agonists R-PIA and adenosine (from

a [^{35}S]GTPγS binding assay), in Chinese hamster ovary (CHO) cells stably expressing A_1ARs are listed in Table 1.3.

	VCP746	**R-PIA**	**Adenosine**
pK_i	7.23 ± 0.17	6.47 ± 0.07	5.53 ± 0.05
pEC_{50}	9.05 ± 0.08	8.60 ± 0.04	7.03 ± 0.06
E_{max}	98 ± 1	98 ± 1	100

Table 1.3 Affinity (pK_i), potency (pEC_{50}) and maximal efficacy (E_{max}) of VCP746, R-PIA and adenosine in CHO cells stably expressing the A_1AR.

While bitopic ligands have previously been identified for G protein-couple receptors (GPCR), VCP746 is the first to show separation of on-target efficacy from undesired on-target adverse effects (Fig. 1.3). To validate the bitopic binding mode for VCP746 at the A_1AR, the interaction between DPCPX (A_1AR-selective antagonist) and VCP746 was assessed by Valant et al. (205) using [^{35}S]GTPγS and ERK1/2 phosphorylation assays in CHO cells. DPCPX induced a decrease in VCP746 potency followed by a depression of E_{max} in both the [^{35}S]GTPγS and ERK1/2 phosphorylation assays suggesting a bitopic mode of interaction with the A_1AR. The study also found that VCP746 had a 30-fold preference for cAMP inhibition relative to ERK1/2 accumulation, unlike CPA and R-PIA (the reference ligand used in the study) which were equipotent in both signaling pathways. Valant et al. further showed that VCP746 was cytoprotective in cardiac myocytes and myoblasts but had no effect on heart rate in isolated rat atria, suggesting a separation of a desired effect (cytoprotection) from an adverse effect (bradycardia) at the A_1AR. Together, these results suggest that VCP746 interacts in a bitopic mode and displays biased agonism at the A_1AR. VCP746 also has no effect on heart rate at concentrations that are cytoprotective.

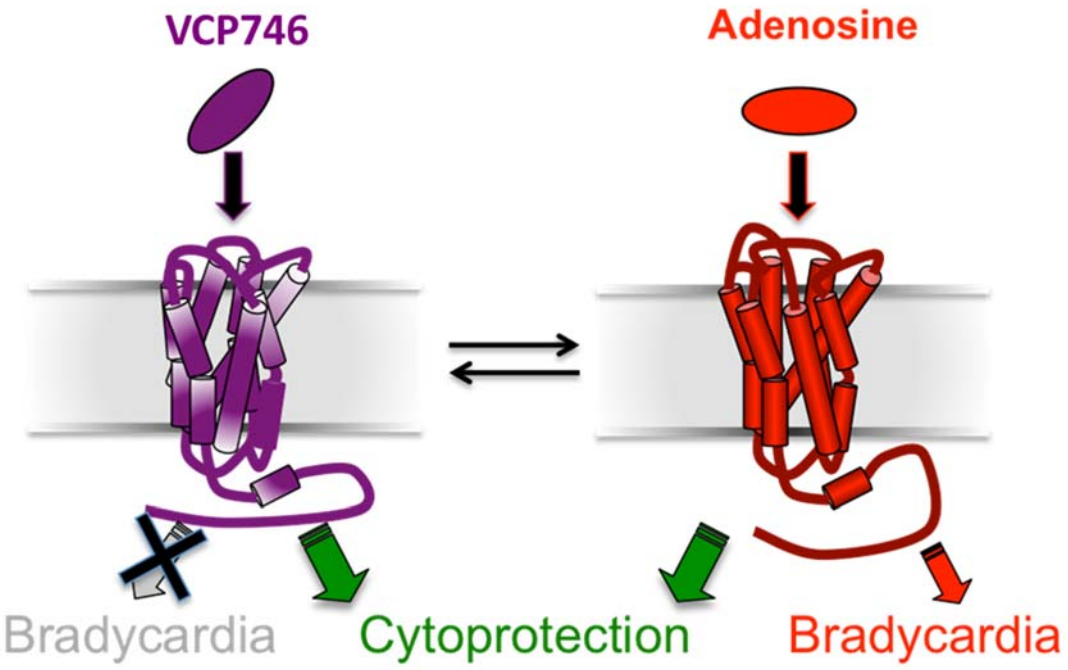

Figure 1.3 The ideal bias properties of a cardioprotective A_1AR therapeutic. VCP746 has been shown to be cytoprotective without causing bradycardia.

Recent evidence has also shown that VCP746 also has higher potency and efficacy at the A_{2B}AR compared to prototypical orthosteric ligands 5'-N-Ethylcarboxamidoadenosine (NECA) and BAY60-6583. The affinity and potency estimates of VCP746, NECA and BAY60-6583 across multiple signaling pathways in CHO cells stably expressing the A_{2B}AR are listed in Table 1.4. Outcomes from [^{3}H]DPCPX binding assays further suggest that VCP746 has a bivalent mode of interaction with the A_{2B}AR, that is VCP746 can potentially simultaneously interact with two distinct sites on the A_{2B}AR.

	pK_I	pEC_{50}			
		Calcium	cAMP	IP	pERK1/2
NECA	5.61 ± 0.30	7.20 ± 0.01	8.04 ± 0.27	6.10 ± 0.39	7.04 ± 0.12
BAY60-6583	5.82 ± 0.32	7.22 ± 0.05	8.03 ± 0.42	5.37 ± 0.79	7.01 ± 0.06
VCP746	7.26 ± 0.12	8.21 ± 0.09	8.04 ± 0.09	7.60 ± 0.23	8.53 ± 0.08

Table 1.4 Affinity (pK_I) and potency (pEC_{50}) estimates of NECA, BAY60-6583 and VCP746 across different signaling pathways in CHO cells stably expressing the A_{2B}AR.

The dual potency of VCP746 at the A_1 and A_{2B}AR may be highly advantageous in the treatment of IR injury given that both receptors are known to be involved – the A_1AR in cardioprotective signaling and the A_{2B}AR in mitigating inflammation. The A_1 and A_{2B}ARs are also implicated in the regulation of cardiac hypertrophy and fibrosis, respectively. As such, VCP746 represents a highly attractive therapeutic approach for modulating not only IR injury but also cardiac remodeling.

1.10 Aims and hypotheses

1.10.1 Ischaemia and reperfusion injury

Hypothesis: VCP746, a novel A_1/A_{2B}AR agonist, is cardiorprotective without any effect on heart rate and mean arterial pressure in the setting of ischaemia and reperfusion injury.

Aim 1: To investigate if VCP746, a novel A_1/A_{2B}AR agonist, reduces infarct size and improves post-ischaemic cardiac function without reducing heart rate in a Langendorff-perfused isolated rat heart model.

Aim 2: To investigate if VCP746, a novel A_1/A_{2B}AR agonist, reduces infarct size without reducing heart rate and mean arterial pressure in a rat myocardial infarction model.

VCP746 will first be tested in an isolated heart model, an environment free from the influences of the immune system, before proceeding to a more physiologically relevant whole animal model of myocardial infarction. In both studies, key parameters such as infarct size (as a percentage of area at risk) and heart rate will be investigated.

1.10.2 Cardiac remodeling

Hypothesis: VCP746, a novel A_1/A_{2B}AR agonist, reduces cardiac remodelling.

Aim 1: To investigate the effect of VCP746, a novel A_1/A_{2B}AR agonist, on cardiac myocyte hypertrophy and cardiac fibroblast collagen synthesis.

Aim 2: To investigate the effect of VCP746, a novel A_1/A_{2B}AR agonist, on cardiac remodelling and function in a long-term rat myocardial infarction model.

VCP746 will first be tested *in vitro* in a neonatal cardiac myocyte and cardiac fibroblast model before proceeding to a more physiologically relevant whole animal LAD occlusion model of cardiac remodelling. Measures of hypertrophy and fibrosis will be undertaken in both studies, along with changes in gene expression. In the whole animal study, changes in cardiac function, protein expression and histology will also be investigated to further determine the effect of VCP746.

Chapter 2 Materials and Methods

2.1 *In vitro* studies

Cultured neonatal rat cardiac myocytes (NCM) and fibroblasts (NCF) were used to determine the effects of adenosine receptor (AR) agonists on hypertrophy and collagen synthesis, respectively.

2.1.1 Animals and ethics approval

NCM and NCF were isolated from 1-2 day old Sprague Dawley (SD) rat pups. All animal usage was approved by the Alfred Medical Research and Education Precinct (AMREP) Animal Ethics Committee-approved protocols in accordance with the National Health and Medical Research Council's (NHMRC) Guide for the Care and Use of Laboratory Animals (ethics approval number: E/0981/2010/M).

2.1.2 Reagents and solutions

10X Ads Buffer

Composition: NaCl 116 mM; KCl 50 mM; $MgSO_4$ 8 mM; Glucose 60 mM; Na_2HPO_4 0.008 mM.

Adjust to pH 7.35 and store at 4°C. Dilute to 1X Ads buffer with sterilized Milli-Q water when required.

Enzyme digestion solution

1X Ads buffer containing 0.8 mg/ml pancreatin and 125 U/ml collagenase.

Use 0.3 ml of enzyme digestion solution per heart.

Minimum essential media (MEM) with 10% new born calf serum (NBCS)

Composition: Powdered MEM dissolved in MilliQ-water; $NaHCO_3$ 26 mM; 1X essential amino acids; non-essential amino acids 100 μM; L-glutamine 2 mM; 1X MEM vitamins; 10% v/v NBCS; 1% antibiotics and antimycotics.

Adjust to pH 7.2. Sterilize using Steritop filters (Millipore, MA, USA) and store at 4ºC.

Percoll stock

9 parts Percoll: 1 part 10X Ads buffer. Store at 4°C.

Top Percoll layer

9 parts Percoll stock: 11 parts 1X Ads buffer. Make fresh when required.

Bottom Percoll layer

13 parts Percoll stock: 7 parts 1X Ads. Make fresh when required.

NCM media for culture/treatment

Composition: Dulbecco's modified eagle medium (DMEM); $NaHCO_3$ 26 mM; 1X essential amino acids; non-essential amino acids 100 μM; sodium pyruvate 1 mM; 1X MEM vitamins. Media was supplemented with insulin 2 mg/L, apo-transferrin 10 mg/L, and 5-bromo-deoxyuridine (BrDu) 0.1 mM before use. NB: BrDu was only used in the first three days to inhibit proliferation of fibroblasts.

Adjust to pH 7.2 and sterilize using Steritop filters. Store at 4ºC.

2.1.3 NCM and NCF isolation

Neonatal NCM and NCF were isolated from 1-2 day old SD rat pups with enzymatic digestion as described in detail previously (206, 207). Hearts were harvested under aseptic conditions and placed into cold PBS solution. After removing the main blood

vessels and atria, the remaining ventricular tissues were washed and gently cut into 6-8 pieces (1-2 mm^2). The chopped tissues were digested by 10x10 min sequential stirring in a Celstir apparatus containing enzyme digestion solution. The Celstir system was placed on a magnetic stirrer using the lowest speed and maintained at 37°C. For each cycle, undigested tissue was allowed to settle; and following each digestion period, the supernatants containing dissociated NCM and NCF were transferred into 50 ml sterile tubes (on ice) in the presence of 10 mL NBCS to inhibit enzyme activity. The first supernatant was discarded because it contained blood cells and cell debris. The remaining supernatant was combined and centrifuged at 1,200 revolutions per minute (rpm) (300xg) for 10 min and the cell pellets were then collected and resuspended in MEM with 10% NBCS. Cells were centrifuged for 10 min and the pellets collected. Cell pellets were resuspended in 1X Ads buffer.

The resuspended cells were loaded above the top layer of a Percoll gradient, consisting of the top and bottom Percoll layers, and centrifuged at 3,000 rpm for 30 min at 4°C without using the brake. Upon completion of centrifugation, the NCF were collected in the upper gradient band and the NCM were collected in the lower band. After transferring each band into separated tubes, cells were washed with 1X Ads twice by centrifuging for 6 min at 1,200 rpm then resuspended in MEM with 10% NBCS.

2.1.4 Cell culture

Briefly, NCM were purified and seeded in gelatin-coated 12-well plates at a density of 300,000 cells/well and maintained in serum-free, high-glucose (4.5g/L) DMEM supplemented with insulin and transferrin. Bromodeoxyuridine (BrdU) was included for the first 3 days and KCl (50 mM) was added to the medium to prevent spontaneous contraction hypertrophy of the plated NCM. NCF were seeded and maintained in high-

glucose (25 mM) DMEM in the presence of 1% antibiotic/antimycotic and 10% FBS. For all experiments, NCF were used at passage 2. All cells were maintained at 37°C in a 5% CO_2 humidified incubator.

2.1.5 Measurement of NCM hypertrophy

NCM hypertrophy was determined by measuring ^{3}H-leucine incorporation as previously described (208-210). After isolation, the number of NCM suspended in MEM with 10% NBCS was counted using a haemocytometer. Purified NCM were seeded at 300,000 cells/well in 12 well plates (BD Falcon, NSW, Australia) coated with 0.1% gelatin. NCM were incubated overnight at 37°C with 5% CO_2. NCM were then maintained in serum-free DMEM supplemented with insulin and apo-transferrin for 48 hours before treatment. KCl (50 mM) was added to the media to prevent contact-induced spontaneous contraction of the plated NCM.(211)

On treatment day, media was changed. NCM were then pre-treated with adenosine receptor agonists. After pre-treatment, interleukin-1 beta (IL-1β; Peprotech, NJ, USA) or tumour necrosis factor α (TNFα; Peprotech, NJ, USA) at 10 ng/mL or angiotensin II (AngII; 100 nM; Auspep, VIC, Australia) were added to cells. ^{3}H-leucine (1 μCi) was added to each well. Cells were incubated at 37°C with 5% CO_2 for a further 48 hrs (60 hrs for AngII-treated cells). After 3 washes with cold 1X PBS, cells were harvested by precipitation with 10% trichloroacetic acid (TCA) on ice for 30 min before solubilisation with 1M NaOH overnight at 4°C. The samples were then neutralized with 1M HCl, and ^{3}H levels were counted in scintillation fluid on a beta counter to determine the levels of ^{3}H-leucine incorporation.

2.1.6 Measurement of NCF collagen synthesis

NCF collagen synthesis was determined at passage 2 by ^{3}H-proline incorporation (209, 212). After isolation, NCF (passage 0) were seeded into T75 cell culture flasks (BD Falcon, NSW, Australia) and maintained in high-glucose (25 mM) DMEM containing 5.33 mM KCl (Invitrogen, VIC, Australia) in the presence of 1% v/v antibiotic/antimycotic (Invitrogen, VIC, Australia) and 10% foetal bovine serum (FBS) (JRH biosciences, VIC, Australia). Cells were incubated at 37°C with 5% CO_2 for 48 hr.

At 80% of confluence, the NCF were sub-cultured. After removing media, NCF were washed 3 times with warm 1X PBS, 2 ml of warm 0.05% trypsin-EDTA was added to each flask. Flasks were placed back into a 37°C incubator for 1-2 min to allow cells to lift off the surface of the flasks. Trypsin was inactivated by adding 8 ml of DMEM containing 10% FBS. NCF (passage 1) were centrifuged at 1,600 rpm for 5 min at room temperature. Cell pellets were washed 3 times and resuspended with DMEM containing 10% FBS. Cells were then split into new flasks (1:3) and incubated at 37°C with 5% CO_2 for 48 hrs.

To seed NCF, steps from trypsinization to re-suspension described above were repeated. NCF (passage 2) were counted and seeded at a density of 50,000 cells/well in 12 well plates in DMEM containing 10% FBS. Plated NCF were incubated at 37°C with 5% CO_2 overnight before serum starving with media containing 0.15 mM vitamin C and 0.5% bovine serum albumin (BSA; Sigma-Aldrich, Castle Hills, NSW, Australia) for 48 hrs.

After changing media, cells were pre-treated with adenosine receptor antagonists for 20 min followed by agonists for 40 min before stimulation with transforming growth factor-β1 (TGF-β1; 10 ng/mL; Peprotech, NJ, USA) or angiotensin II (100 nM). ^{3}H-proline (1 μCi) was added to each well. After 48 hrs of further incubation, cells were harvested by TCA precipitation and ^{3}H-proline incorporation was determined using methods similar to NCM hypertrophy assessment described above.

2.1.7 Measurement of cell viability

MTT assay was used to determine cell viability as previously described (213, 214). NCM and NCF were seeded in 96 well plates at a density of 50,000 cells/well. After serum starving for 48 hrs, cells were treated with adenosine receptor agonists in the presence or absence of antagonists, and cytokines as described in 2.1.5 and 2.1.6. 3-(4,5-dimethylthiazol-2-yl)-2,5-diphenyltetrazolium bromide (MTT; Sigma Aldrich, NSW, Australia) (10.0 ng/ml) was added to each well and the cells were incubated at 37°C with 5% CO_2 for 4 hr. The media was removed and isopropanol (100 μl/well) was added, the plates were placed back into the incubator for 30 min. Absorbance was measured on a microplate reader (SPECTROstar Nano; BMG LABTECH, Ortenberg, Germany) at a wavelength of 570 nm with background subtraction at 690 nm.

2.1.8 Quantitative measurement of mRNA in NCM and NCF

After 48 hours of serum starvation, cultured NCM and NCF were pre-treated with adenosine receptor antagonists for 20 min (NCF only), followed by VCP746 for 40 min and lastly, stimulated for 24 hours before harvesting. IL-1β (10 ng/mL), TNF-α (10 ng/mL) and AngII (100 nM) were used to stimulate hypertrophy-associated gene expression in NCM while AngII (100 nM) and TGF-β1 (10 ng/mL) were used to stimulate pro-fibrotic gene expression in NCF. Total RNA was extracted using an RNA

isolation kit (RNAqueous, Ambion, TX, USA) according to manufacturer's instruction. Reverse transcription was then performed in a thermocycler. Reaction mixture (Table 2.1) was heated to 25°C for 10 min, 42°C for 12 min, 95°C for 5 min, and cooled to 4°C.

Reagent	Volume (μl)/reaction
PCR Buffer II (10X)	4
$MgCl_2$	8
dNTPs	16
Random Hexamers	2
Nuclease free water	2
RNAse inhibitor	2
MultiScribe	2
RNA	4
Total	**40**

Table 2.1 Composition of reverse transcription reaction mixture for cDNA synthesis.

After reverse transcription to cDNA with MultiScribe (Applied Biosystems, Foster City, CA, USA), triplicate cDNA aliquots were amplified using either sequence specific primers (Table 2.2; Geneworks, Adelaide, SA, Australia) with SYBR Green detection (for pro-fibrotic genes in NCF) or TaqMan® Gene Expression Assays (for pro-hypetrophic genes in NCM).

Following the addition of the reaction mixture (Table 2.3 and Table 2.4) into PCR plates, the plates were covered with optical adhesive film (Applied Biosystems, CA, USA) and spun in a centrifuge at 3,000 rpm for 5 min at 4°C to remove air bubbles.

Gene	Primer sequence
TGF-β1	Forward: 5’ CCAGCCGCGGGACTCT 3’
	Reverse: 5’ TTCCGTTTCACCAGCTCCAT 3’
CTGF	Forward: 5’ GCGGCGAGTCCTTCCAA 3’
	Reverse: 5’ CCACGGCCCCATCCA 3’
Collagen I	Forward: 5’ TGCCGATGTCGCTATCCA 3’
	Reverse: 5’ TCTTGCAGTGATAGGTGATGTTCTG 3’
ANP	Forward: 5’ ATCTGATGGATTTCAAGAACC 3’
	Reverse: 5’ CTCTGAGACGGGTTGACTTC 3’
β-MHC	Forward: 5’ TTGGCACGGACTGCGTCATC 3’
	Reverse: 5’ GAGCCTCCAGAGTTTGCTGAAGGA 3’
GAPDH	Forward:5’ GACATGCCGCCTGGAGAAAC 3’
	Reverse: 5’ AGCCCAGGATGCCCTTTAGT 3’
18S	Forward: 5’ TCGAGGCCCTGTAATTGGAA 3’
	Reverse: 5’ CCCTCCAATGGATCCTCGTT 3’

Table 2.2 Primer sequences used in RT-PCR.

RT-PCR was performed with QuantStudio 12K Flex Real-Time PCR System (Life Technologies) to quantify mRNA expression of transforming growth factor-β1 (TGF-β1), connective tissue growth factor (CTGF) and collagen I (Col I) in NCF, and atrial natriuretic peptide (ANP), β-myosin heavy chain (β-MHC) and alpha skeletal actin (α-SKA) in NCM. The primer pairs were designed using Primer Express 2.0 software (Applied Biosystems) based on published sequences. GAPDH and 18s rRNA were used as endogenous controls in all experiments to correct for the expression of each gene in NCM and NCF, respectively.

Reagent	Volume (µl)
SYBR Green master mix	5
Forward Primer	0.5
Reverse Primer	0.5
Nuclease free water	3
cDNA	1
Total	**10**

Table 2.3 Composition of RT-PCR reaction mixture in each well using SYBR Green detection for NCF gene expression.

Reagent	Volume (µl)
Buffer A	0.5
PCR Buffer II (10X)	0.5
$MgCl_2$	1.4
dNTPs	0.8
Primer probe mix	0.5
Nuclease free water	5.25
AmpliTaq Gold (ATG)	0.05
CDNA	1
Total	**10**

Table 2.4 Composition of RT-PCR reaction mixture in each well using TaqMan assay for NCM gene expression.

2.1.9 Materials

N^6-Cyclopentyladenosine (CPA) was purchased from Sigma-Aldrich (Castle Hills, NSW, Australia). Trans-4-[(2-Phenyl-7H-pyrrolo[2,3-d]pyrimidin-4-

yl)amino]cyclohexanol (SLV320), 2-(2-Furanyl)-7-[3-(4-methoxyphenyl)propyl]-7H-pyrazolo[4,3-e][1,2,4]triazolo[1,5-c]pyrimidin-5-amine (SCH442416) and 8-[4-[4-(4-Chlorophenzyl)piperazide-1-sulfonyl)phenyl]]-1-propylxanthine (PSB603) were purchased from Tocris Bioscience (Bristol, UK). The A_1/A_{2B}AR agonist VCP746 was synthesised at the Monash Institute of Pharmaceutical Sciences. Stock solutions were prepared in DMSO and kept at -20˚C until used.

2.1.10. Statistical analysis

Data expressed as mean ± SEM. Statistical significance was defined as $P<0.05$ as determined by one-way analysis of variance (ANOVA) with Dunnett's multiple comparisons post hoc analysis. All statistical analyses were performed using GraphPad Prism 6.

2.2 *Ex vivo study*

2.2.1 Animals and ethics approval

Adult male Sprague-Dawley rats used in the present study were obtained from Monash Animal Services, Monash University. Rats were maintained in-house at the Monash Institute of Pharmaceutical Sciences animal house at 22^{o}C with a constant 12 hour light/dark cycle. Animals had free access to rat chow and water ad libitum. The experimental protocols were approved by the Monash University Standing Committee of Animal Ethics in Animal Experimentation (ethics approval number: MIPS.2014.11), Faculty of Pharmacy and Pharmaceutical Sciences, Monash University.

2.2.2 Langendorff-perfused isolated heart preparation

Male Sprague-Dawley rats (250-350 g) were anaesthetized with sodium pentobarbital (60 mg/kg) administered by intraperitoneal route, a thoracotomy was done, and the hearts were rapidly excised into ice-cold perfusion buffer. The hearts were retrogradely perfused through the aorta at a constant pressure of 80 mmHg with modified Krebs-Henseleit buffer containing 120 mM NaCl, 4.7 mM KCl, 1.2 mM KH_2PO_4, 1.2 mM $MgSO_4$, 0.5 mM EDTA, 22 mM $NaHCO_3$, 11 mM glucose and 2.5 mM CaCl. The perfusion buffer was equilibrated with 95% O_2 and 5% CO_2 at 37^oC. The buffer was filtered through an in-line sterile 0.22 μm Sterivix-GV filter unit (Millipore, Billerica, MA) to remove microparticulate matter. The left atrium was removed, and the left ventricle was vented with a polyethylene tube through the apex for Thebesian drainage, which prevented intraventricular pressure development. For measurement of left ventricular developed pressure, a fluid filled latex balloon (ADInstruments, Bella Vista, NSW, Australia) was inserted into the left ventricle via the mitral valve. The balloon was connected to the physiological pressure transducer (MLT844, ADInstruments) and inflated with a 500 μL glass syringe to obtain approximately 5 - 10 mmHg left ventricular diastolic pressure. The heart was submerged into the heat-jacketed Krebs-Henseleit buffer maintained at 37^oC throughout the experiment. Perfusion fluid temperate was monitored using T-type implantable thermocouple (MLT1401; ADInstruments). Coronary perfusion pressure was measured using the physiological pressure transducer attached to a 3-way valve immediately above the aortic cannula. Perfusion reservoir and aorta cannula connected to a Minipuls 3 peristaltic pump (Gilson SAS, Villers Le Del, France) was attached to PowerLab (8/30; ADInstruments) via STH Pump controller (ADInstruments). Continuous in-line measurement of coronary perfusion flow was monitored by appropriately calibrated pump which was

recorded along with coronary perfusion pressure, on the computer by PowerLab data acquisition system (ADInstruments). The left ventricular pressure signals were acquired continuously using PowerLab and digitally processed by using ChartPro version 5.5.6 software (ADInstruments) to measure left ventricular systolic and developed pressure, heart rate and dP/dt_{max}. Difference of systolic and diastolic pressures was used to obtain left ventricular developed pressure (LVDP).

All hearts were equilibrated for at least 20 minutes to allow for stabilization. After stabilization, hearts were subjected to 30 minutes of no-flow normothermic global ischaemia and 60 minutes of reperfusion. Ischaemia was attained by completely stopping the perfusate inflow and immersing the heart in perfusate buffer saturated with 95% N_2 and 5% O_2 in the heart chamber. After no-flow global ischaemia, reperfusion was achieved by restarting the perfusion in-line flow. To examine adenosine receptor-mediated cardioprotective effects on functional recovery and infarct size reduction, hearts were perfused with perfusate containing the indicated agonist and antagonist at predetermined concentrations for 15 minutes at the start of reperfusion. When antagonists were used, they were perfused for 5 minutes before addition with agonist for 15 minutes. In the present study, 30 minutes of global ischaemia and 60 minutes of reperfusion protocol was selected based on previous studies in our laboratory.

2.2.3 Infarct size measurement

At the end of the experiment, hearts were removed and frozen at -20ºC. The frozen hearts were sectioned into transverse slices of 1.5 mm thickness and stained by incubation in 1% 2, 3, 5-triphenyltetrazolium chloride (TTC; Sigma-Aldrich, St. Louis, MO) for 15 minutes at 37ºC. After fixing overnight in 10% neutral buffered formalin, heart sections were photographed using a digital camera. The area of infarction and risk

zone was measured using ImageJ 1.46r software (National Institute of Health). Metabolically-active tissue was stained red and considered non-infarcted tissue while metabolically-inactive tissue remained pale and considered infarcted tissue. The area at risk was calculated as total ventricular area minus cavities. Infarct size was expressed as a percentage of the risk area.

2.2.4 Materials

N^6-Cyclopentyladenosine (CPA) was purchased from Sigma-Aldrich (Castle Hills, NSW, Australia). Trans-4-[(2-Phenyl-7H-pyrrolo[2,3-d]pyrimidin-4-yl)amino]cyclohexanol (SLV320) and 8-[4-[4-(4-Chlorophenzyl)piperazide-1-sulfonyl)phenyl]]-1-propylxanthine (PSB603) were purchased from Tocris Bioscience (Bristol, UK). The A_1/A_{2B}AR agonist VCP746 was synthesised at the Monash Institute of Pharmaceutical Sciences. Stock solutions were prepared in DMSO and kept at -20˚C until used.

2.2.5 Statistical Analysis

Data expressed as mean ± SEM. Infarct size data was analysed by one-way ANOVA followed by Dunnet's post-hoc test. Cardiac functional data were analysed by two-way ANOVA followed by Dunnet's post-hoc test. All statistical analyses were performed using GraphPad Prism 6. A two-sided P-value of less than 0.05 was considered statistically significant.

2.3 *In vivo* studies

2.3.1 Anaesthetised rat model

2.3.1.1 Animals and ethics approval

8-week old male Sprague-Dawley (SD) rats were obtained from Monash Animal Services, Monash University. Rats were maintained in-house at the Monash Institute of Pharmaceutical Sciences animal house at 22˚C with a constant 12 hour light/12 hour dark cycle. Animals had free access to rat chow and water ad libitum. All experiments were conducted under approval from the Monash Institute of Pharmaceutical Sciences Animal Ethics Committee (ethics approval number: MIPS2014.11).

2.3.1.2 Measurement of heart rate and systolic blood pressure

Rats were anaesthetised with an intraperitoneal (IP) injection of sodium pentobarbital (0.1 mL/100 g rat body weight). The trachea was intubated before a catheter was inserted into the jugular vein for intravenous (IV) administration of compounds and saline. The carotid artery was also catheterised for the measurement of systolic blood pressure (SBP) and heart rate (HR) using a Gould Statham Physiological pressure transducer (Gould Instruments, Oxnard, CA, USA) connected to a Power Lab System (ADInstruments, Sydney, NSW, Australia). After surgery, rats were equilibrated for 20 mins to allow for stabilisation before compounds were administered. Between each bolus dose, the catheter was flushed with 150 µL of 0.9% NaCl. SBP and HR were allowed to return to baseline before administration of a subsequent dose. SBP and HR were continuously monitored and digitally processed using ChartPro version 5.0.2.1024 software (ADInstruments).

2.3.2 Acute rat myocardial infarction model

2.3.2.1 Animals and ethics approval

Outbred 8-week old male Sprague-Dawley rats were obtained from the Animal Resource Centre (Murdoch, WA, Australia). They were given free access to commercial standard rat chow (Norco Co-Operative Ltd., NSW, Australia) and tap water and housed in stable conditions at 22^{o}C with a 12 hour light/dark cycle during the entire study unless mentioned otherwise. All experiments adhered to the guidelines of the Animal Welfare and Ethics Committee of the St. Vincent's Hospital and National Health and Medical Research Council (NHMRC) of Australia. The animal ethics committee approval number was 034/12.

2.3.2.2 Myocardial infarction

Myocardial infarction (MI) was induced in Sprague-Dawley rats by temporary occlusion of the left anterior descending coronary artery (LAD). Animals were anaesthetised with 60 mg/kg sodium pentobarbitone intraperitoneally (IP), intubated and placed on a respirator with 100% O_2 supplementation. Body temperature was monitored and maintained at 37^{o}C with the use of a heat pad and lamp. To measure heart rate (HR) and mean arterial pressure (MAP), a 2-F_r miniaturized combined catheter-micromanometer (Model SPR-838 Millar instruments, TX, USA) was inserted into the right common carotid artery. All readings were recorded using LabChart 8 (ADIntruments). The jugular vein was catheterised for IV fluid and drug administration. A left thoracotomy was performed to gain access to the heart. The pericardium was removed and the LAD was identified. To occlude the LAD, a 6-0 prolene suture was passed under the vessel and a knot was made around a small piece

of polyethylene tubing and the vessel. Regional myocardial ischaemia was confirmed by epicardial cyanosis and hypokinesia. After 30 min of ischaemia, the suture was released to allow for 120 min of reperfusion.

2.3.2.3 Infarct size measurement

At the end of reperfusion, the ligature at the occlusion site was permanently tied off. Evans Blue (5%; 1 mL) was then infused intravenously to distinguish the non-ischaemic zone (stained blue) from the area at risk (unstained). Hearts were briefly excised and immediately sliced into 4-5 transverse sections. The sections were then incubated in 1% 2, 3, 5-triphenyltetrazolium chloride (TTC; Sigma-Aldrich, St. Louis, MO) for 15 minutes at 37ºC. After fixing overnight in 10% neutral buffered formalin, heart sections were photographed using a digital camera. Non-ischaemic, viable tissue was stained blue by Evans Blue; ischaemic but viable tissue was stained red by metabolised TTC; while necrotic tissue was white or pale as TTC remains white (unmetabolised). The area of infarction and risk zone was measured using ImageJ 1.46r software (National Institute of Health). Infarct size was expressed as a percentage of the area at risk.

2.3.3 Long-term rat myocardial infarction model

2.3.3.1 Animals and ethics approval

As described above (refer to 2.3.2.1).

2.3.3.2 Myocardial infarction

Myocardial infarction (MI) was induced in Sprague-Dawley rats by temporary occlusion of the left anterior descending coronary artery (LAD). Animals were

anaesthetised with 60 mg/kg sodium pentobarbitone intraperitoneally (IP), intubated and placed on a respirator with 100% O_2 supplementation. Body temperature was monitored and maintained at 37^{o}C with the use of a heat pad and lamp. The jugular vein was catheterised for IV fluid and drug administration. A left thoracotomy was performed to gain access to the heart. The pericardium was removed and the LAD was identified. To occlude the LAD, a 6-0 prolene suture was passed under the vessel and a knot was made around a small piece of polyethylene (PE) tubing and the vessel. Regional myocardial ischaemia was confirmed by epicardial cyanosis and hypokinesia. After 30 min of ischaemia, the suture was released to allow for reperfusion. The chest was then closed, and the muscle and skin closed in layers. Buprenorphine was administered (0.03 mg/kg sc) for post-operative pain. Sham animals were treated identically except that the prolene suture was not tied.

2.3.3.3 Preparation of osmotic minipumps

Each rat in the study was implanted with two osmotic minipumps (Bio-scientific Pty. Ltd., Sydney, NSW, Australia). Two minipumps were required in each rat to achieve suitable drug levels based on *in vitro* studies. To avoid compromising the viability of the right external jugular vein to be used for haemodynamic measurements (2.3.3.6), only one minipump was utilised for intravenous delivery (via the left external jugular vein) while the second minipump utilised subcutaneous delivery.

Subcutaneous delivery

Osmotic minipumps were purchased from Bio-scientific Pty. Ltd. (Sydney, NSW, Australia). Vehicle or drug solution was drawn up into a syringe with a filling tube (supplied with pumps). The filling tube was then inserted through the opening at the top of the pump. Held in an upright position, the pump was then slowly filled with solution

to avoid introduction of air bubbles. The syringe and the filling tube were then removed and a flow moderator was inserted fully into the body of the pump.

Intravenous delivery

The pump was filled as above. The translucent cap at the end of the flow moderator was then removed, revealing a short steel tube protruding from the white flange. A rat jugular catheter (Bio-scientific Pty. Ltd., Sydney, NSW, Australia) was then filled with solution using the filling tube and syringe. With the syringe still attached at the distal end, the tubing of the catheter was then attached to the flow moderator. The syringe was then carefully removed.

Priming

The prefilled pumps with or without catheters were placed in 0.9% saline at 37^{o} C overnight prior to implantation.

Implantation of osmotic minipumps

Pumps were prepared one day prior to implantation as described above. Minipumps were implanted 1 week after induction of MI. Rats were anaesthetised with Alfaxan 1.5 mL/kg via tail vein injection, intubated and maintained anaesthetised with 2% isoflurane. Briefly, the jugular vein was catheterised with polyethylene (PE) tubing and a loading dose of drug or vehicle was administered with a syringe just before implantation of the minipump. The PE tubing was then removed and the catheter of the minipump was inserted through the same entry in the jugular vein. The catheter was secured in place with silk suture. Using a haemostat, a pocket was made under the skin in the back. The first minipump (with jugular catheter) was carefully inserted into the pocket followed by the second minipump (subcutaneous drug delivery). Immediately

post-surgery, animals were administered buprenorphine (0.03 mg/kg sc) for post-operative pain.

2.3.3.4 Blood pressure

Systolic blood pressure was measured in conscious rats using an occlusive tail-cuff plethysmography attached to a pneumatic pulse transducer (PowerLab, ADInstruments, Australia). The readings were recorded using the software Chart 5 (PowerLab, ADInstruments, Australia). For each animal, blood pressure readings were taken until 5 readings were obtained within a range of 5 mmHg and averaged.

2.3.3.5 Echocardiography

Echocardiography was performed in lightly anaesthetised animals (ketamine 3.75 mg/100g and xylazine 0.5 mg/100g, i.p.) using a Vivid 7 (GE Vingmed, Horten, Norway) echocardiography machine with a 10 MHz phased array probe. Parasternal short-axis views of the heart at the mid-papillary level were used to obtain measures of posterior wall thickness in diastole (LVPWd), and left ventricular internal dimension in diastole (LVIDd) and systole (LVIDs). Fractional shortening (FS) was calculated according to standard formula: FS (%) = [(LVIDd – LVIDs)/LVIDd] x 100. Parasternal long-axis views of the heart were used to obtain measures of left ventricular end diastolic and systolic volume (LVEDV and LVESV, respectively). Ejection fraction (EF) was calculated according to the standard formula: EF (%) = [(LVEDV – LVESV)/LVEDV] x 100.

Doppler images were obtained from the apical 4-chamber views of the heart. Early and late transmitral peak diastolic flow velocity (E and A waves) and mitral valve inflow E wave deceleration time (DT), isovolumic relaxation time (IVRT) were measured.

Diastolic filling was evaluated by determining the E/A ratio from the peak velocity of E and A mitral flow and DT. Tissue Doppler imaging was also performed to assess peak early and late (E′ and A′) diastolic tissue velocity at the septal side of the mitral annulus. All parameters were assessed using an average of three consecutive cardiac cycles and calculations were made in accordance with the American Society of Echocardiography guidelines (215).

2.3.3.6 Cardiac catheterisation

Cardiac catheterization was performed at the end of the study as previously published (216). Briefly, animals under anaesthesia with pentobarbitone (Lethabarb) (60 mg/kg, i.p.) were placed on a warming pad (37 °C) and ventilated. A 2-F_r miniaturized combined catheter-micromanometer (Model SPR-838 Millar instruments, TX, USA) was inserted into the right common carotid artery to obtain aortic blood pressure and then advanced into the left ventricle (LV) to obtain LV pressure-volume loops when stable. The loops were recorded at steady state and during transient preload reduction, achieved by occlusion of the inferior vena cava and portal vein with the ventilator turned off and the animal apnoeic. Parallel conductance values of the heart muscle was obtained by the injection of approximately 100 µL of 10% NaCl into the right atrium. Calibration from Relative Volume Units (RVU) conductance signal to absolute volumes (in µL) was undertaken using a previously validated method of comparison to known volumes in Perspex wells. The following validated parameters were assessed using LabChart 8 (ADInstruments): stroke volume (SV), the slope of the end systolic pressure-volume relationship (ESPVR), the slope of the end diastolic pressure-volume relationship (EDPVR), heart rate (HR), Tau (τ Logistic), and the slope of the preload recruitable stroke work relationship (PRSW).

2.3.3.7 Metabolic caging

Prior to metabolic caging, 0.5 mL blood was collected from the tail vein, centrifuged at 3200 rpm for 10 min. Blood plasma (100 μL) was collected for plasma creatinine analysis. Rats were then individually housed in metabolic cages for 24 hr, where they were given free access to tap water and standard laboratory chow (219). Rats in the perindopril treatment group were given perindopril in drinking water. Food and water intake, and urine volume was recorded. An aliquot of urine (1 ml) was collected from the 24-hour urine sample and stored at -20°C for subsequent analysis of urinary creatinine and protein (220). Urine creatinine, plasma creatinine and urine protein was measured by autoanalyzer (Roche Instruments Inc., CA, USA). Creatinine clearance and 24 hr urine protein were calculated using the following formula (221):

24 hr Urine protein (mg/day) = Urine protein (g/L) x 24 hr urine volume (ml)

$$\text{Creatinine clearance (ml/min)} = \frac{\text{Urine creatinine (μmol/day)}}{\text{Plasma creatinine (μmol/L)}} \times 1000 \times \frac{1}{24 \times 60}$$

Glomerular filtration rate (GFR; ml/min/kg) was calculated as creatinine clearance (ml/min) over weight (kg).

2.3.3.8 Tissue collection

At the completion of obtaining pressure-volume loops, blood was withdrawn from the abdominal aorta for determination of conductance measures. The heart and lungs were then removed and weighed. The atria and right ventricle was dissected from the LV and all tissues weighed. The LV was cross sectioned into 3 portions. The base of the LV was embedded in Tissue-Tek® O.C.T compound. The middle portion was fixed in 10% neutral-buffered formalin (NBF). The apex was separated into infarct and non-infarct

tissue in MI-induced animals and cut into smaller pieces before being snap-frozen in liquid nitrogen for molecular biology.

2.3.3.9 Histopathology

Formalin-fixed heart tissues were placed in histo-cassettes and processed overnight (Department of Pathology, St. Vincent's Hospital, Melbourne, Australia). Tissues were embedded in paraffin moulds and 4 µm sections were cut using a rotary microtome (Leica Biosystems). Tissue sections were floated in a 42 ˚C water bath and collected on silanated glass microscope slides. Prior to staining, sections were dewaxed in 2 changes (2x) of histolene for 5 min each time and hydrated through graded ethanols: 100% ethanol 2x 3 min each time, 70% ethanol 1x 3 min. Sections were then rehydrated in dH_2O for 5 min.

Interstitial fibrosis

LV tissue sections were incubated in picrosirius red (Merck, Vic, Australia) reagent for 1 hr. Slides were then washed briefly in 2 changes of acidified water (1% acetic acid). Sections were dehydrated through graded ethanol (2x 70%, 2x 100%) for 2 min each and histolene (2x 5 min) before being mounted with DPX (BDH laboratory supplies, Poole, UK). Tissue sections stained with picrosirius red were analysed for interstitial fibrosis using Aperio ScanScope Console v.8.0.0.1058 (Aperio Technologies, Inc) at x20 magnification. Interstitial fibrosis in the remote zone (Fig. 2.1), excluding perivascular fibrosis, was selected for its intensity of red staining, and the percentage area was calculated using a pre-set algorithm. The intensity and algorithm was maintained constant for the analysis of all sections.

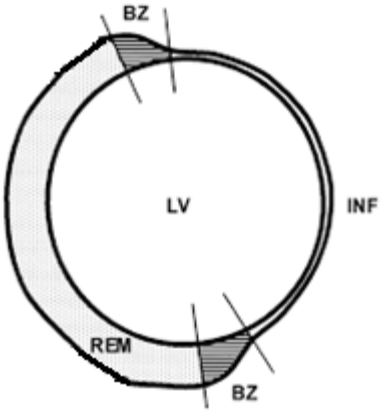

Figure 2.1 Heart section illustrating left ventricle (LV), infarct zone (INF), border zone (BZ), and remote zone (REM). Image adapted from Loennechen et al. (222).

Infarct size measurement

Infarct size was assessed morphologically and slides were digitally scanned using Aperio ScanScope Console v.8.0.0.1058 for infarct size analysis. Infarct size was expressed as an averaged percentage of the endocardial and epicardial scarred circumferences of the LV.

Haematoxylin and eosin staining

LV tissue sections were stained with haematoxylin and eosin to assess the morphology of cardiomyocytes. After dewaxing and rehydration, sections were incubated in Mayer's haematoxylin (Amber Scientific, WA, Australia) for 4 mins and dipped in tap water to remove excess staining. Sections were then dipped in Scott's tap water for 1 min and then briefly in tap water. Slides were then incubated in eosin (BASF Australia Ltd., Auckland, New Zealand) for 3 min to give the cytoplasm shades of pink. Sections were then dehydrated in 100% ethanol 3x 3 min each time and then in histolene 2x 5 min each time before coverslipped using DPX.

Sections were scanned and analysed for each animal using Aperio ScanScope Console v.8.0.0.1058. Myocytes in the same plane, as assessed by selecting cells with similar sized nuclei in the remote zone were outlined and the average myocyte cross-sectional area calculated from 25 myocytes per LV.

2.3.3.10 Immunohistochemistry

Sections were dewaxed as previously described in 2.3.3.9. Antigen retrieval was performed to unmask cross linked antigens. Sections were placed in pre-heated 0.01 M citrate buffer and boiled in a microwave oven for 10 min before being washed with PBS 3x 5 min each time. Sections were then circled with a Dako pen to create a barrier to liquids before incubated in 3% H_2O_2 (Sigma Aldrich, USA) for 15 min to quench endogenous peroxidase activity. Slides were washed with PBS 3x 5 min each time.

Collagen I staining

Sections were incubated with Dako Protein Block, Serum Free (Dako, CA, USA) for 30 min at room temperature. Sections were then incubated with goat anti-collagen I (Southern Biotechnology Associates, Inc. Birmingham, AL, USA) primary antibody (1:100 dilution) overnight at 4˚C. On the following day, slides were washed with PBS 3x 5 min each time and incubated with HRP-rabbit anti-goat secondary antibody for 1 hr, followed by PBS wash (3x 5 min each time). Localisation of the peroxidase conjugates was achieved using 3,3'-diaminobenzidine tetrahydrochloride (DAB, Dako, CA, USA) as a chromagen. DAB was applied to all sections until the target stained brown under microscope according to the manufacturer's instruction (around 1 min). Slides were washed thoroughly with running tap water for 10 min. Sections were then dipped in haematoxylin for 4 min and rinsed in tap water to remove excess staining.

After that, slides were dipped in Scott's tap water for 1 min and rinsed in tap water. Sections were then dehydrated, cleared and mounted as in 2.3.3.9.

Sections were scanned and analysed for collagen I content using Aperio ScanScope Console v.8.0.0.1058 at x20 magnification. Collagen I content in the remote zone, excluding perivascular fibrosis, was selected for its intensity of brown staining, and the percentage area was calculated using a pre-set algorithm

Macrophage infiltration (CD68 staining)

Sections were incubated with normal goat serum (1:5 dilution) for 30 min at room temperature. Sections were then incubated with mouse monoclonal CD68 (Serotec, Raleigh NC, USA) primary antibody (1:300 dilution) overnight at 4˚C. On the following day, slides were washed with PBS 3x 5 min each time and incubated with Dakocytomation Envision+ system labelled polymer (HRP-linked) anti-mouse (Dako, CA, USA) secondary antibody for 30 min, followed by PBS wash (3x 5 min each time). Localisation of the peroxidase conjugates was achieved using 3,3'-diaminobenzidine tetrahydrochloride (DAB, Dako, CA, USA) as a chromagen. DAB was applied to all sections until the target stained brown under microscope according to the manufacturer's instruction (around 40 s). Slides were washed thoroughly with running tap water for 10 min. Sections were then dipped in haematoxylin for 4 min and rinsed in tap water to remove excess staining. After that, slides were dipped in Scott's tap water for 1 min and rinsed in tap water. Sections were then dehydrated, cleared and mounted as described in 2.3.3.9.

Sections were scanned and analysed for each animal using Aperio ScanScope Console v.8.0.0.1058. The total number of macrophages (CD68 immunoreactive cells) in the infarct zone of the LV was individually counted for each animal.

2.3.3.11 Quantitative mRNA expression

Total RNA was extracted from frozen tissues using Ambion RNAqueous kit (Ambion, TX, USA) according to manufacturer's instruction. RNA (20 ng/µL for genes of interest and 2 ng/µL for housekeeping gene) was reverse transcribed to cDNA with Multiscribe (Table 2.5). Reverse transcription was performed in a thermocycler. Triplicate cDNA aliquots were amplified using sequence-specific primers (Geneworks, SA, Australia) (Table 2.6) with SYBR Green detection (Applied Biosystems).

Reagent	**Volume (µL)/reaction**
PCR Buffer II (10x)	4
$MgCl_2$	8
dNTPs	16
Random Hexamers	2
Nuclease free water	2
RNAse inhibitor	2
Multiscribe	2
RNA	4
Total	**40**

Table 2.5 Composition of reverse transcription mixture for cDNA synthesis

Gene	Primer sequence
TGF-β1	Forward: 5’ CCAGCCGCGGGACTCT 3’
	Reverse: 5’ TTCCGTTTCACCAGCTCCAT 3’
CTGF	Forward: 5’ GCGGCGAGTCCTTCCAA 3’
	Reverse: 5’ CCACGGCCCCATCCA 3’
Collagen I	Forward: 5’ TGCCGATGTCGCTATCCA 3’
	Reverse: 5’ TCTTGCAGTGATAGGTGATGTTCTG 3’
TIMP2	Forward: 5’ CTCGGCAGTGTGTGGGGTC3’
	Reverse: 5’ CGAGAAACTCCTGCTTGGGG 3’
ANP	Forward: 5’ ATCTGATGGATTTCAAGAACC 3’
	Reverse: 5’ CTCTGAGACGGGTTGACTTC 3’
β-MHC	Forward: 5’ TTGGCACGGACTGCGTCATC 3’
	Reverse: 5’ GAGCCTCCAGAGTTTGCTGAAGGA 3’
GAPDH	Forward:5’ GACATGCCGCCTGGAGAAAC 3’
	Reverse: 5’ AGCCCAGGATGCCCTTTAGT 3’

Table 2.6 Primer sequences used in RT-PCR.

Composition of the Real-Time Polymerase Chain Reaction (RT-PCR) reaction mixture is shown in Table 2.7. Following the addition of the reaction mixture into PCR plates, the plates were covered with optical adhesive film (Applied Biosystems, CA, USA) and spun in a centrifuge at 3000 rpm for 5 min to remove air bubbles. RT-PCR was performed with QuantStudio 12K Flex Real-Time PCR System (Life Technologies) to quantify mRNA expression of TGF-β1, CTGF, collagen I, TIMP2, ANP and β-MHC. Quantitation was standardized to the housekeeping gene GAPDH.

Reagent	Volume (µl)
SYBR Green master mix	5
Forward Primer	0.5
Reverse Primer	0.5
Nuclease free water	3
cDNA	1
Total	**10**

Table 2.7 Composition of RT-PCR reaction mixture in each well.

2.3.3.12 Protein extraction

Frozen tissue was homogenised with 1 mL of tissue lysis buffer using a polytron homogeniser. After centrifugation for 15 min at 4˚C, the supernatant was collected for subsequent Bradford assay and Western blot analysis.

2.3.3.13 Bradford assay

Protein concentrations were measured by Bradford assay. Protein samples were diluted 1:5 with dH_2O. A bovine serum albumin (BSA) standard curve with a concentration range from 0.0125 to 0.8 µg/mL was generated from serial 1:2 dilutions using a 4 µg/mL BSA stock solution. Protein samples and BSA standards (5 µL each) were added in triplicate to 96-well plates. Diluted (1:5) Bradford reagent (200 µL; Bio-Rad, CA, USA) was added to each well. The plates were shaken and the absorbance was measured using a microplate reader (SPECTROstar Nano, BMG Labtech, Ortenberg, Germany) at a wavelength of 595 nm. Protein concentrations of the samples were calculated from the standard curve.

2.3.3.14 Western blot analysis

Western blot analysis was performed as per manufacturer's protocol. Lysed tissue protein was separated using sodium dodecyl sulphate polyacrylamide gel electrophoresis (SDS-PAGE) on the basis of molecular weight. After that, the protein was transferred onto nitrocellulose membranes to visualise specific proteins in complex antigenic mixtures.

Reagents and solutions

Tissue lysis buffer

Composition: Tris-HCl 20 mM, NaCl 250 mM, EDTA 2 mM, EGTA 2 mM, Glycerol 10%, β-glycerophosphate 40 mM, NP40 0.5% or 0.5% Triton X-100, Leupeptin 10 µg/µl, Aprotinin 10 µg/µl, Pepstatin 1µM, Phenylmethylsulfonylfluoride 1 mM, DTT 1 mM, Phosphatase inhibitor cocktail-1 1 µl/ml, Phosphatase inhibitor cocktail-2 1 µl/ml, NaF 0.5 mM, Sodium Pyrophosphate 2.5 mM. The lysis buffer was made fresh with Milli-Q water.

2x Sample buffer

Composition: Tris-HCl (pH 6.8) 125 mM, sodium dodecyl sulfate (SDS) 4% w/v, Glycerol 20% v/v, β-mercaptoethanol 10% v/v, Bromophenol blue 0.02 mg/ml. Store at -20°C.

5x Running buffer

Composition: Tris base 0.124 M, glycine 0.96 M, SDS 0.5% w/v.

Make with distilled water (dH_20), adjust to pH 8.3 and store at 4°C.

Dilute 1:5 with Milli-Q water when required.

Transfer buffer

Composition: Tris base 0.025 M, glycine 0.192 M, CH_3OH 20% v/v.

Make fresh with dH_2O.

10x Tris buffered saline (TBS)

Composition: Tris base 0.2 M, NaCl 1.37 M.

Adjust to pH 7.6 with concentrated HCl. Store at 4°C.

Tris buffered saline - Tween 20 (TBST)

Composition: 10xTBS 100 ml, dH_20 900 ml, Tween 20 1 ml.

Make fresh when required.

5% blotto in TBST

5 g skim milk powder in 100 ml TBST. Make fresh when required.

5% BSA in TBST

5 g BSA powder in 100 ml TBST. Make fresh when required.

Preparation

Sample buffer was added to equal amounts of protein (30 µg) at 1:1 (v/v) ratio. Mixtures were boiled at 100°C for 5 min.

The gel apparatus was assembled using a glass plate sandwich in a gel casting stand. A 10% separating gel (recipe in Table 2.8) was prepared and the gel mix was cast between the sandwich using a pipette followed by an overlay of 1 ml of water saturated

n-butanol to form a layer. The gel was allowed to set (~ 45 min) prior to removing the n-butanol.

Reagent	10%
dH_2O	4.05 ml
1.5M Tris-HCl pH 8.8	2.50 ml
30% Acrylamide/bis	3.30 ml
10% SDS	100 µl
10% APS	50 µl
TEMED	5 µl
Total	**10 ml**

Table 2.8 Separating gel recipe (1.5 mm gel). SDS, sodium dodecyl sulfate; APS, ammonium persulfate; TEMED, tetramethylethylenediamine.

A 4% stacking gel (recipe in Table 2.9) was prepared and poured on top of the set separating gel until the gel reached the top of the glass plate. A comb was inserted to create wells and the gel was allowed to set (~30 min). After gel set, the comb was removed from stacking gel.

Reagent	**4%**
dH_2O	6.40 ml
0.5M Tris-HCl pH 6.8	2.50 ml
30% Acrylamide/bis	1.00 ml
10% SDS	100 µl
10% APS	200 µl
TEMED	20 µl
Total	**~10 ml**

Table 2.9 Stacking gel recipe (1.5 mm gel). SDS, sodium dodecyl sulfate; APS, ammonium persulfate; TEMED, tetramethylethylenediamine.

SDS-PAGE

The gel was placed into clamping frame and electrode assembly. The inner chamber was placed into a mini tank, and running buffer was then added into the inner chamber (between gels) up to the top of the glass plate and outer chamber ~ 4 cm high. After loading prepared protein samples and molecular weight marker (BenchMark™ Pre-Stained Protein Ladder, 10 µl, Invitrogen) into wells in the gel, voltage of 120V was applied along the gel until dye front reaches the bottom of the gel (~ 2 hours).

Transfer

Nitrocellulose membrane (Amersham Biosciences), filter paper and fibre pad were soaked in transfer buffer for at least 1 hr. Transfer sandwich was set up as laying a fibre pad, 3x filter paper, nitrocellulose membrane, gel, 3x filter paper and a fibre pad in order. The transfer sandwich was clamped in a cassette and placed into an electrode

module (the black side of the cassette facing the black side of the electrode module). The module was then placed into a tank containing transfer buffer. The separated protein samples were electrophoretically transferred to the membrane under a voltage of 100V for ~ 2 hr at 4°C. After transferring, the membrane was taken out, stained with Ponceau solution for 2-3 min to locate the protein bands, and washed with dH_2O.

Immunoblotting

The membrane was incubated with 5% BSA/blotto in TBST for 1 hr at room temperature. Diluted primary antibody (10 ml) was added onto the membrane and incubated overnight at 4˚C (Table 2.10). The membrane was washed with TBST for 3x 5 min before adding secondary antibody diluted in 5% BSA/blotto in TBST (10 ml). The membrane was then incubated for 1 hr at room temperature before washing with TBST for 5x 5 min. Specific bands were visualized by enhanced chemiluminescence reagents (Thermo Scientific), (223) (223) and then the intensity was analysed using Image Lab version 5.2.1 (Bio-Rad Laboratories).

Primary antibody	Isotype	Dilution	Secondary antibody	Dilution
Phospho-NFκB #3033 (Cell Signalling Technology)	Rabbit monoclonal IgG	1:1000 in 5% BSA in TBST	Anti-rabbit IgG, HRP-linked #7074	1:2000
MMP2 #4022 (Cell Signalling Technology)	Rabbit polyclonal Ab	1:1000 in 5% blotto in TBST	Anti-rabbit IgG, HRP-linked #7074	1:2000
TIMP2 #4022 (Cell Signalling Technology	Rabbit monoclonal IgG	1:1000 in 5% blotto in TBST	Anti-rabbit IgG, HRP-linked #7074	1:2000
Pan-actin #8456 (Cell Signaling Technology)	Rabbit monoclonal IgG	1:2000 in 5% blotto in TBST	Anti-rabbit IgG, HRP-linked #7074	1:4000

Table 2.10 Antibodies for Western blot analysis

2.3.4 Materials

N^6-Cyclopentyladenosine (CPA; A_1AR-selective agonist), 5'-N-ethylcarboxamidoadenosine, (NECA; non-selective AR agonist) and 8-cyclopentyl-1,3-dipropylxanthine (DPCPX; A_1AR-selective antagonist) were purchased from Sigma-Aldrich, Castle Hills, NSW. Capadenoson was purchased from MedChemExpress (Shanghai, China). Perindopril (Coversyl; Servier Australia, Hawthorn, Melbourne, VIC, Australia) 10 mg tablets were obtained from St. Vincent's Hospital Pharmacy. The A_1/A_{2B}AR agonist VCP746 was synthesised at the Monash Institute of Pharmaceutical Sciences. Stock solutions were prepared in DMSO and kept at -20˚C until used.

2.3.5 Statistical analysis

Data expressed as means ± SEM. Significance was determined by a one-way ANOVA or two-way ANOVA (only for HR and MAP data from the acute rat myocardial infarction study) followed by Dunnet's post-hoc test. All statistical analyses were performed using GraphPad Prism 6. A two-sided P-value of less than 0.05 was considered statistically significant.

Chapter 3 Effect of VCP746 on blood pressure and heart rate in an anaesthetised rat model

3.1 Introduction

Adenosine receptors are known to exert haemodynamic effects on the cardiovascular system. The activation of the A_1AR suppresses sinoatrial (SA) and atrioventricular (AV) nodal activity, resulting in a reduction of heart rate (140, 224). This is achieved through several possible mechanisms including the activation of G protein-coupled inwardly rectifying potassium (GIRK) channels, the suppression of the hyperpolarisation-activated cyclic nucleotide-gated "funny" current (I_f) and the inhibition of the inward calcium current (I_{Ca}) (139). The hypotensive effect of adenosine is largely attributed to the activation of the A_{2A}AR (225). However, evidence suggests that not only the A_{2A}AR but also the A_{2B}AR play a role in vasodilation, mainly acting through ATP-dependent K^+ channels and nitric oxide dependent mechanisms (226-228). On the other hand, the A_1AR have previously been observed to oppose the vasodilatory effect of A_{2A}AR by inhibiting increased cAMP production (154).

VCP746 was previously reported to be a biased A_1AR agonist with no effect on heart rate (205). In the study, VCP746 (comprising adenosine linked to a positive allosteric modulator, VCP171), a rationally-designed molecule, engenders biased signalling at the A_1AR. VCP746 was observed to be cytoprotective in cells subjected to simulated ischaemia but does not affect rat atrial beat rate, unlike the prototypical A_1AR agonist CPA which was cytoprotective but produced significant bradycardic effects. The findings suggest that VCP746 could possibly confer cardioprotection while producing minimal, if any, effect on heart rate, effectively separating on-target efficacy from on-target side effects (205). With this in mind, we first sought to determine if VCP746

produces any adverse effects in the form of heart rate and/or blood pressure reduction in a more physiologically-relevant, anaesthetised rat model.

3.2 Aim

To evaluate heart rate and blood pressure effects of VCP746 in an anaesthetised rat model.

3.3 Study design and methods

Male Sprague-Dawley rats were administered bolus doses of vehicle, CPA (0.3 μg/kg → 30 μg/kg), and VCP746 (3 μg/kg → 1000 μg/kg) intravenously. Surgery and functional measurements were performed using protocols detailed in Chapter 2.3.1.2. Baseline measurements of systolic blood pressure (SBP) and heart rate (HR) were obtained after stabilisation. Maximal reduction in HR and SBP was measured after each bolus dose. Heart rate and systolic blood pressure data were expressed as a 'reduction from baseline' against dose.

3.4 Results

3.4.1 Effects of VCP746 on heart rate and systolic blood pressure

Baseline HR and SBP of the rats were determined to be 430.0 ± 11.2 BPM and 142.2 ± 6.9 mmHg, respectively. To evaluate the effects of the novel adenosine receptor agonists on heart rate (HR) and systolic blood pressure (SBP), bolus doses of CPA (0.3

μg/kg → 30 μg/kg) and VCP746 (3 μg/kg → 1000 μg/kg) were administered intravenously in anaesthetised rats (Fig. 3.1a, c). Due to the limited solubility of VCP746, increasing concentrations of DMSO in the vehicle were required to prevent compound precipitation at the higher doses. Vehicle effect on HR and BP was found to be present at the 300 (55% DMSO) and 1000 μg/kg (70% DMSO) doses of VCP746 but not at 100 μg/kg (7% DMSO) (Fig. 3.1a, c). At 30 μg/kg (maximum CPA dose), CPA significantly reduced HR by 325.3 ± 64.4 BPM while VCP746 had no significant effect, producing a HR reduction of 6.3 ± 6.7 BPM (Fig 3.1b). CPA also significantly reduced SBP by 103.0 ± 11.1 mmHg while VCP746 did not significantly reduce SBP (SBP reduction of 3.8 ± 1.6 mmHg) at 30 μg/kg (Fig. 3.1d). The reduction of SBP following CPA treatment is likely due to the reduction in cardiac output caused by reduction in HR rather than vasodilation. The HR and SBP reduction produced by VCP746 was found to be no different to that produced by vehicle at all doses (Fig. 3.1). When reduction of HR and SBP were measured again 2 min post-infusion (minimum time needed for vehicle-mediated changes to return to baseline), we observed that VCP746 and vehicle no longer had any effect on HR or SBP at any dose (Fig. 3.1e, f). In contrast, CPA-mediated reduction in HR and SBP was found to remain significant 2 min post-infusion.

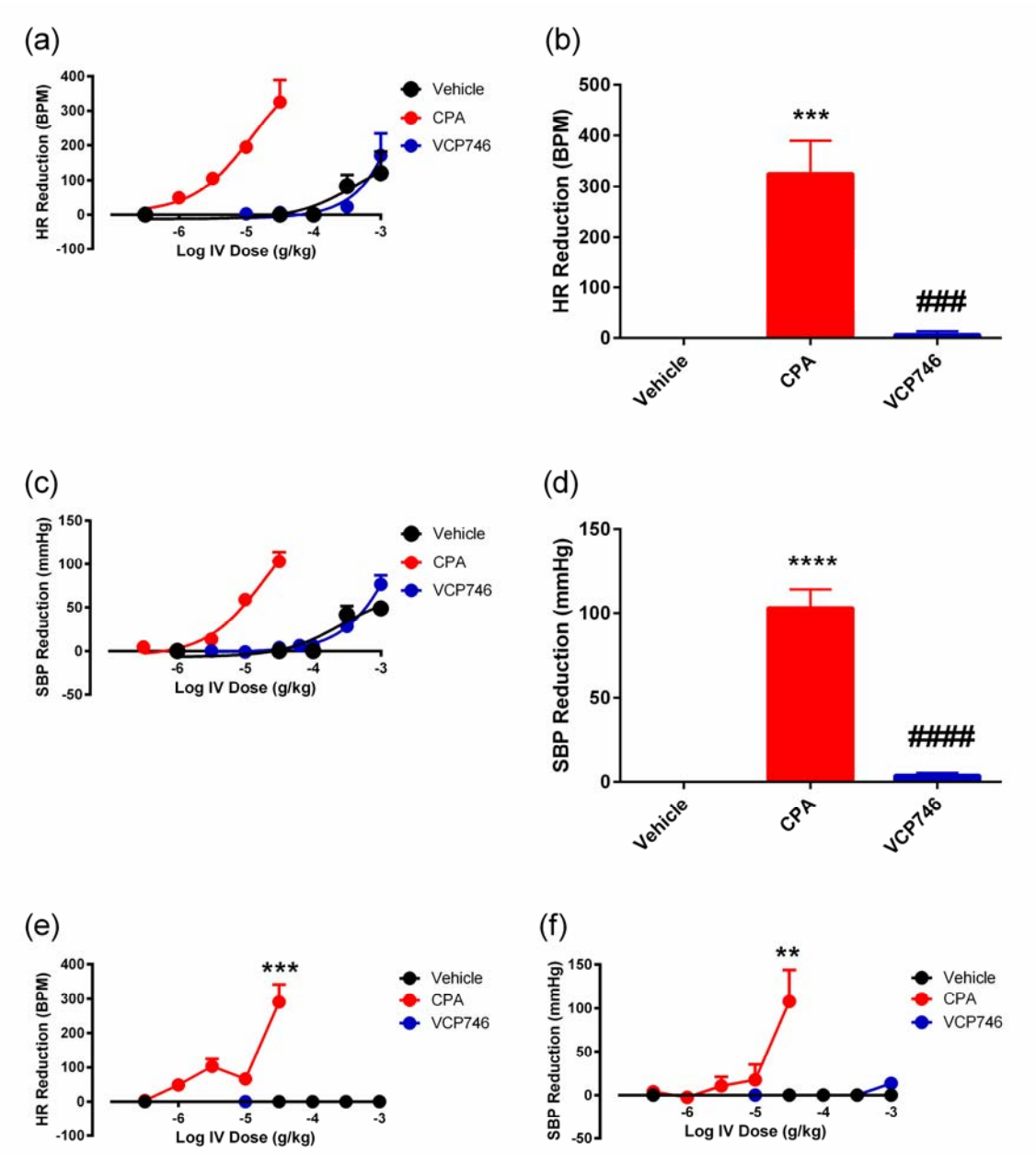

Figure 3.1 Heart rate (HR) and systolic blood pressure (SBP) were determined from pressure signals from the carotid artery using a physiological transducer while ligands were administered intravenously into the jugular vein. Dose-response curves of CPA, VCP746 and vehicle on (a) HR and (c) SBP reduction. At 30 µg/kg, the maximum CPA dose tested, CPA produced a significant (b) HR and (d) BP reduction compared to vehicle, while VCP746 had no significant effect. (e) HR and (f) SBP reduction was measured again 2 min post-infusion, which is the minimum time needed for vehicle-mediated changes to return to baseline. VCP746 and vehicle no longer had any effect on HR and SBP while the effect of CPA remains significant. Data are the mean ± S.E.M. expressed as reduction in HR measured in beats per minute (BPM) and reduction in BP in millimetres of mercury (mmHg), n = 3 – 5. **P<0.01, ***P<0.001 and ****P<0.0001 vs. vehicle. $^{###}$P<0.001 and $^{####}$P<0.0001 vs. CPA.

3.5 Discussion

VCP746 was investigated for haemodynamic effects in an anaesthetised rat model and compared to the prototypical A_1AR agonist, CPA. At the 300 and 1000 μg/kg doses, VCP746 displayed an apparent effect on SBP and HR. However, this effect was no different to that observed in the vehicle control group, suggesting a 'vehicle effect' rather than an on-target effect by VCP746. While this does not explicitly prove that VCP746 alone has no effect on HR and SBP at 300 and 1000 μg/kg, the evidence strongly suggests so, as an additive effect on HR/SBP reduction (on top of the vehicle curve) would be observed following VCP746 treatment otherwise. Up to the 100 μg/kg dose, a dose greater than what confers maximal cardioprotection in rats (refer to Chapter 4), VCP746 produced negligible haemodynamic effects. On the other hand, CPA reduced HR and SBP from doses as low as 1 μg/kg and 3 μg/kg, respectively, while at 30 μg/kg, HR and SBP was reduced by 325.3 ± 64.4 BPM and 103.0 ± 11.1 mmHg, respectively (Fig. 3.1). The effects of CPA and VCP746 were compared at 30 μg/kg (Fig. 3.1b, d) as this was the maximum CPA dose tolerable by rats in the study; at this dose VCP746 is also known to produce a near-maximal infarct-sparing effect in rats (refer to Chapter 4). When HR and SBP were measured again at 2 min post-infusion, the effect of CPA was found to remain persistent and significant while VCP746 and vehicle no longer had any effect (Fig. 3.1e, f). This data again suggests that the HR and SBP lowering effect of VCP746 seen in Fig. 3.1a, c was due to vehicle as there was no difference between VCP746 and vehicle-mediated effects 2 min post-infusion while the effect of CPA remained.

A large body of evidence supports that A_1AR-activation typically reduces heart rate and this likely explains the bradycardic effect of the prototypical A_1AR-selective

agonist, CPA (140, 143, 229). As such, the reduction in SBP by CPA is most likely the result of reduced cardiac output subsequent to A_1AR-mediated decrease in heart rate, and not vasodilation, which is typically an A_{2A}AR-mediated effect. While VCP746 was previously shown to be a potent A_1AR agonist (205), VCP746 failed to display any effect on HR in this study. We hypothesise that VCP746, an A_1AR agonist known to display biased agonism, stabilises a unique receptor conformation that is biased away from signalling pathways that promote heart rate reduction.

One limitation to this study is the assessment of heart rate and blood pressure in only anaesthetised animals but not conscious animals. Indeed, the use of telemetry would provide valuable insight into changes in heart rate and blood pressure in conscious animals in response to not only acute but also chronic VCP746 administration (230). The use of sodium pentobarbital in this study was based on the prospect that future studies on the potential cardioprotective effect of VCP746 would be carried out (chapter 4). Sodium pentobarbital was chosen based on its inherent lack of cardioprotective effects and widely-accepted use in ischaemia/reperfusion (IR) models (45, 125). In contrast, while inhaled anaesthetic agents such as isoflurane are safer and more convenient to use, they are known to be cardioprotective (231). The use of inhaled anaesthetics was therefore avoided as they could influence results in experiments investigating cardioprotection.

Overall, this study has found that VCP746 – which was designed to engender biased signalling in the A_1AR (205) – has no significant effect on HR and SBP, suggesting that VCP746 does not activate signalling pathways that promote the reduction of heart rate and blood pressure, unlike prototypical A_1AR agonists such as CPA. These findings support the notion that ligands can be designed to be biased away from signalling pathways that promote side effects, thus opening an avenue for developing

therapeutics with an improved side effect profile. Further studies to determine the biased profile responsible for the lack of heart rate reduction of VCP746 are of great interest.

Chapter 4 VCP746-mediated cardioprotection in models of ischaemia and reperfusion injury (Langendorff-perfused isolated rat heart and acute rat myocardial infarction models)

4.1 Introduction

It is well-accepted that adenosine receptors (AR) are involved in conferring cardioprotection in ischaemic hearts. Of the four AR subtypes, the A_1AR is the most extensively studied and was the first to be associated with cardioprotection. Numerous studies, both *in vitro* and *in vivo*, have highlighted the key role played by the activation A_1AR in conferring cardioprotection (refer to Chapter 1.4.1). The mechanisms underlying A_1AR-mediated cardioprotection are yet to be fully uncovered although signalling pathways such as the MEK1/2-ERK1/2 (44) and the mitoK_{ATP} (232) pathways are heavily implicated.

A substantial body of research has also demonstrated that synergistic cardioprotection resulting from the activation of both the A_1 and A_2AR also exists. Lasley and colleagues (125) were the first to show in *in vivo* rat myocardium that blockade of the A_2ARs with an A_{2A}/A_{2B}AR antagonist, ZM241385, abolished A_1AR agonist-mediated infarct size reduction to the same extent as an A_1AR antagonist, DPCPX. This finding suggested that occupation and activation of the A_{2A} and/or A_{2B}AR, for instance by endogenous adenosine, is necessary for A_1AR-mediated cardioprotection.

VCP746 was previously shown to be cytoprotective in rat cardiac myoblasts and cardiac myocytes subjected to simulated ischaemia (205). In this chapter, we sought to investigate the cardioprotective effects of VCP746 in more physiologically-relevant systems, firstly in the isolated rat heart and secondly in an *in vivo* rat myocardial infarction model. Furthermore, the effect of VCP746 on heart rate and blood pressure will also be examined in these models to determine if VCP746 could indeed confer cardioprotection without significant haemodynamic effects.

4.2 Aims

To investigate the cardioprotective effect of VCP746 in a Langendorff-perfused isolated rat heart and a rat myocardial infarction model. To determine if VCP746 reduces heart rate and blood pressure at concentrations that are cardioprotective.

4.3 Study design and methods

Langendorff-perfused isolated rat heart model

Male Sprague-Dawley rats were randomised into the following groups: Control (DMSO 0.1%), CPA (100 nM), VCP746 (1 μM), VCP746 (10 nM), VCP746 (1 μM) + SLV320 (100 nM) and VCP746 (1 μM) + PSB603 (100 nM). Surgical procedures and functional measurements were performed using protocols as per Chapter 2.2.2. All hearts were subjected to 30 minutes of global ischaemia followed by 60 minutes of reperfusion. Agonists were infused for 15 minutes at the onset of reperfusion. Where antagonists were used, they were infused 5 minutes prior to agonist infusion. After the experiment, infarct size was measured as detailed in Chapter 2.2.3.

Acute rat myocardial infarction model

Male Sprague-Dawley rats were randomised into the following groups: vehicle control 1 (10% DMSO in saline), DPCPX (100 μg/kg), VCP746 (80.8 μg/kg), NECA (10 μg/kg), VCP746 (80.8 μg/kg) + DPCPX (100 μg/kg), vehicle control 2 (50% DMSO in saline) and Capadenoson (100 μg/kg). Surgical procedures were performed using protocols as per Chapter 2.3.2.2. To measure heart rate (HR) and mean arterial pressure (MAP), a 2-F_r miniaturized combined catheter-micromanometer (Model SPR-838

Millar instruments, TX, USA) was inserted into the right common carotid artery. All readings were recorded using LabChart 8 (ADIntruments). All animals were subjected to 30 min of regional ischaemia via LAD occlusion followed by 120 min of reperfusion. Agonists were given as an IV bolus dose at the onset of reperfusion. Where antagonists were used, they were given as an IV bolus dose 5 mins prior to reperfusion. After the experiment, infarct size was measured as detailed in Chapter 2.3.2.3.

4.4 Results

4.4.1 Effect of VCP746 on post-ischemic functional recovery in the isolated rat heart model

Post-ischaemic LVDP and contractility (dP/dt_{max}) were significantly reduced at the end of the reperfusion period in ischaemic control isolated rat hearts (32.5 ± 6.2% and 32.4 ± 5.2% of baseline, respectively, Fig. 4.1). LVDP and contractility were significantly improved in CPA- (100 nM) and VCP746 (1 μM)-treated hearts compared to control hearts at the end of the reperfusion period (LVDP: 89.1 ± 14.2% and 69.2 ± 6.6% vs. 32.5 ± 6.2% of baseline, respectively; dP/dt_{max}: 84.5 ± 17.6% and 64.7 ± 6.9% vs. 32.4 ± 5.2% of baseline, respectively). VCP746-mediated increase in post-ischaemic contractility and LVDP recovery was abolished in the presence of SLV320 (A_1AR antagonist; 100 nM) and PSB603 (A_{2B}AR antagonist; 100 nM), suggesting that activation of both receptors were required to mediate the protective effect of VCP746.

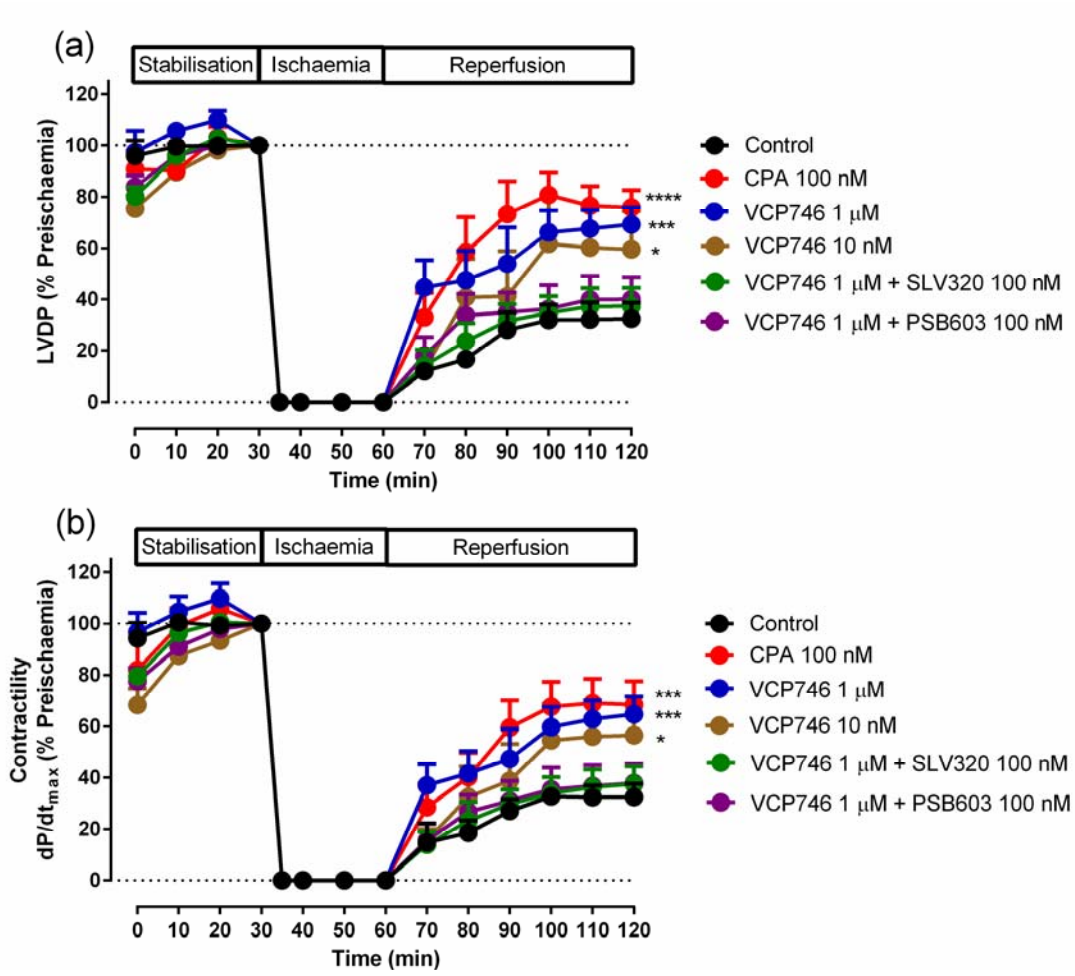

Figure 4.1 (a) LVDP and (b) contractility (dP/dt_{max}) of hearts during global ischaemia and reperfusion. VCP746 treatment significantly improved (a) LVDP and (b) contractility, an effect blocked by co-treatment with SLV320 and PSB603. LVDP and contractility data were normalised to baseline values and expressed as % preischaemia. Data were expressed as mean ± SEM, n = 5. *P<0.05, ***P<0.001, ****P<0.0001 vs. control)

4.4.2 Effect of VCP746 on infarct size in the isolated rat heart model

Infarct size measured at the end of reperfusion was significantly reduced in CPA- (100 nM) and VCP746-treated (1 μM) hearts compared to control hearts (10.1 ± 1.7% and 14.7 ± 2.6% vs. 32.1 ± 4.2% area at risk, respectively; Fig. 4.2).

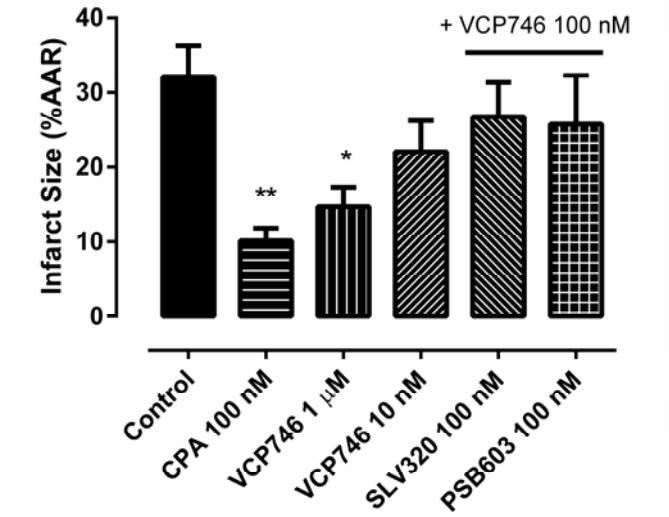

Figure 4.2 Myocardial infarct size measurement in isolated rat hearts after global ischaemia and reperfusion injury. Treatment with CPA (100 nM) and VCP746 (1 μM) significantly reduced infarct size. Co-treatment with SLV320 or PSB603 blunted the infarct-sparing effect of VCP746. After ischaemia and reperfusion, hearts were stained with TTC and infarct size was quantified as percentage area at risk. Data were expressed as mean ± SEM, n = 5. *P<0.05, **P<0.01 vs. control.

VCP746-mediated infarct size reduction was blunted by SLV320 (A_1AR antagonist) and PSB603 (A_{2B}AR antagonist), suggesting that VCP746 requires the activation of the A_1 and A_{2B}AR to confer cardioprotection.

4.4.3 Effect of VCP746 on heart rate in the isolated rat heart model

Infusion of CPA at the onset of reperfusion led to a significant reduction in heart rate (Fig. 4.3). When CPA infusion was stopped, heart rate returned to control level. Heart rates of VCP746-treated hearts and hearts co-treated with VCP746 and SLV320 were no different to heart rate of control hearts throughout the entire reperfusion phase, indicating that neither of the compounds had an effect on heart rate.

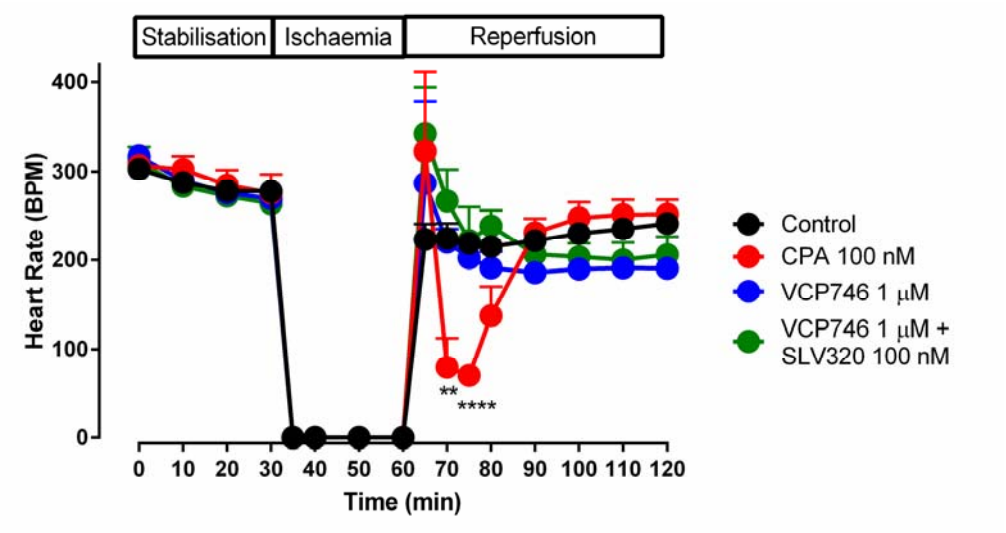

Figure 4.3 Heart rate measurement in isolated rat hearts. CPA infusion at the onset of reperfusion resulted in a significant decrease in heart rate. Neither VCP746 nor VCP746 + SLV320 infusion had a significant effect on heart rate. Data expressed as mean ± SEM, n = 5. **P<0.01, ****P<0.0001 vs. control.

4.4.4 Effect of VCP746 on heart rate and mean arterial pressure in the rat myocardial infarction model

Baseline heart rate (HR) and mean arterial pressure (MAP) of treatment groups were not found to be significantly different to that of their respective vehicle groups (Fig. 4.4). Heart rate of rats treated with the non-selective adenosine receptor agonist NECA was significantly reduced compared to heart rate in the vehicle control group (Fig. 4.4a). 20 min post-infusion, heart rate in NECA-treated hearts was observed to no longer be significantly different to the vehicle control group and eventually returned to baseline. In contrast, the biased A_1/A_{2B} adenosine receptor agonist VCP746 produced no effect on heart rate. Similarly, VCP746 produced no effect on MAP but NECA infusion led to a significant reduction in MAP that persisted until the end of reperfusion (Fig. 4.4b).

Due to the limited solubility of Capadenoson, a vehicle with higher percentage of solvent (50% DMSO) was used to prevent precipitation (Fig. 4.4c, d). Capadenoson produced no significant effect on MAP compared to its vehicle control group (Fig. 4.4d). However, we observed that Capadenoson infusion led to a statistically significant, albeit modest, heart rate reduction (Fig. 4.4c). This effect on heart rate was also persistent and remained until the end of reperfusion.

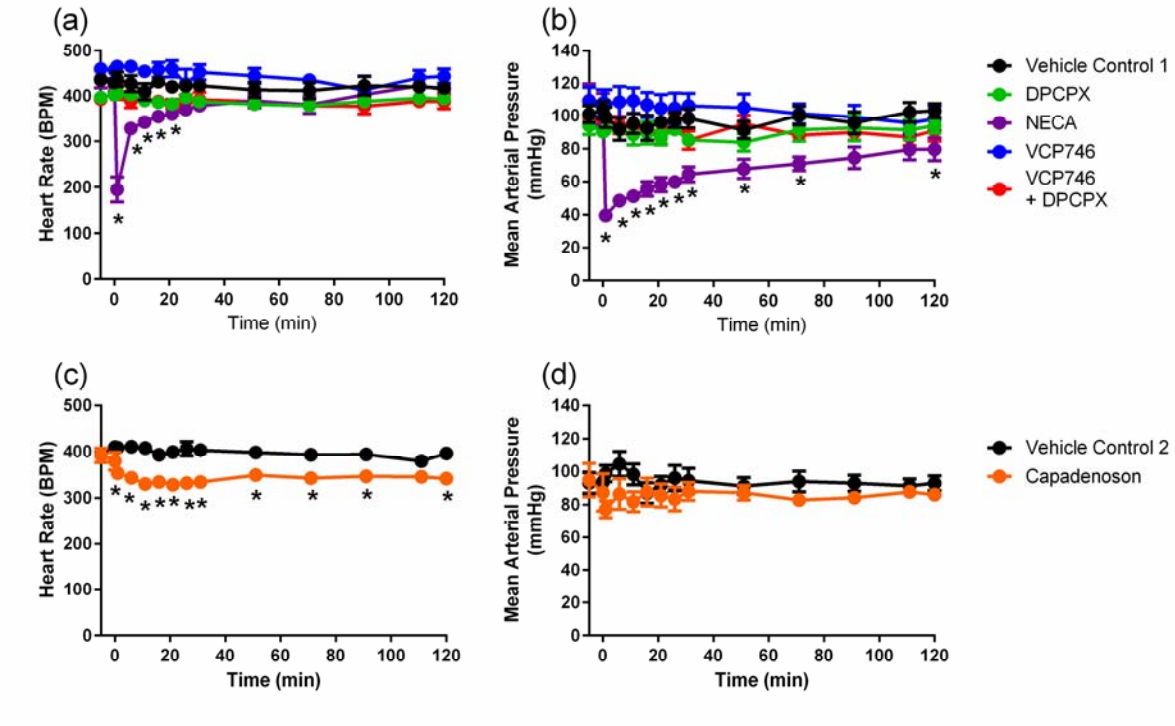

Figure 4.4 Heart rate and mean arterial pressure at reperfusion. Effect of DPCPX, VCP746, NECA, VCP746 + DPCPX and Capadenoson on (a, c) heart rate and (b, d) mean arterial pressure. X-axis is expressed as time (min) after start of reperfusion beginning at -5 min (5 min before reperfusion) and ending at 120 min. Heart rate and mean arterial pressure expressed as BPM and mmHg, respectively. Data expressed as mean ± SEM, n = 6-8. *P<0.05 vs. respective vehicle control.

4.4.5 Effect of VCP746 on infarct size in the rat myocardial infarction model

Infarct size in both vehicle control 1 and vehicle control 2 groups are not significantly different to one another (Fig. 4.5). Hearts treated with NECA or VCP746 were found to have significantly smaller infarct sizes compared to hearts in their respective control group, vehicle control 1 group (34.9 ± 3.8% and 30.7 ± 2.0% AAR vs. 52.3 ± 2.0%, respectively). Hearts treated with Capadenoson were also found to have significantly smaller infarct sizes compared to hearts in its respective control group, vehicle control 2 (37.8 ± 2.2% vs. 51.0 ± 2.1%).

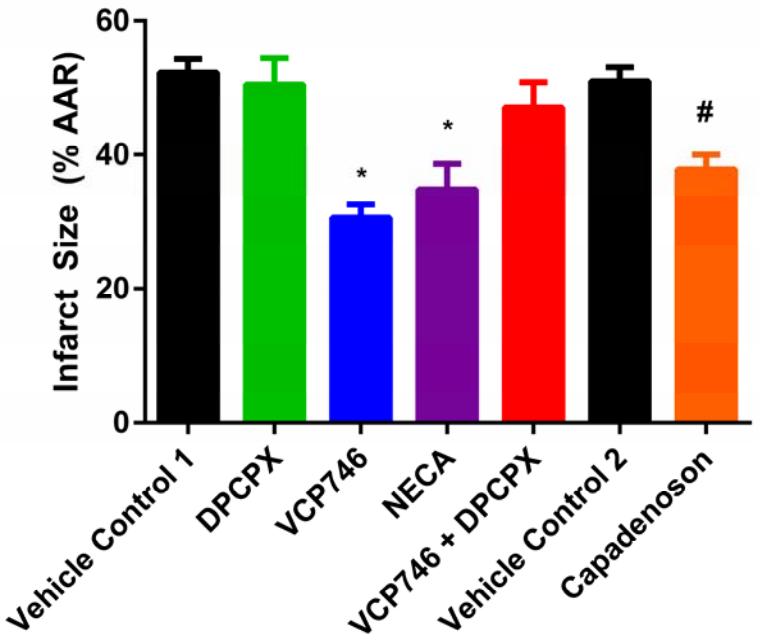

Figure 4.5 Adenosine receptor agonist and antagonist effects on infarct size post-myocardial infarction and reperfusion. Infarct size is expressed as percentage of area at risk (% AAR). Data expressed as mean ± SEM, n = 6-8. *P < 0.05 vs. Vehicle Control 1; #P < 0.05 vs. Vehicle Control 2.

The A_1AR antagonist, DPCPX alone did not have a significant effect on infarct size. The infarct-sparing effect of VCP746 was abolished when co-administered with DPCPX, as infarct size in the VCP746 + DPCPX group was no different to infarct size in the vehicle control 1 group.

4.5 Discussion

Langedorff-isolated rat heart model

In the isolated rat heart model, VCP746 and CPA reduced infarct size and improved post-ischaemic functional recovery as assessed by dp/dt_{max} (contractility) and left ventricular developed pressure (LVDP). VCP746-mediated infarct size reduction and post-ischaemic functional recovery was attenuated not only by SLV320 (A_1AR antagonist), but also by PSB603, the A_{2B}AR antagonist. The present findings suggest that synergistic activation of both the A_1 and A_{2B}AR is required to confer full cardioprotection following ischaemia/reperfusion injury, supporting previous studies that have found that full cardioprotection by an A_1AR agonist cannot be achieved without co-activation of the A_{2A} and/or A_{2B}AR. Urmaliya and colleagues previously observed that CPA-mediated cardioprotection in isolated mouse hearts is dependent on the cooperative activation of A_{2A}/A_{2B}AR by endogenous adenosine (48). Lasley and colleagues also found that blockade of the A_{2A} and A_{2B}AR abolished 2-Chloro-N^6-cyclopentyladenosine (CCPA; A_1AR agonist)-mediated cardioprotection in *in vivo* rat myocardium (125). In the present study, VCP746 administration was found to have no effect on heart rate, whereas the prototypical A_1AR agonist CPA was found to reduce heart rate significantly when compared to the vehicle group. This outcome was in

accordance to what was observed in anaesthetised rats (Chapter 3) where CPA produced a significant heart rate reduction at doses where VCP746 had no effect.

Taken together, the results of this *ex vivo* study support the findings of Valant et al. where VCP746 was observed to reduce cell death in ischaemic cardiac myocytes but had no effect on isolated atrial HR, in contrast to CPA which was equally cytoprotective but produced a pronounced reduction in atrial HR (205). The present study has shown that VCP746 has no effect on heart rate at concentrations that are cardioprotective. Furthermore, the cardioprotective effects of VCP746 are not only A_1AR-mediated but also dependent on the activation of A_{2B}AR, presumably by endogenous adenosine.

A limitation of the isolated heart model is the exclusion of the immune system and thus inflammation, which contributes to cardiac injury following ischaemia and reperfusion (172). In this study, the isolated heart model was used specifically to evaluate the direct cardioprotective effects of VCP746 without the complexity of the inflammatory component of ischaemia/reperfusion injury. Further evaluation of VCP746 in a more physiologically-relevant *in vivo* model is therefore warranted. Another potential limitation in this study is the use of unpaced hearts. In addition to its intrinsic cardioprotective properties, CPA also potently reduces heart rate. Indeed, heart rate reduction could reduce myocardial energy and oxygen demand and thus improve outcomes of myocardial ischaemia (233). As such, without pacing, it is impossible to compare the cardioprotective effects of CPA to VCP746 independent of heart rate effects. However, the use of paced hearts would introduce an artificial aspect into the disease model used in this study. As we were more interested in investigating the effects of the compounds in a system that mimics the disease as closely as possible, the use of paced hearts was avoided.

Acute rat myocardial infarction study

To evaluate VCP746 in a more physiologically-relevant system, a rat myocardial infarction model was utilised. Myocardial infarction is a dynamic event that involves various inflammatory cytokines such as tumour necrosis factor-α (TNF-α) and interleukin-1β (IL-1β) and immune cells, such as mast cells, macrophages and neutrophils (234-236). The extent of inflammation in the myocardium - as a result of ischaemia/reperfusion injury - significantly influences final infarct size and patient outcomes in the clinical setting (32, 172). While investigating the effects of VCP746 on inflammation and immune cell recruitment is out of the scope of this study, we sought to investigate the effect of VCP746 on infarct size in a whole animal where interplay between multiple systems in the body occurs. VCP746 was found to significantly reduce infarct size in rat hearts, via an A_1AR-dependent mechanism, at a dose that had no effect on heart rate or mean arterial pressure. This was unlike the prototypical non-selective AR agonist NECA that produced an infarct-sparing effect along with a reduction in heart rate and mean arterial pressure.

Capadenoson, an A_1AR agonist that has been shown to display biased agonism in our lab (237), was effective at reducing infarct size and did not reduce mean arterial pressure, similar to VCP746. However, Capadenoson produced a modest but significant reduction in heart rate. It is possible that the observed effects of Capadenoson on infarct size and heart rate is due to a bias towards pathways that promote cell survival and away from pathways that promote bradycardia, albeit an imperfect bias. While bradycardic effects have previously been a hindering dose-limiting factor for cardioprotective drug candidates in the clinic, a modest reduction in heart rate, in contrast, may be beneficial for reducing the oxygen demand of the injured heart without hypo-perfusing end organs (238).

Potential cardioprotective signalling pathways and mechanisms

The mechanisms by which AR activation confer cardioprotection has been widely studied. Activation of ARs is thought to activate G protein-mediated pro-survival RISK (reperfusion injury salvage kinase) signalling pathways. These kinases, which include ERK1/2 (48), PI3K (239), Akt (240), and PKC (241), have been shown to confer powerful cardioprotection when activated at myocardial reperfusion. These signalling pathways have been shown to converge at downstream mitochondrial K_{ATP} (mitoK_{ATP}) channels. When opened, the mitoK_{ATP} channels inhibit the opening of the mitochondrial permeability transition pore (MPTP), thus preserving mitochondrial function and cell surviva (242). Of the ARs, the A_1 subtype appears to more directly protect myocardial tissue during IR, that is, via activation of the RISK pathways. Given that VCP746 is a potent A_1AR agonist, this is likely to be the main mechanism of action of VCP746 at the myocardium.

There is also evidence that activation of A_{2B}AR at reperfusion protects the heart by inactivating GSK (Glycogen Synthase Kinase)-3β and subsequently modulating MPTP opening (243). However, the direct cardioprotective role of A_{2B}AR remains in question as many studies have failed to demonstrate the benefits of activating myocardial A_{2B}AR post-MI (126, 172). Rather, Koeppen et al. (172) showed that it is the activation of A_{2B}AR on bone marrow derived inflammatory cells (such as neutrophils), and not cardiomyocytes, that confers cardioprotective effects. In addition, depletion of A_{2B}AR from these inflammatory cells also led to significantly increased myocardial injury. A_{2B}AR. Using enzyme-linked immunosorbent assay (ELISA), Koeppen and colleagues found that A_{2B}AR activation dampen TNF-α release from inflammatory cells. These results suggest that A_{2B}AR activation on inflammatory cells is cardioprotective by

decreasing TNF-α release and limiting inflammatory responses during reperfusion post-ischaemia.

As a potent agonist at both A_1 and A_{2B}ARs, VCP746 may confer cardioprotection through any of these mechanisms. While the present study has demonstrated the powerful cardioprotective effect of VP746 in both the *ex vivo* and *in vivo* setting, the mechanisms of action of VCP746 remain unelucidated. As such, further studies investigating the means by which VCP746 reduces myocardial injury during IR is warranted.

Conclusion

Overall, the results of the acute rat myocardial infarction study have shown that VCP746 is cardioprotective with no effect on heart rate or blood pressure and that this effect is mediated by the activation of the A_1AR. We hypothesise that as a biased agonist, VCP746 preferentially activates signalling pathways that promote cell survival over signalling pathways that lead to bradycardia. Further mechanistic studies on VCP746 are required to confirm this hypothesis and to determine the biased profile responsible for the agonist's observed cardioprotective effects in the absence of bradycardia.

Chapter 5 Effect of VCP746 on Cardiac Myocyte Hypertrophy and Cardiac Fibroblast Collagen Synthesis

5.1 Introduction

During myocardial infarction (MI), the acute loss of myocardium results in an abrupt increase in load, initiating a host of intracellular signalling processes that begins and modulates reparative changes, including left ventricular (LV) dilatation, hypertrophy and scar formation, among many events (54). It is well-established that left ventricular function is a key predictor of survival post-MI, which in turn is largely determined by infarct size (55). However, a number of cardioprotective therapies have failed in the clinic despite strong preclinical evidence that they reduce infarct size. This possibly results from the relative inability of most cardioprotective drug candidates to control the remodelling process following MI. The major components contributing to the remodelling process are cardiac hypertrophy and cardiac fibrosis.

In response to triggers such as wall stretch, cytokines, and neurohormones, cardiomyocytes undergo pathological hypertrophy. These triggers lead to changes in cardiac gene expression described as the reactivation of the 'foetal gene programme'. Foetal genes such as atrial natriuretic peptide (ANP), β-myosin heavy chain (β-MHC) and α-skeletal actin (α-SKA) are often upregulated in pathological hypertrophy (72, 244). Injury to the heart also evokes complex cellular responses in non-muscular cells, the most prominent of which are the cardiac fibroblasts. Cardiac fibrosis can be stimulated by various cytokines including transforming growth factor-β1 (TGF-β1) and angiotensin II (Ang II). These cytokines upregulate fibrogenic genes such as collagen I, connective tissue growth factor (CTGF) and TGF-β1, and together they stimulate collagen synthesis, and ultimately lead to increased extracellular matrix deposition (80, 81).

Various studies have implicated a role for adenosine receptors in regulating and attenuating cardiac hypertrophy (177) and fibrosis (102). We were therefore interested to determine if the A_1/A_{2B}AR biased agonist VCP746 has anti-hypertrophic and anti-fibrotic effects, in addition to the compound's established cardioprotective effects (205). With this in mind, we first utilised an *in vitro* model of hypertrophy and fibrosis to preliminarily evaluate VCP746 for any anti-remodelling properties.

5.2 Aim

To determine whether VCP746 has anti-hypertrophic and anti-fibrotic effects in NCM and NCF, respectively.

5.3 Study design and methods

Neonatal cardiac myocytes and fibroblasts were isolated and cultured as per Chapter 2.1. NCM were pre-treated with DMSO (Control; 0.1%), VCP746 or prototypical A_1AR agonist, CPA and then stimulated with IL-1β, TNF-α or Ang II to induce hypertrophy. NCF were pre-treated with DMSO (Control; 0.1%), VCP746 in the absence or presence of SLV320 (A_1AR antagonist), SCH442416 (A_{2A}AR antagonist) or PSB603 (A_{2B}AR antagonist), and then stimulated with Ang II or TGF-β1 to induce collagen synthesis. ^{3}H-leucine and ^{3}H-proline incorporation was used as an index for cardiac myocyte hypertrophy and cardiac fibroblast collagen synthesis, respectively. MTT toxicity assay was used to determine cell viability. RT-PCR was performed to measure change in expression of pro-hypertrophic and pro-fibrotic genes. Detailed experimental protocols can be found in Chapter 2.1.

5.4 Results

5.4.1 Cardiac Myocyte Hypertrophy

IL-1β (Fig. 5.1a, d), TNF-α (Fig. 5.1b, e) and Ang II (Fig. 5.1c, f) significantly stimulated NCM hypertrophy as determined by ^{3}H-leucine incorporation (up to 120.4 ± 3.0%, 124.3 ± 2.0% and 124.8 ± 2.0% of control, respectively). Pre-treatment of NCM with the prototypical A_1AR agonist, CPA (1 nM – 1 μM) concentration-dependently reduced IL-1β- (Fig. 5.1a), TNF-α- (Fig. 5.1b) and Ang II- (Fig. 5.1c) stimulated ^{3}H-leucine incorporation (104.8 ± 3.2%, 103.9 ± 2.5% and 104.9 ± 1.5% of control, respectively, at 1 μM CPA concentration). The novel A_1AR biased agonist VCP746 (0.1 nM – 100 nM) also concentration-dependently reduced IL-1β- (Fig. 5.1d), TNF-α- (Fig. 5.1e) and Ang II- (Fig. 5.1f) stimulated ^{3}H-leucine incorporation (90.8 ± 3.8%, 91.7 ± 4.0% and 98.4 ± 4.2% of control, respectively; 100 nM VCP746 concentration). At only 10 nM, VCP746 significantly reduced TNF-α- and Ang II-stimulated hypertrophy while CPA (at the same concentration) had no significant effect, indicating that VCP746 is more potent than CPA at inhibiting NCM hypertrophy.

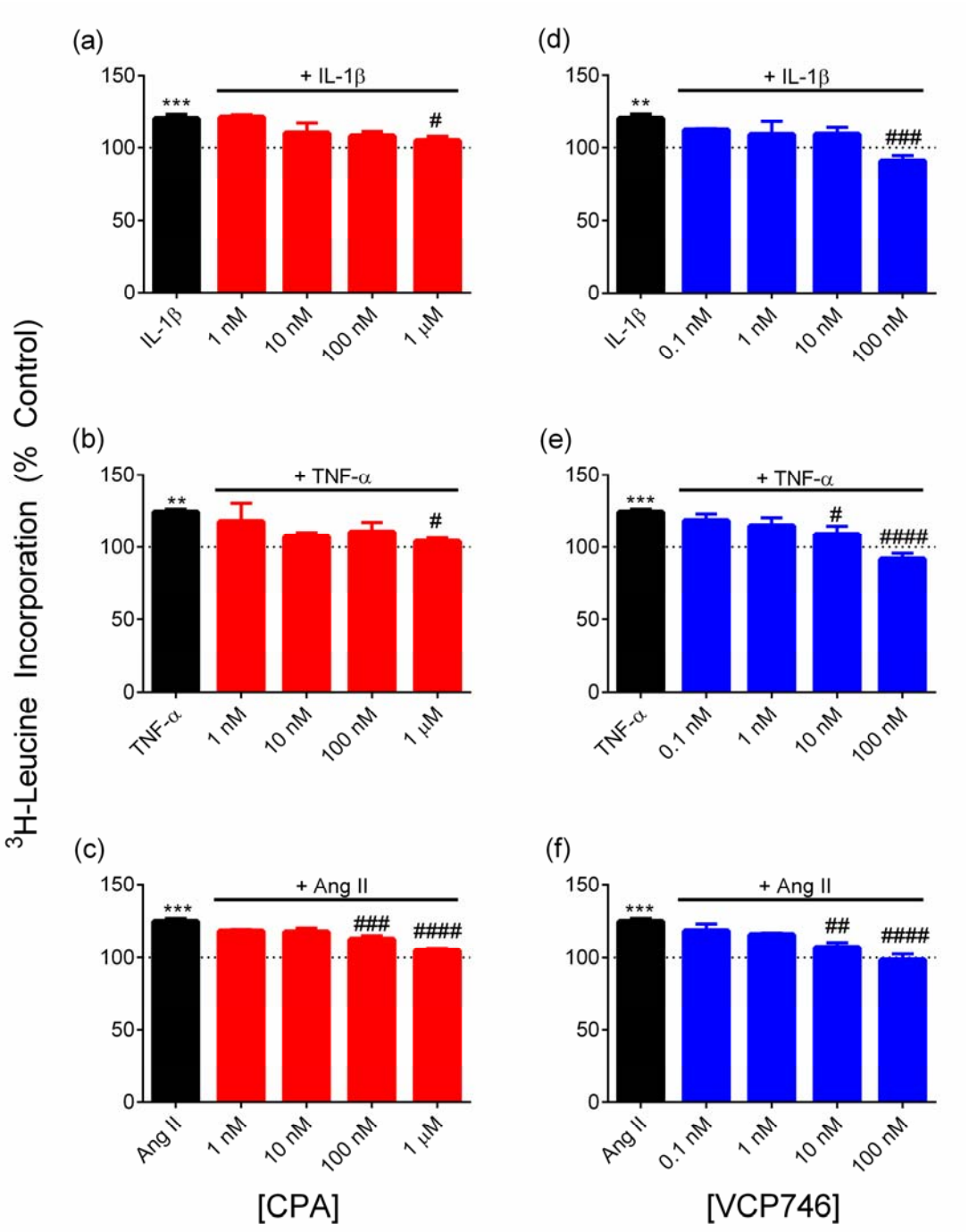

Figure 5.1 CPA and VCP746 reduced cardiac myocyte hypertrophy as assessed by ^{3}H-leucine incorporation. ^{3}H-leucine incorporation analysis demonstrated that IL-1β, TNF-α and Ang II stimulated rat cardiac myocyte hypertrophy. Co-treatment of these cells with CPA (a-c), and VCP746 (d-f), lead to a concentration-dependent, significant reduction in IL-1β- (a, d), TNF-α- (b, e) and AngII- (c, f) stimulated cardiac myocyte hypertrophy. Data presented as means ± SEM, n = 4-5. **P<0.01, ***P<0.001 vs. 100%. $^{\#}$P<0.05, $^{\#\#\#}$P<0.001, $^{\#\#\#\#}$P<0.0001 vs. IL-1β, TNF-α or Ang II.

5.4.2 Measurement of cardiac myocyte viability

The MTT assay was used to investigate whether the observed inhibitory effects of CPA and VCP746 on NCM ^{3}H-leucine incorporation were due to reduced cell viability. Neither CPA (100 nM and 1 μM) nor VCP746 (10 nM and 100 nM), in the presence of IL-1β (Fig. 5.2a), TNF-α (Fig. 5.2b) or Ang II (Fig. 5.2c), had any effect on cell viability as determined by MTT assay, demonstrating that the inhibition of NCM ^{3}H-leucine incorporation by the adenosine receptor agonists was not due to a reduction in cell viability.

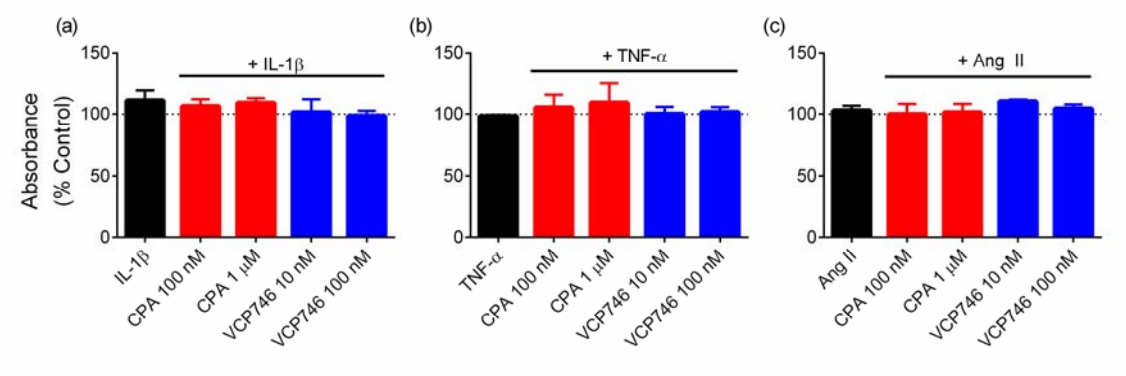

Figure 5.2 CPA and VCP746 does not reduce cardiac myocyte viability. The effects of CPA, and VCP746, on cardiac myocyte viability were analysed with the MTT assay. Treatment of cardiac myocytes with CPA (100 nM and 1 μM), and VCP746 (10 nM and 100 nM), in the presence of IL-1β (a), TNF-α (b) and Ang II (c) did not affect cell viability. Data presented as means ± SEM, n = 3 – 5.

5.4.3 Quantitative measurement of pro-hypertrophic gene expression

Real-time PCR analysis from total RNA extracted from NCM stimulated with IL-1β, TNF-α and Ang II for 24 h showed that these cytokines significantly increased ANP, β-MHC and α-SKA mRNA expression (Fig. 5.3), with the exception of α-SKA mRNA expression mediated by IL-1β (Fig. 5.3c) and Ang II (Fig. 5.3i), for which the effect on gene expression was not statistically significant.

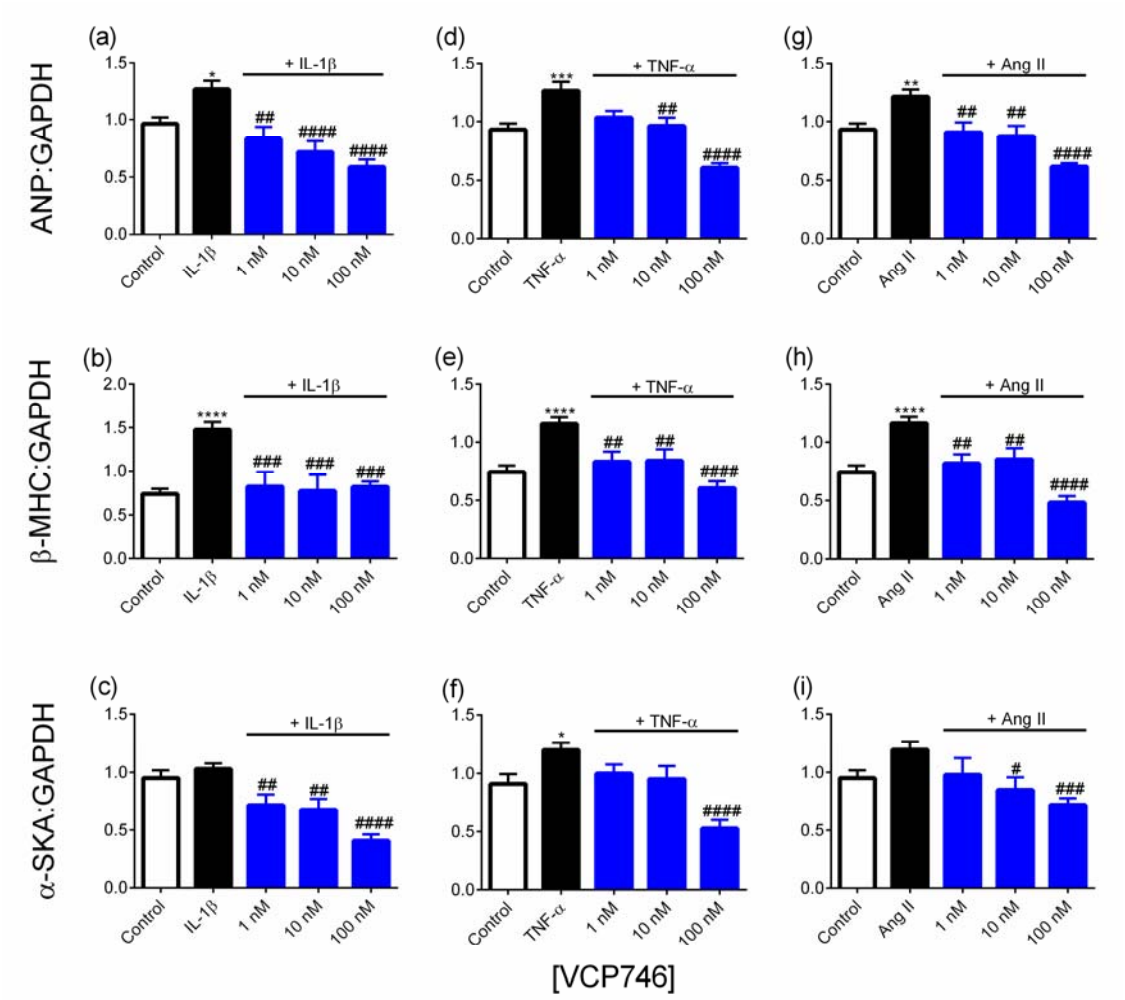

Figure 5.3 Effects of VCP746 on cardiac myocyte pro-hypertrophic gene expression. After 24 h of incubation, IL-1β, TNF-α and Ang II stimulated ANP (a, d, g), and β-MHC (b, e, h) mRNA expression in cardiac myocytes. Only TNF-α significantly increased α-SKA (f) mRNA expression. Pre-treatment of cardiac myocytes with VCP746 resulted in the suppression of IL-1β- (a-c), TNF-α- (d-f) and Ang II (g-i) -stimulated ANP, β-MHC and α-SKA mRNA expression. Data presented as mean ± SEM, n = 4 – 5. *P<0.05, **P<0.01, ***P<0.001, ****P<0.0001 vs. control. $^{\#}$P<0.05, $^{\#\#}$P<0.01, $^{\#\#\#}$P<0.001, $^{\#\#\#\#}$P<0.0001 vs. IL-1β, TNF-α or Ang II.

Pre-treatment of NCM with VCP746 (1 nM – 100 nM) resulted in the inhibition of ANP, β-MHC and α-SKA mRNA expression stimulated by IL-1β (Fig. 5.3a-c), TNF-α (Fig. 5.3d-f) or Ang II (Fig. 5.3g-i). This effect by VCP746 was potent; a concentration as low as 1 nM was sufficient to return the mRNA expression of the hypertrophy biomarkers to control levels.

5.4.4 Cardiac fibroblast collagen synthesis

Ang II and TGF-β1 significantly stimulated NCF collagen synthesis over control levels as determined by ^{3}H-proline incorporation (Fig. 5.4; 139.16 ± 9.8% and 193 ±7.1% of untreated control, respectively). Pre-treatment of NCF with VCP746 (0.1 nM – 1 μM) produced a concentration-dependent reduction in TGF-β1 and Ang II-stimulated ^{3}H-proline incorporation (Fig. 5.4a). The addition of SLV320, an A_1AR-selective antagonist, or an A_{2A}AR-seletive antagonist, SCH442416 had no effect on VCP746-mediated reduction in NCF collagen synthesis. However, the addition of PSB603 (A_{2B}AR-selective antagonist) abolished the inhibitory effects of VCP746. These data indicate that VCP746 decreases collagen synthesis in NCF through activation of the A_{2B}AR and not the A_1 or A_{2A}AR.

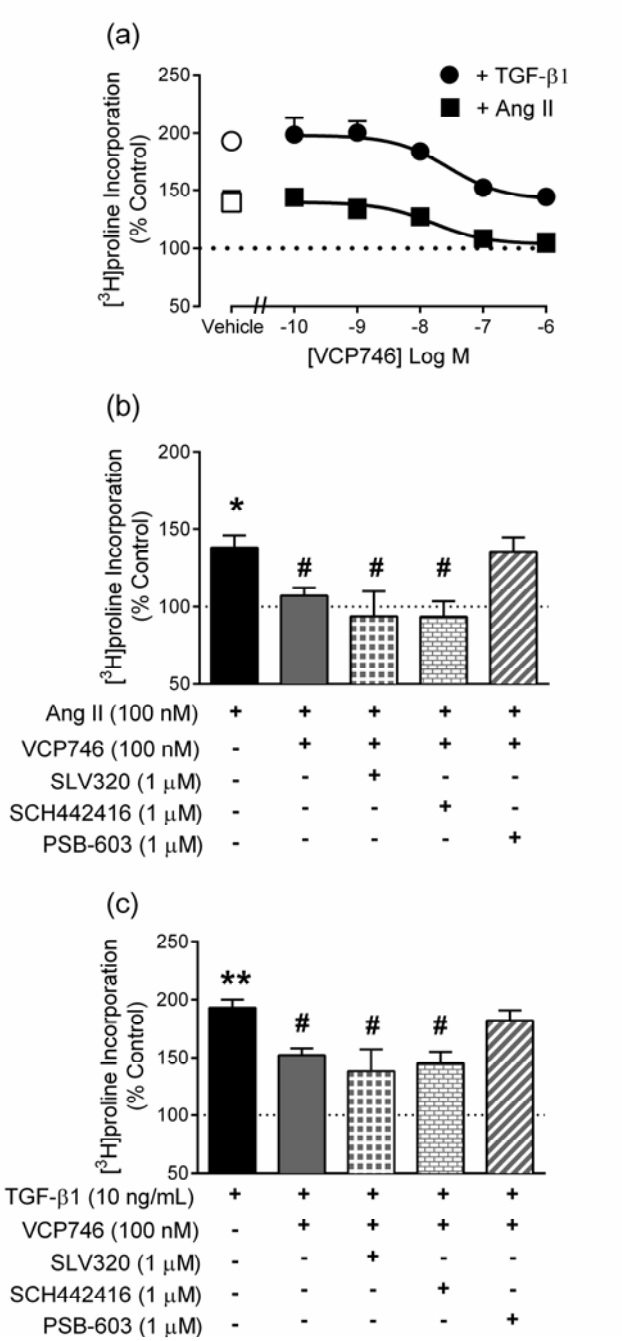

Figure 5.4 VCP746 stimulated potent inhibition of collagen synthesis in NCF. (a) VCP746 mediated a concentration-dependent inhibition of Ang II- and TGF-β1-stimulated collagen synthesis in rat NCF as determined by ^{3}H-proline incorporation. The inhibitory effect of VCP746 on (b) Ang II- and (c) TGF-β1-stimulated collagen synthesis was blocked by an A_{2B}AR antagonist (PSB603) but not by an A_1AR-selective antagonist (SLV320) or an A_{2A}AR-selective antagonist (SCH442416). Data presented as mean ± SEM, n = 4 – 5. *P<0.05 and **P<0.01 vs. control. $^{\#}$P<0.05 vs. TGF-β1 or Ang II.

5.4.5 Measurement of cardiac fibroblast viability

A potential limitation of using ^{3}H-proline incorporation as an index of collagen synthesis is that a reduction in cell viability could lead to a false interpretation of reduced in ^{3}H-proline incorporation and thus collagen synthesis. We therefore performed an MTT assay to assess if VCP746 and/or the antagonists were reducing NCF viability (Fig. 5.5).

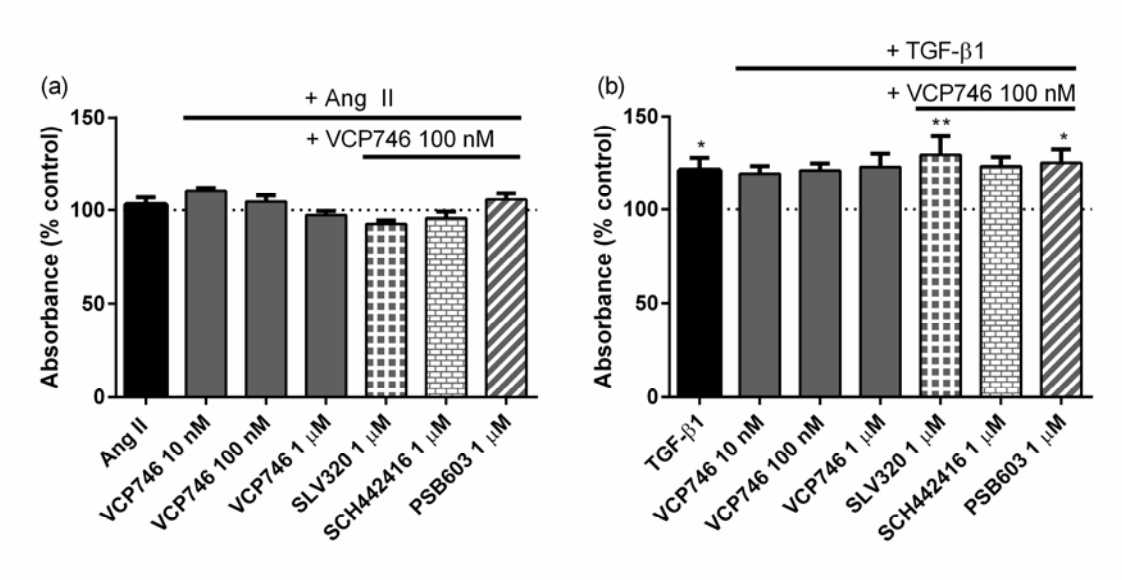

Figure 5.5 VCP746 does not reduce cardiac myocyte viability. The potential effects of VCP746 on cardiac fibroblast viability was analysed with the MTT assay. Treatment of cardiac fibroblasts with VCP746 in the absence or presence of antagonists with (a) Ang II and (b) TGF-β1 stimulation did not reduce cell viability. However, increased absorbance was detected in cells stimulated with (b) TGF-β1, indicating an increase in cell number. Data presented as means ± SEM, n = 3 – 5. *P<0.05, **P<0.01 vs. control.

Results demonstrate that neither VCP746 nor the addition of antagonists reduced cell viability indicating that the observed reduction in ^{3}H-proline incorporation mediated by VCP746 reflected an anti-fibrotic effect and not a reduction in NCF viability.

Treatment with TGF-β1 (Fig. 5.5b) did however lead to increased absorbance, indicative of increased cell numbers.

5.4.6 Quantitative measurement of fibrogenic gene expression

Quantitative real-time PCR analysis of total RNA extracted from NCF stimulated with Ang II or TGF-β1 for 24 h significantly increased Col I, CTGF and TGF-β1 mRNA expression levels compared to control, with the exception of TGF-β1-stimulated TGF-β1 expression, which showed a trend towards an increase but did not reach statistical significance (Fig. 5.6). Pre-treatment with VCP746 resulted in the inhibition of Col I, CTGF and TGF-β1 mRNA expression stimulated by Ang II (Fig. 5.6a, c and e) or TGF-β1 (Fig. 5.6b, d and f). The addition of SLV320 (A_1AR antagonist) or SCH442416 (A_{2A}AR antagonist) had little effect on VCP746-mediated decreases in fibrogenic gene expression. In contrast, the use of PSB603 (A_{2B}AR antagonist) abolished the inhibitory effect of VCP746 on Col I, CTGF and TGF-β1 mRNA expression, further indicating that VCP746-mediated anti-fibrotic effects are downstream of A_{2B}AR (and not A_1 or A_{2A}AR) activation.

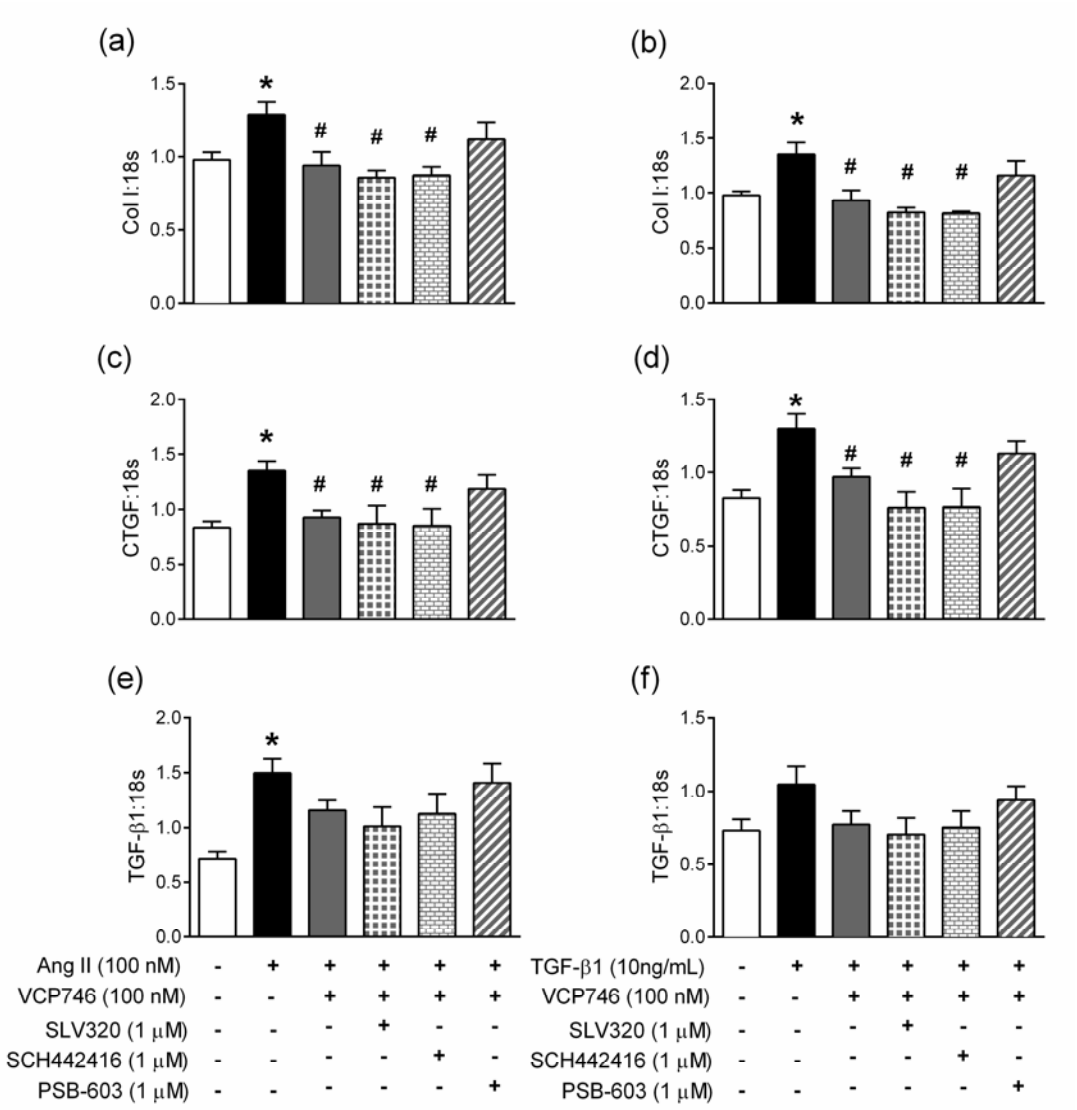

Figure 5.6 VCP746 inhibits fibrogenic gene expression in cardiac fibroblasts. Ang II and TGF-β1 stimulated (a, b) Col I, (c, d) CTGF and (e, f) TGF-β1 mRNA expression in NCF. Pre-treatment with VCP746 significantly attenuated (a, c) Ang II- and (b, d) TGF-β1-stimulated Col I and CTGF mRNA expression but not TGF-β1 mRNA expression. The inhibitory effect of VCP746 was blocked by an A_{2B}AR antagonist, PSB603, but not by an A_1AR antagonist (SLV320) or A_{2A}AR antagonist (SCH442416). Data presented as means ± SEM, n = 3 – 5. *P<0.05 vs. control, $^{\#}$P<0.05 vs. Ang II or TGF-β1.

5.5 Discussion

In the present study, we first showed that IL-1β, TNFα and Ang II stimulated NCM hypertrophy, an effect that was inhibited by CPA, a prototypical A_1AR agonist, and by VCP746, in a concentration-dependent manner. This result was concurrent with what was observed by Liao et al. who were able to inhibit TNF-α induced rat NCM hypertrophy with CPA treatment (70). It is a possibility that compound-induced cytotoxicity could lead to reduced NCM viability and cell numbers, and subsequently a false interpretation of reduced ^{3}H-leucine incorporation. Results from the MTT assay suggests that neither CPA nor VCP746 were cytotoxic at the two highest concentrations tested and that the observed reduction in ^{3}H-leucine incorporation mediated by the two compounds were indeed due to anti-hypertrophic signalling and not reduced NCM viability.

Stimulation of NCM with IL-1β, TNF-α and Ang II also led to an increase in the mRNA expression of ANP and β-MHC. In our hands, only TNF-α significantly increased mRNA expression of α-SKA in NCM while Ang II-induced α-SKA expression only trended towards increased expression at the time point of measurement – it is possible that this time point did not capture peak Ang II stimulation of α-SKA gene expression and hence expression levels of the marker did not reach statistical significance. Irrespective of species, cardiac myocytes respond to hypertrophic stimuli with changes in gene expression (244). The molecular changes that occur in pathological hypertrophy resemble what is observed in foetal cardiac development and hence the reactivation of the 'foetal gene programme' is always said to occur during cardiac hypertrophy. Treatment of cells stimulated with IL-1β, TNF-α, and Ang II with VCP746 revealed that VCP746 was very potent at reducing the expression of the

hypertrophic biomarkers ANP, β-MHC and α-SKA (245). VCP746 attenuated the expression of ANP, β-MHC and α-SKA at concentrations as low as 1 nM.

In cardiac fibroblasts, Ang II and TGF-β1 were shown to increase collagen synthesis, an effect that was attenuated by the addition of VCP746. Using PSB603, an A_{2B}AR antagonist, the inhibitory effect of VCP746 on collagen synthesis was reversed, suggesting that the anti-fibrotic effect of VCP746 was dependent upon the activation of the A_{2B}AR. Antagonists for the A_1AR and the A_{2A}AR failed to abrogate the effect of VCP746, indicating that these receptors were not involved in reducing collagen synthesis. The relative importance of the A_{2B}AR over other AR subtypes as a key regulator of cardiac fibrosis is perhaps unsurprising as data suggest that the A_{2B}AR is the most abundantly expressed subtype in rat cardiac fibroblasts (127, 132). Similar to the findings in cardiac myocytes, the MTT assay conducted on cardiac fibroblasts revealed that neither VCP746 nor subtype-selective antagonists reduced NCF viability and that reduction in ^{3}H-proline incorporation was due to anti-fibrotic signalling. Cells treated with TGF-β1 – a cytokine well known for promoting cardiac fibroblast proliferation (246) – registered a greater absorbance, suggesting increased cell numbers. This may, at least in part, explain the apparent inability of VCP746 to bring TGF-β1-induced ^{3}H-proline incorporation back to unstimulated control levels, as cell number and thus baseline ^{3}H-proline incorporation is significantly greater in TGF-β1-treated cells than in unstimulated control cells.

In response to cardiac injury, pro-fibrotic gene expression is upregulated in fibroblasts in an attempt to repair the damaged myocardium. Ang II is able to stimulate fibrogenesis in the heart directly, independent of its pressor actions (247). Also highly implicated in myocardial fibrosis is the cytokine TGF-β1. Cardiac fibroblasts are not only a target but also a source of TGF-β1 activity (248). Therefore, we sought to

determine if VCP746 could regulate the stimulation of fibrogenic gene expression by Ang II and TGF-β1. Indeed, we found that VCP746 attenuated the upregulation of Col I, TGF-β1 and CTGF, genes that contribute to fibrosis, via A_{2B}AR activation (and not the A_1 or A_{2A}AR). Taken together, the results from our cardiac fibroblast study suggest that VCP746, a potent A_{2B}AR agonist, represents an effective pharmacological agent for the treatment of myocardial fibrosis.

The potential pathways and mechanisms by which ARs reduce hypertrophy and fibrosis are not fully known. Interestingly, while signalling proteins such as ERK1/2 and p38 are involved in cardiac hypertrophy and adenosine-induced cardioprotection, adenosine receptor agonists have been shown to have no effect on these proteins in phenylephrine-stimulated cardiac myocytes (100). Evidence has shown, however, that activation of ARs can reduce Ang II and endothelin-1-stimulated RhoA activation and downstream cofilin phosphorylation, proteins that have previously been associated with cardiac hypertrophy (249). There is also evidence demonstrating that AR-mediated anti-hypertrophic effects are mediated by sarcolemmal (sarc) K_{ATP} and mitoK_{ATP} channels (176). As such, it appears that these channels are not only involved in acute cardioprotection (250, 251), but also in reducing cardiac myocyte hypertrophy. In cardiac fibroblasts, NECA-mediated reduction in Ang II-stimulated collagen production has been shown to involve an A_2AR-G_s-adenylate cyclase-cAMP-dependent pathway (252). Additionally, it was found that, rather than phosphorylating PKA, this pathway leads to the activation of exchange factor directly activated by cAMP (Epac). This A_2AR-mediated reduction in collagen production was also shown to be dependent on PI3K (a common downstream mediator of Epac) activation as treatment with LY-294002, a PI3K inhibitor, abrogated the effect of NECA on collagen production. Interestingly, ERK1/2 (also a downstream mediator of Epac) inhibition by PD-98059

(MEK-ERK1/2 inhibitor) had no effect on NECA-mediated reduction in collagen production. While currently available data give us a glimpse of how ARs may reduce cardiac remodelling, more studies are required before the full extent of AR-mediated anti-hypertrophic/fibrotic pathways can be unravelled and understood.

A clear limitation of this study would be the use of only a single inducer of hypertrophy or collagen synthesis for each treatment group: IL-1β, TNFα or Ang II for myocytes, and Ang II or TGF-β1 for fibroblasts. In cardiac remodelling and heart failure, a myriad of factors (biomechanical, neurohormonal and inflammatory) that will determine progression and severity of the condition come into play. The purpose of this study was to serve as an initial screen for any potential anti-hypertrophic and/or anti-fibrotic effects that VCP746 may possess and thus the use of a single inducer capable of stimulating hypertrophy or collagen synthesis was deemed sufficient. Furthermore, using a single inducer for each group helps delineate the specific circumstances by which VCP746 may work to reduce hypertrophy and fibrosis. A whole animal study where multiple systems and inducers are involved is therefore warranted to further investigate the role of VCP746 as an anti-remodelling therapeutic (refer to Chapter 6). While the present study has shown that VCP746 is efficacious in reducing hypertrophy and collagen synthesis (via measurements of leucine/proline incorporation and gene expression), the signalling mechanisms by which these effects are achieved remains undetermined. As such, further studies are required to understand the signalling pathways that are activated and modulated by VCP746 in the context of cardiac cell remodelling.

In summary, VCP746 has potent anti-hypertrophic and A_{2B}AR-mediated anti-fibrotic effects in cardiac myocytes and fibroblasts, respectively. In addition to being a biased agonist that elicits cardioprotection in the absence of haemodynamic side effects, this

study has demonstrated that VCP746 also confers anti-remodelling effects in cardiac cells. As such, VCP746 represent a highly attractive pharmacological agent for modulating maladaptive cardiac remodelling especially in the setting of ischaemia and reperfusion injury, given its already-established cardioprotective effects.

Chapter 6 Therapeutic Role of VCP746 in a Long-Term Rat Myocardial Infarction Model

6.1 Introduction

Improvements in therapy and care for patients suffering from myocardial infarction (MI) have led to a steady decline in patient mortality (52). However, heart failure secondary to MI (as a result of maladaptive cardiac remodelling) has become a major source of morbidity and mortality (52, 53). Left ventricular (LV) remodelling secondary to MI manifests clinically as a change in shape, function, size and composition of the LV myocardium. The initial phase of post-MI LV remodelling involves infarct expansion which occurs as a result of the degradation of inter-myocyte collagen struts by matrix metalloproteinases (MMPs) released by invading inflammatory cells. Due to this increase in fibrillar collagen degradation, a loss of structural integrity ensues, causing myocyte slippage, wall thinning, ventricular dilation and subsequently, an elevation of diastolic and systolic wall stresses (54). Alterations in wall stress serves as a strong stimulus for cardiac myocyte hypertrophy mediated by myocardial stretch, neurohormonal activation and activation of local renin-angiotensin system (RAS) (58). In addition to hypertrophy, the initial inflammatory response, characterised by elevated levels of cytokines, promotes the activation and proliferation of myofibroblasts which is responsible for scar formation and wound healing post-MI (253).

While cardiac hypertrophy and fibrosis is initially beneficial as a means to compensate for cardiomyocyte death and normalising wall stress, progressive hypertrophy and fibrosis will eventually lead the heart into a decompensated, deformed state. As such, cardiac remodelling is generally accepted as a key determinant for the progression of heart failure. In response to pressure/volume overload, cytokines, and neurohormones in the failing heart, cardiac myocytes undergo pathological hypertrophy characterised

by the activation of the foetal gene programme (upregulation of genes such as α-skeletal actin and ANP) (254) and downregulation of adult cardiac genes such as α-myosin heavy chain (255). Cardiac fibrosis – defined as the excessive accumulation of extracellular matrix in the heart – is also stimulated as a result of the actions of cytokines such as TGF-β1 and IL-6 on cardiac fibroblasts (248).

A number of *in vitro* and *in vivo* studies have found that adenosine receptors, in particular the A_1 and A_{2B}AR, are involved in the regulation of cardiac hypertrophy (177) and fibrosis (102), respectively. We, therefore, sought to determine if the *in vitro* anti-hypertrophic and anti-fibrotic effects of VCP746 could be extended into an *in vivo* disease model. Most *in vivo* myocardial infarction models involve the permanent ligation of the left anterior descending (LAD) artery where only the post-ligation remodelling aspect of the model is investigated. We wanted to investigate not only the direct anti-hypertrophic/fibrotic effects of VCP746 but also the effect of VCP746-mediated infarct size reduction on post-MI cardiac remodelling and LV function. Therefore, the present study utilised a temporary LAD occlusion model whereby infarct-sparing VCP746 intervention is possible at the onset of reperfusion.

6.2 Aim

To investigate the effect of VCP746 on cardiac remodelling and function in a long-term rat myocardial infarction model.

6.3 Study design and methods

Adult 8-week old male Sprague-Dawley rats (n = 61) were randomised into 6 groups (Fig. 6.1).

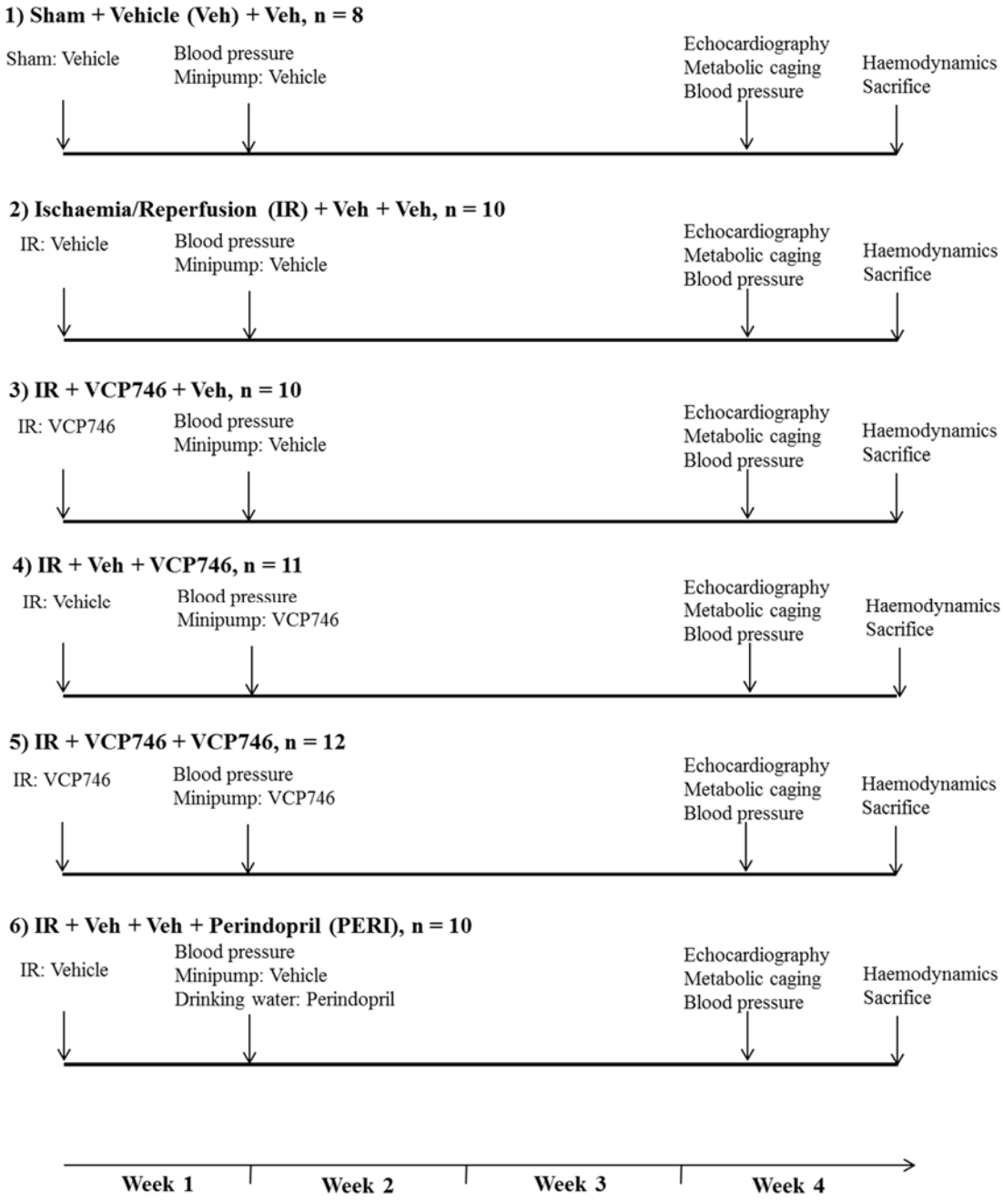

Figure 6.1 Timeline of the study protocol

Rats in all groups except sham were subjected to regional ischaemia via LAD occlusion for 30 min followed by reperfusion. 6-0 prolene sutures were slipped around the LAD but not tightened in sham rats. The first intervention following IR was an IV infusion of Veh (10% DMSO) or VCP746 (80.8 μg/kg) at reperfusion, followed by the second intervention one week later, implantation of minipumps containing Veh (60% DMSO) or VCP746 (4.4 mg/mL). In the case of group 6, perindopril (angiotensin converting enzyme inhibitor; ACEI) was administered in drinking water at 20 mg/800 mL to achieve a dose of 2 mg/kg/day. Minipumps (2) were implanted subcutaneously into every animal, one delivering continuous IV Veh or VCP746, and the other delivering the same treatment (Veh or VCP746) but subcutaneously according to groups.

Rats in the IR + Veh + Veh + PERI group were given free access to drinking water containing perindopril (0.025 mg/mL) immediately after minipump implantation.

In week 4 post-MI, tail-cuff blood pressure measurement, echocardiography and metabolic caging were performed. Prior to sacrifice, haemodynamic parameters were measured. Cardiac tissue was harvested for histopathology, immunohistochemistry, and protein and gene expression analysis as described previously.

6.4 Results

6.4.1 Infarct Size

Rats in the IR + Veh + Veh group were found to have an infarct size of 40 ± 1.2% (Fig. 6.2). Rats administered bolus VCP746 infusion at the onset of reperfusion were found to have significantly smaller infarct sizes, that is, 22.5 ± 2.5% in the IR + VCP746 + Veh group and 25.4 ± 2.4% in the IR + VCP746 + VCP746 group. Infarct size in rats

not treated with VCP746 at reperfusion (IR + Veh + VCP746 and IR + Veh + Veh + PERI groups) was no different to infarct size in IR + Veh + Veh rats.

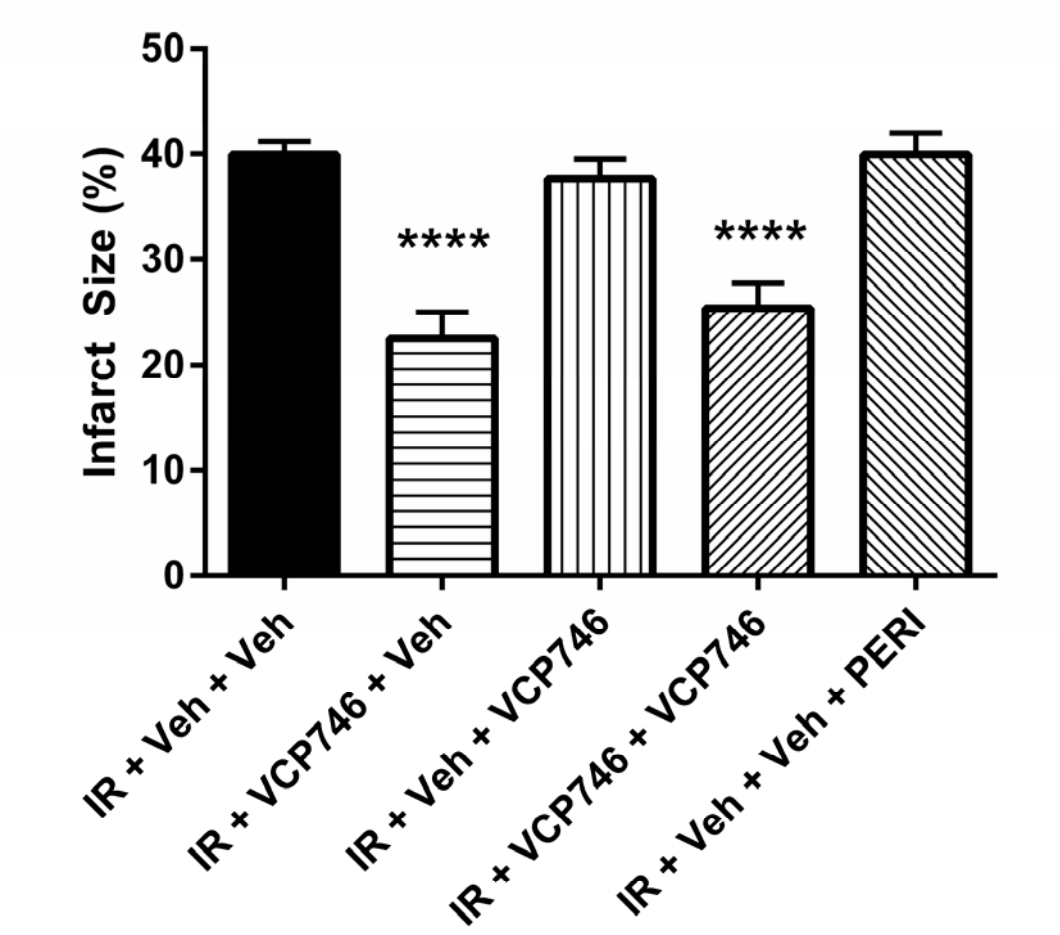

Figure 6.2 Infarct size as expressed as an averaged percentage of the endocardial and epicardial scarred circumferences of the left ventricle. Treatment groups receiving bolus VCP746 at reperfusion had significantly smaller infarct sizes compared to the IR + Veh + Veh group. Data expressed as mean ± SEM. ****P<0.0001 vs. IR + Veh + Veh.

6.4.2 Blood pressure

Conscious systolic blood pressure (SBP) before pump implantation (Pre-pump) and on week 4 (Post-pump) was not found to be different in all groups except the IR + Veh +

Veh + PERI group (Fig. 6.3). Likely as a result of the anti-hypertensive effects of perindopril, Post-pump SBP of rats in the IR + Veh + Veh + PERI group was also significantly lower than Post-pump SBP of rats in the sham-operated and IR + Veh + Veh groups.

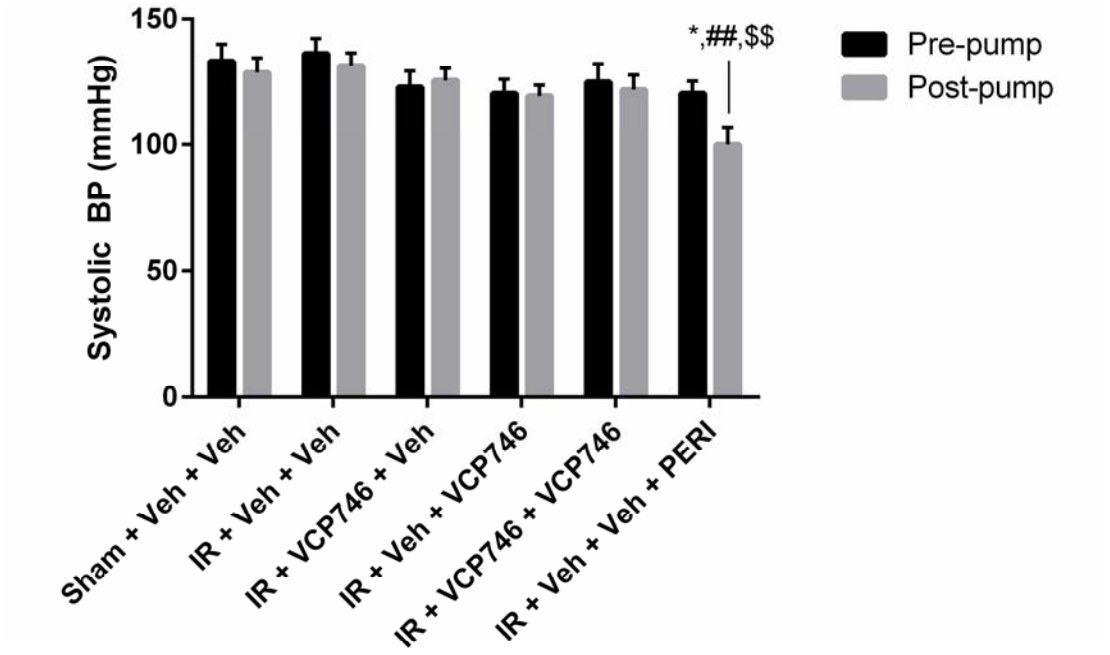

Figure 6.3 Systolic blood pressure (SBP) assessed immediately prior to minipump implantation (Pre-pump) and during week 4 (Post-pump). Post-pump SBP in the IR +Veh + Veh + PERI group was significantly lower than its respective Pre-pump SBP and Post-pump SBP of the sham and IR + Veh + Veh groups. Data expressed as mean ± SEM. *P<0.05 vs. respective Pre-pump, $^{\#\#}$P<0.01 vs. sham (Post-pump), $^{\$\$}$P<0.01 vs. IR + Veh + Veh (Post-pump).

6.4.3 Tissue weights

There was no significant difference in body weight among groups. Lung, left ventricular, heart and atrial weights as a ratio of body weight (BW) were significantly greater in the IR + Veh + Veh group compared to sham-operated rats (Table 6.1). Treatment with VCP746 bolus infusion at the start of reperfusion alone (IR + VCP746

+ Veh) led to a trend towards a reduction in all tissue to body weight ratios compared to the IR + Veh + Veh group.

	Sham + Veh + Veh	IR + Veh + Veh	IR + VCP746 + Veh	IR + Veh + VCP746	IR + VCP746 + VCP746	IR + Veh + Veh + PERI
BW (g)	416.1 ± 16.6	441 ± 10.1	431.5 ± 15.2	453 ± 13.5	446.1 ± 12.1	393.9 ± 6.3
HW:BW (mg/g)	2.66 ± 0.10	3.17 ± 0.06 ***	2.94 ± 0.06	2.77 ± 0.07 ##	2.82 ± 0.08 ##	2.71 ± 0.07 ###
LW:BW (mg/g)	3.32 ± 0.11	3.78 ± 0.11 **	3.64 ± 0.07	3.24 ± 0.10 ###	3.36 ± 0.09 ##	3.50 ± 0.08
LV:BW (mg/g)	1.86 ± 0.08	2.15 ± 0.04 **	2.00 ± 0.03	1.90 ± 0.05 #	1.91 ± 0.06 #	1.82 ± 0.06 ###
AW:BW (mg/g)	0.23 ± 0.01	0.34 ± 0.02 **	0.30 ± 0.03	0.29 ± 0.02	0.32 ± 0.02 **	0.30 ± 0.01

Table 6.1 Heart weight (HW), lung weight (LW), left ventricular weight (LV) and atrial weight (AW) as corrected with body weight (BW). Data expressed as mean ± SEM. **P<0.01, ***P<0.001 vs. sham. $^{\#}$P<0.05, $^{\#\#}$P<0.01, $^{\#\#\#}$P<0.001 vs. IR + Veh + Veh.

Rats in the IR + Veh + VCP746 and IR + VCP746 + VCP746 groups were found to have significantly lower tissue to body weight ratios compared to rats in the IR + Veh + Veh group, with the exception of AW:BW. Treatment with VCP746 or perindopril had no effect on AW:BW.

6.4.4 Echocardiography

Significant reductions in ejection fraction (EF) and fractional shortening (FS) were observed in IR + Veh + Veh rats compared to sham-operated rats (EF: 46.8% vs. 70.4%; FS: 16.5% vs. 48.8%; Fig. 6.4, Table 6.2). Rats in all VCP746- and PERI-treated groups had significantly increased EF and FS compared to rats treated with only vehicle in the IR + Veh + Veh group. Left ventricular end diastolic (LVEDV) and systolic volume (LVESV), and left ventricular internal diameter during diastole (LVIDd) and systole (LVIDs) in the VCP746- or PERI-treated animals were not significantly different compared to the IR + Veh + Veh group.

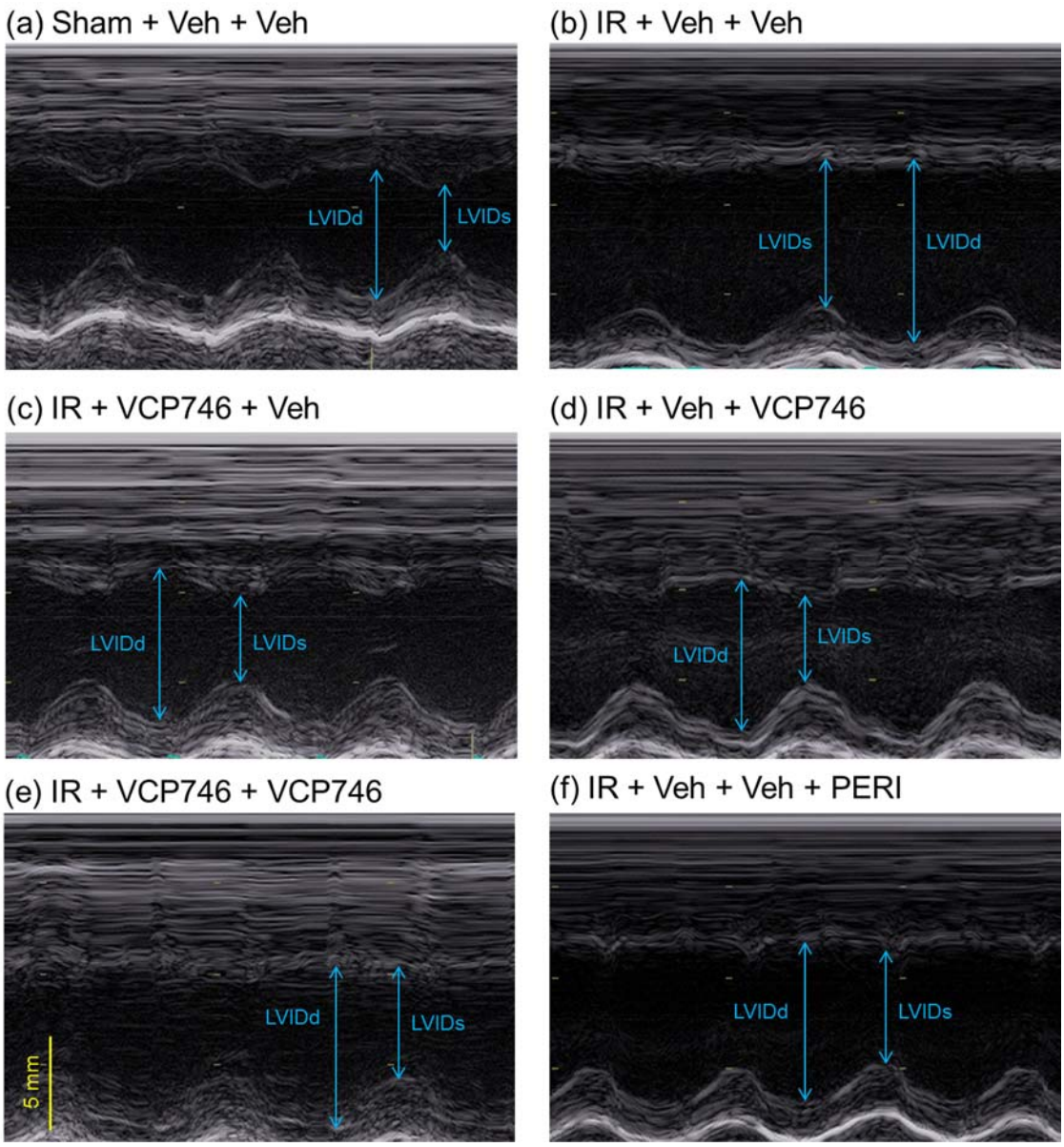

Figure 6.4 Representative 2D echocardiograms. LVIDd, left ventricular internal diameter during diastole; LVIDs, left ventricular internal diameter during systole. Fractional shortening (FS) = [(LVIDd – LVIDs)/LVIDd] x 100.

	Sham	IR + Veh + Veh	IR + VCP746 + Veh	IR + Veh + VCP746	IR + VCP746 + VCP746	IR + Veh + Veh + PERI
LVEF (%)	70.4 ± 1.6	46.8 ± 1.2 ****	60.2 ± 3.6 *, ##	56.7 ± 1.9 **, #	60.5 ± 2.9 *, ##	57.4 ± 2.9 **, #
LVEDV (mL)	0.51 ± 0.03	0.63 ± 0.04	0.64 ± 0.04	0.77 ± 0.05 **	0.72 ± 0.06 *	0.65 ± 0.04
LVESV (mL)	0.15 ± 0.01	0.33 ± 0.02 ***	0.26 ± 0.03	0.36 ± 0.02 ****	0.29 ± 0.04 **	0.27 ± 0.02 *
FS (%)	48.8 ± 1.7	16.5 ± 1.4 ****	32.4 ± 3.3 ***, ###	28.1 ± 1.7 ****, ##	31.6 ± 3.1 ***, ###	28.9 ± 2.9 ****, ##
LVIDd (mm)	7.48 ± 0.25	9.26 ± 0.39 **	9.16 ± 0.33 **	10.34 ± 0.28 ****	9.58 ± 0.31 ***	9.26 ± 0.35 **
LVIDs (mm)	3.83 ± 0.20	7.73 ± 0.36 ****	6.32 ±0.43 ***	7.46 ± 0.29 ****	6.54 ± 0.51 ****	6.68 ± 0.43 ****
LVPWD (mm)	2.06 ± 0.18	2.02 ± 0.12	2.12 ± 0.14	1.75 ± 0.16	1.90 ± 0.15	1.80 ± 0.08
SV (mL)	0.36 ± 0.02	0.30 ± 0.02	0.38 ± 0.03	0.44 ± 0.04 ##	0.43 ± 0.03 ##	0.37 ± 0.03
IVRT (ms)	21.1 ± 2.9	23.6 ± 1.8	21.4 ± 1.9	20.6 ± 1.0	20.1 ± 1.6	21.0 ± 1.7
LV Mass (g/m^2)	1.44 ± 0.05	1.81 ± 0.13	1.86 ± 0.13 *	1.74 ± 0.12	1.87 ± 0.08 *	1.51 ± 0.05
E wave velocity (m/s)	0.98 ± 0.07	0.97 ± 0.04	1.10 ± 0.04	1.07 ± 0.05	1.13 ± 0.06	0.97 ± 0.05
A wave velocity (m/s)	0.49 ± 0.04	0.54 ± 0.03	0.51 ± 0.06	0.40 ± 0.04	0.40 ± 0.04	0.51 ± 0.05
E/A ratio	2.30 ± 0.49	1.85 ± 0.09	2.77 ± 0.70	3.01 ± 0.34	3.26 ± 0.52	2.02 ± 0.15
E' wave velocity (cm/s)	4.05 ± 0.38	4.32 ± 0.17	4.38 ± 0.17	4.81 ± 0.31	4.22 ± 0.25	4.72 ± 0.24
A' wave velocity (cm/s)	2.88 ± 0.21	3.15 ± 0.24	3.23 ± 0.35	3.23 ± 0.32	3.06 ± 0.22	3.25 ± 0.22
E'/A' ratio	1.49 ± 0.24	1.37 ± 0.14	1.48 ± 0.18	1.59 ± 0.16	1.53 ± 0.13	1.48 ± 0.07

Table 6.2 Echocardiographic parameters at week 4. Data expressed as mean ± SEM. LVEF, left ventricular ejection fraction; LVEDV and LVESV, LV end diastolic and end systolic volume; FS, fractional shortening; LVIDd and LVIDs, LV internal diameter during diastole and systole; LVPWD, LV posterior wall dimension; SV, stroke volume; IVRT, isovolumic relaxation time. *P<0.05, **P<0.01, ***P<0.001, ****P<0.0001 vs. sham. $^{\#}$P<0.05, $^{\#\#}$P<0.01 $^{\#\#\#}$P<0.001 vs. IR + Veh + Veh.

6.4.5 Haemodynamic parameters

On completion of the study, haemodynamic measurements were obtained for all animals by pressure-volume loop analysis (Figure 6.5). End systolic pressure-volume relationship (ESPVR) was found to be significantly lower in the IR + Veh + Veh group compared to the sham group (Table 6.3). ESPVR in the IR + VCP746 + Veh, IR + VCP746 + VCP746 and IR + Veh + Veh + PERI was significantly improved compared to the IR + Veh + Veh group. There was also a trend towards improved ESPVR in the

IR + Veh + VCP746 group. There was no significant difference in heart rate (HR) among the groups, including the VCP746-treated groups, suggesting that chronic treatment with VCP746 does not affect heart rate.

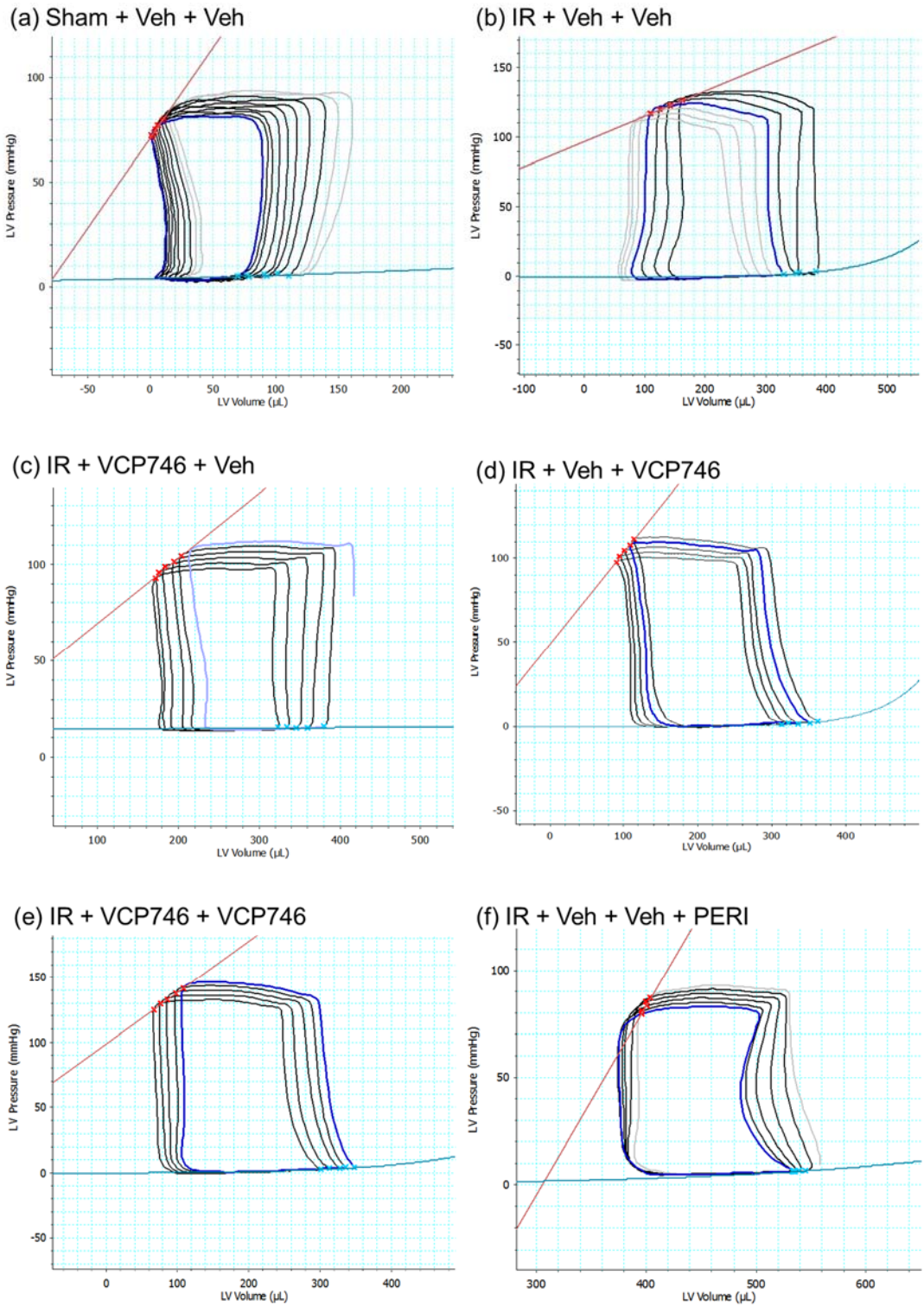

Figure 6.5 Representative pressure-volume loops

	Sham	IR + Veh + Veh	IR + VCP746 + Veh	IR + Veh + VCP746	IR + VCP746 + VCP746	IR + Veh + Veh + PERI
ESPVR (mmHg/µL)	0.94 ± 0.22	0.11 ± 0.02 **	0.87 ± 0.15 ##	0.60 ± 0.22	0.64 ± 0.12 #	0.79 ± 0.15 #
EDPVR (mmHg/µL)	0.018 ± 0.004	0.027 ± 0.004	0.021 ± 0.004	0.018 ± 0.005	0.022 ± 0.006	0.013 ± 0.004
dP/dt_{max} (mmHg/s)	7655 ± 751	7179 ± 543	8753 ± 1070	8007 ± 776	6959 ± 774	7495 ± 1057
$-dP/dt_{min}$ (mmHg/s)	8709 ± 808	6603 ± 410	8905 ± 822	7756 ± 674	6813 ± 934	6339 ± 531
Pes (mmHg)	116.5 ± 8.3	96.1 ± 4.5	130.4 ± 9.5 #	118.7 ± 12.1	113.4 ± 9.2	103.3 ± 8.2
Ped (mmHg)	7.3 ± 0.8	6.6 ± 1.5	9.9 ± 1.6	9.5 ± 1.8	11.7 ± 2.7	9.6 ± 1.2
PRSW (mmHg)	78.3 ± 11.1	50.8 ± 10.9	84.8 ± 10.4	75.7 ± 24.6	82.3 ± 13.7	83.3 ± 14.6
τ (ms)	10.5 ± 1.0	10.5 ± 0.6	11.4 ± 0.8	12.2 ± 1.3	13.5 ± 1.6	11.7 ± 0.4
HR (BPM)	348 ± 12	368 ± 8	371 ± 13	353 ± 9.9	350 ± 8.8	375 ± 14
SV (µL)	198 ± 33	183 ± 12	225 ± 20	230 ± 42	232 ± 18	223 ± 19

Table 6.3 Haemodynamic parameters assessed at week 4. Data expressed as mean ± SEM. ESPVR and EDPVR, slope of end systolic and end diastolic pressure-volume relationship; dP/dt_{max} and dP/dt_{min}, peak rates of pressure rise and decline; Pes and Ped, end systolic and diastolic pressures; PRSW, slope of preload recruitable stroke work relationship; τ, tau logistic; HR, heart rate; SV, stroke volume. **P<0.01 vs. sham. $^{\#}$P<0.05, $^{\#\#}$P<0.01 vs. IR + Veh + Veh.

6.4.6 Cardiac interstitial fibrosis

Cardiac interstitial fibrosis in the remote zone of the myocardium determined by picrosirius red staining was significantly increased in IR + Veh + Veh rats compared to sham-operated rats (Fig. 6.6a, b, g). Picrosirius red staining was significantly reduced in all VCP746- and perindopril-treated groups compared to the IR + Veh + Veh group (Fig. 6.6b-g).

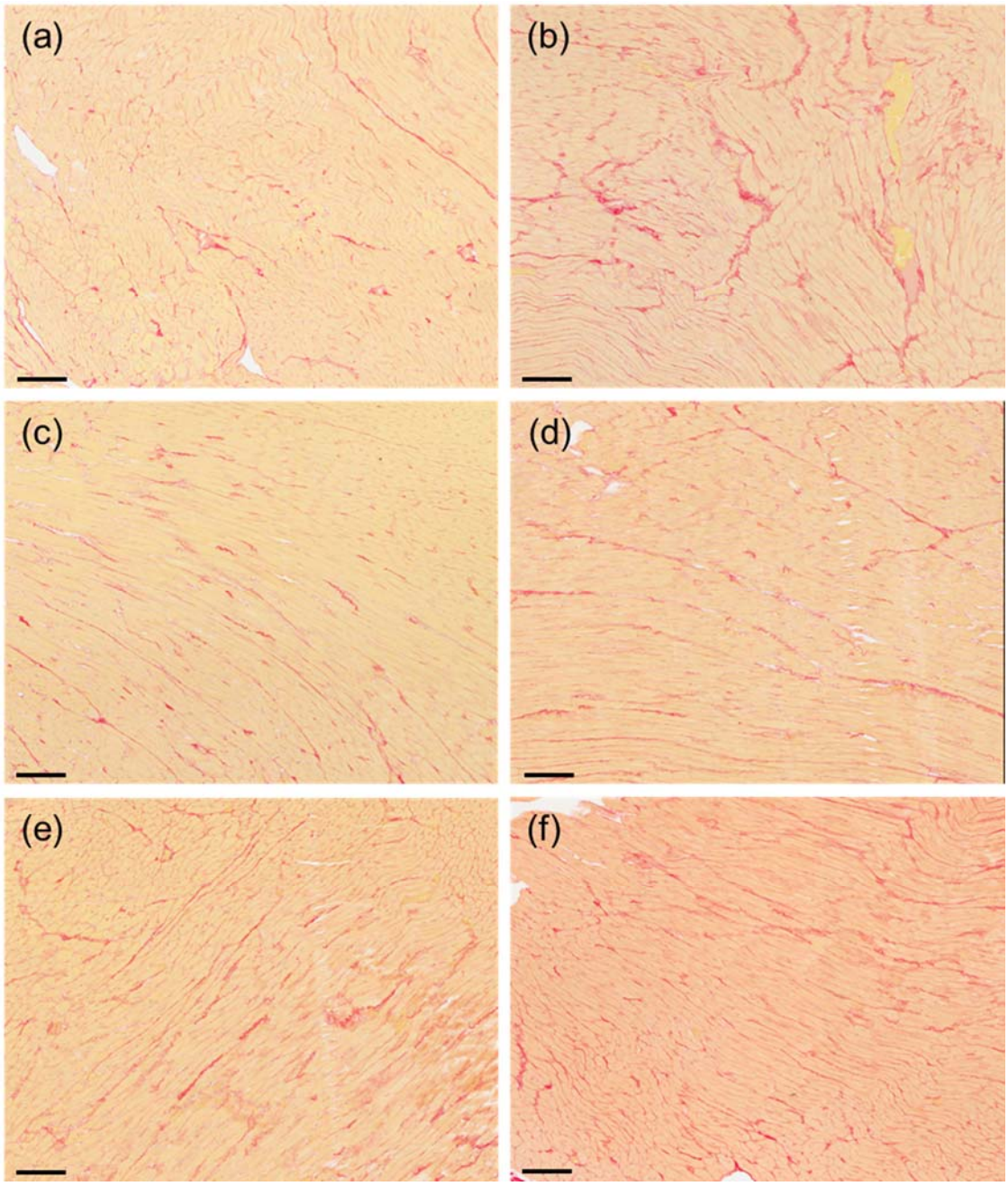
(a)
(b)
(c)
(d)
(e)
(f)

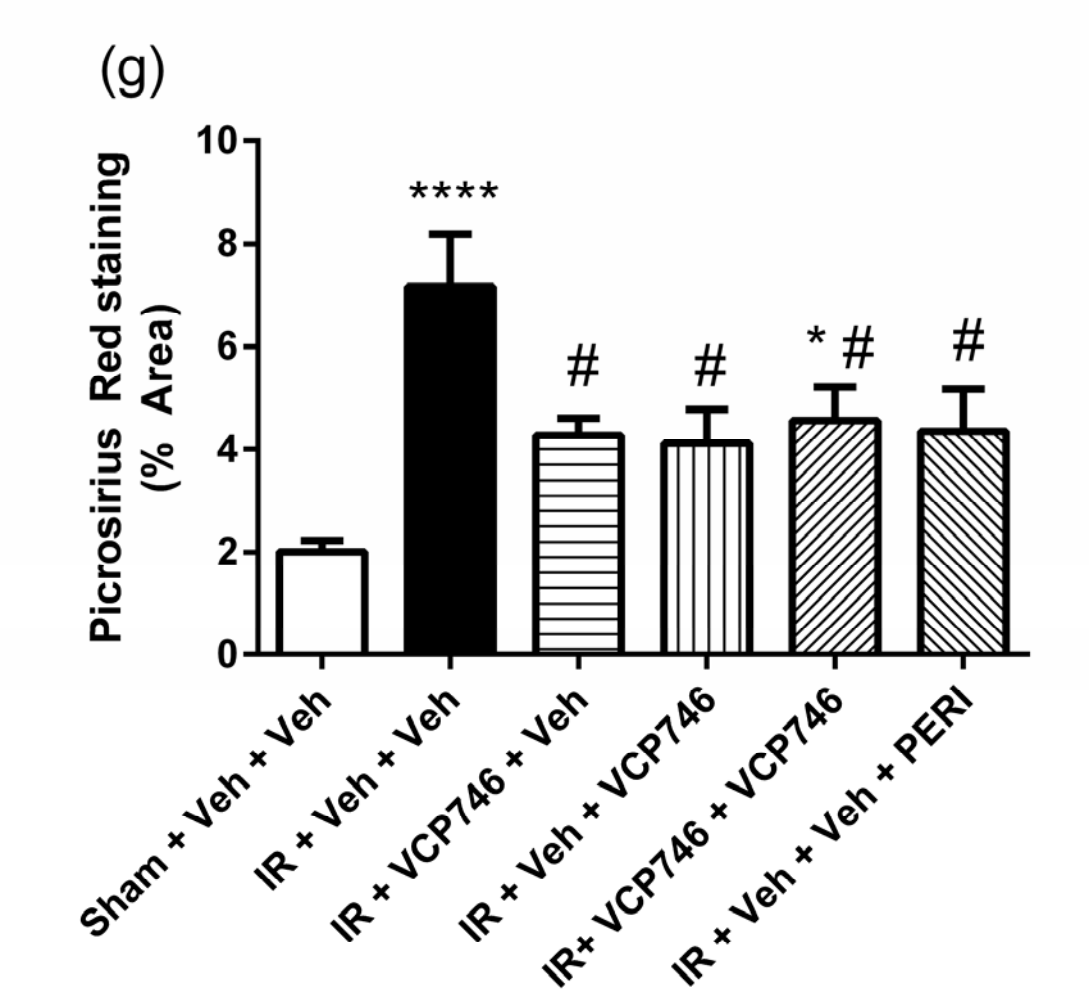

Figure 6.6 Representative images of the LV remote zone with picrosirius red staining for the following groups (a) Sham + Veh + Veh, (b) IR + Veh + Veh, (c) IR + VCP746 + Veh, (d) IR + Veh + VCP746, (e) IR + VCP746 + VCP746, (f) IR + Veh + Veh + PERI. Scale bar, 100 μm. Quantitation of picrosirius red staining (g) for all groups. Data expressed as mean ± SEM. *P<0.05, ****P<0.0001 vs. sham. #P<0.05 vs. IR + Veh + Veh.

6.4.7 Cardiac myocyte cross-sectional area

Myocyte cross-sectional area in the remote zone of the myocardium was elevated in IR + Veh + Veh rats compared to sham-operated rats (Fig. 6.7a, b, g). Myocyte size was significantly smaller in all VCP746- and PERI-treated animals compared to animals in

the IR + Veh + Veh group (Fig. 6.7b-g).

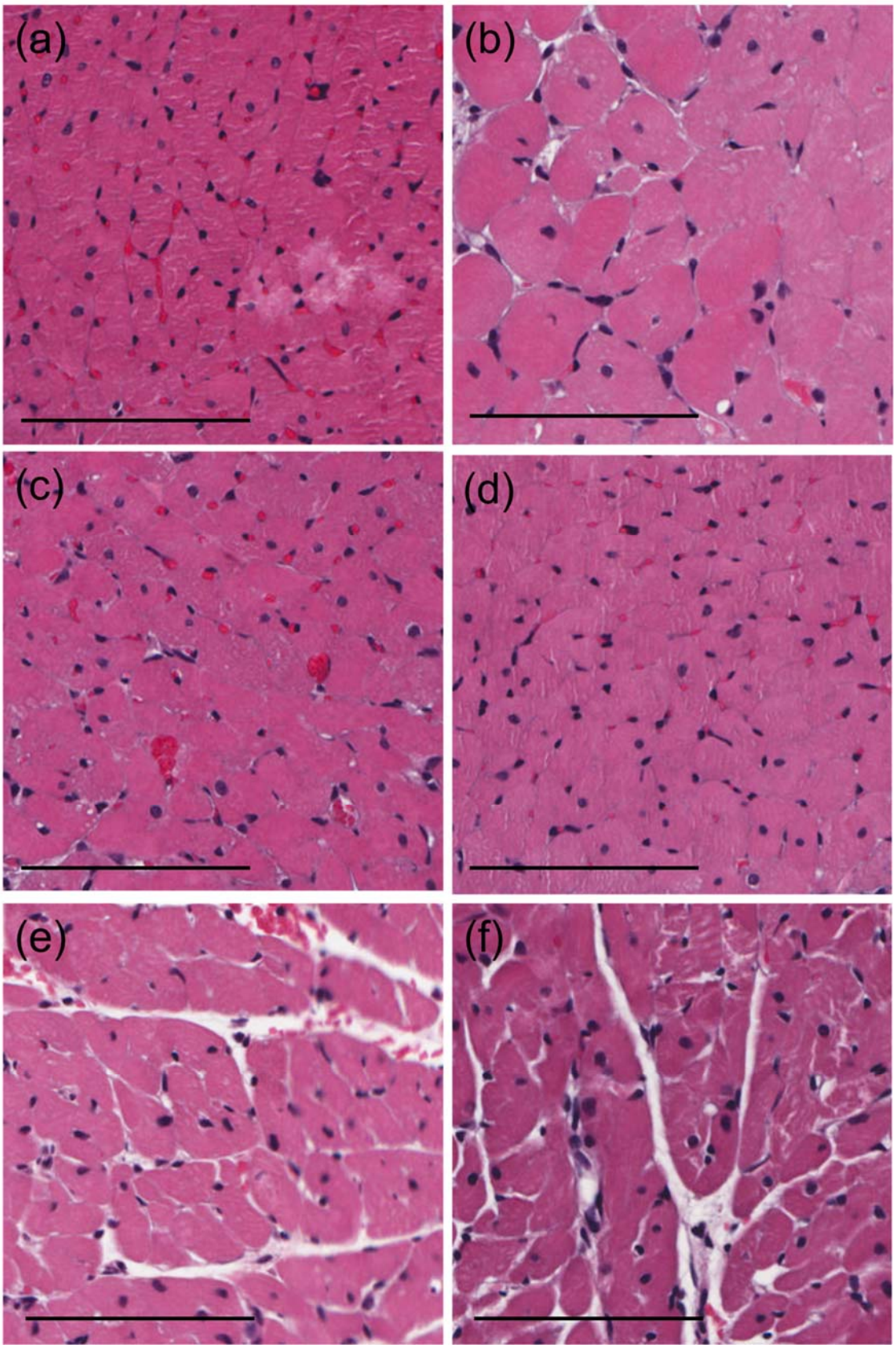

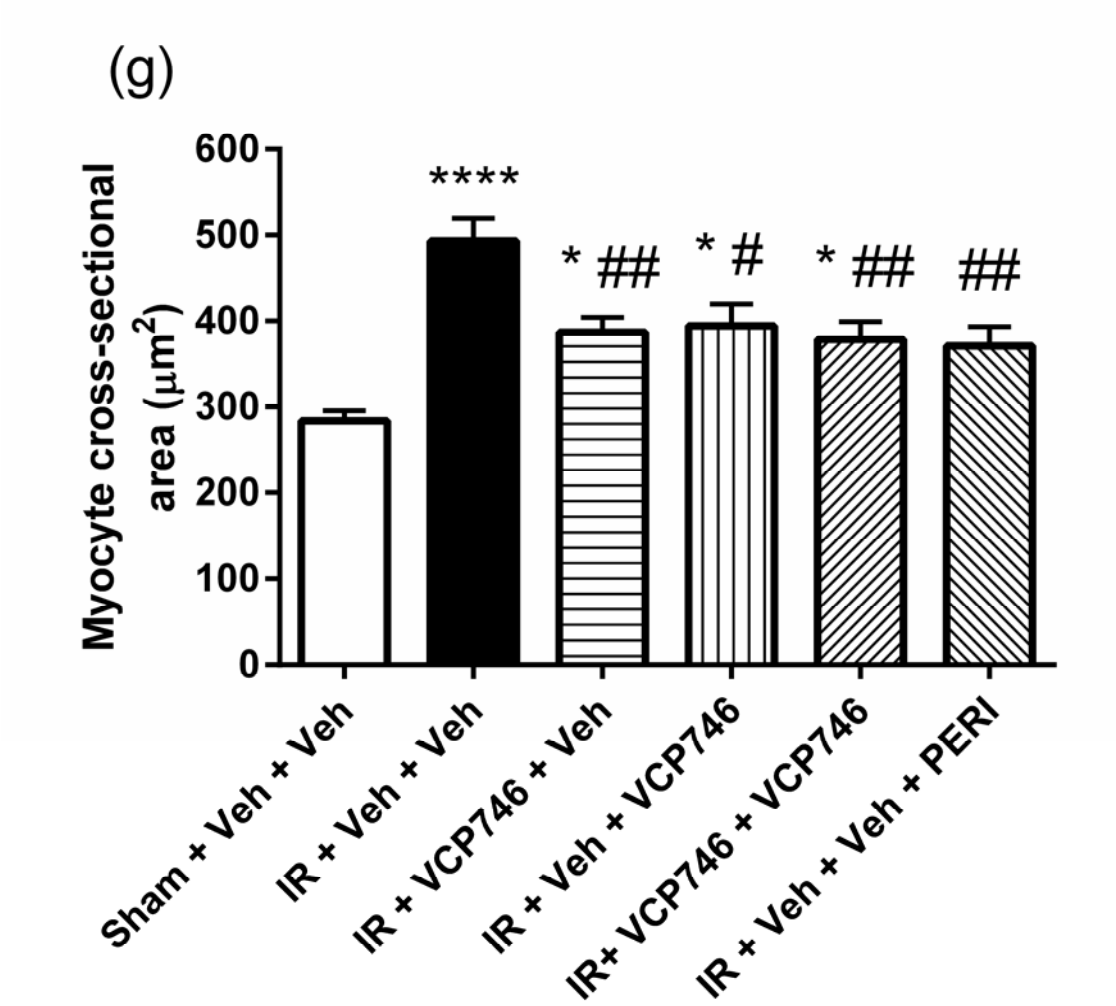

Figure 6.7 Representative images of the LV remote zone with haematoxylin and eosin staining of myocytes for the following groups (a) Sham + Veh + Veh, (b) IR + Veh + Veh, (c) IR + VCP746 + Veh, (d) IR + Veh + VCP746, (e) IR + VCP746 + VCP746, (f) IR + Veh + Veh + PERI. Scale bar, 100 μm. Quantitation of myocyte cross-sectional area (g) for all groups. Data expressed as mean ± SEM. *P<0.05, ****P<0.0001 vs. sham. $^{\#}$P<0.05, $^{\#\#}$P<0.01 vs. IR + Veh + Veh.

6.4.8 Cardiac collagen I

Collagen I expression in the remote zone of the myocardium was significantly elevated in the IR + Veh + Veh group compared to the sham group (Fig. 6.8a, b, g). Collagen I expression was significantly reduced in all VCP746- and perindopril-treated groups compared to the IR + Veh + Veh group (Fig. 6.8b-g).

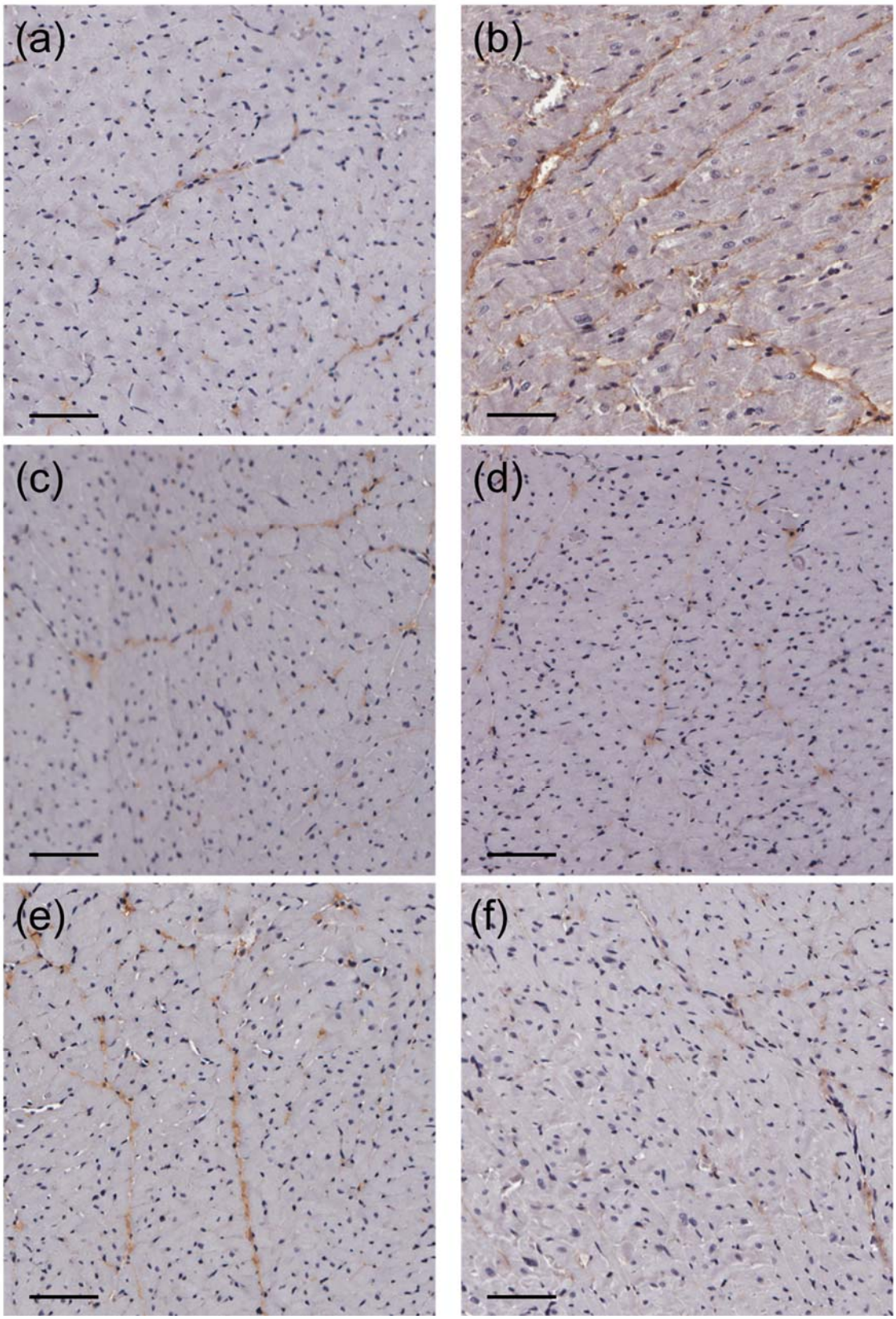
(a)
(b)
(c)
(d)
(e)
(f)

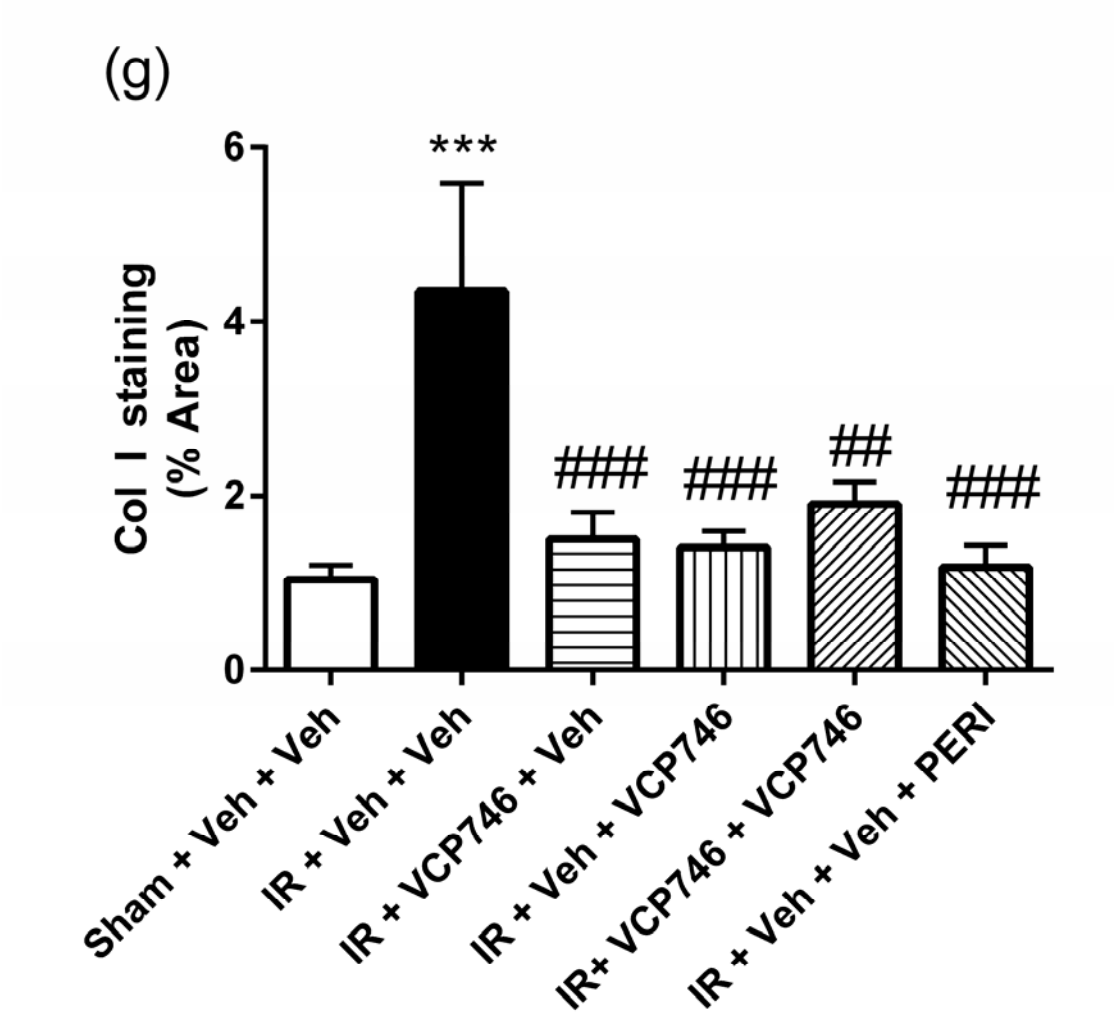

Figure 6.8 Representative images of the LV remote zone with collagen I immunostaining for the following groups (a) Sham + Veh + Veh, (b) IR + Veh + Veh, (c) IR + VCP746 + Veh, (d) IR + Veh + VCP746, (e) IR + VCP746 + VCP746, (f) IR + Veh + Veh + PERI. Scale bar, 100 μm. Quantitation of collagen I (g) for all groups. Data expressed as mean ± SEM. ***P<0.001 vs. sham. $^{\#\#}$P<0.01, $^{\#\#\#}$P<0.001 vs. IR + Veh + Veh.

6.4.9 CD68

Rats in the IR + VCP746 + Veh group had a significantly lower number of CD68+ macrophages within the infarct zone compared to the IR + Veh + Veh group (Fig. 6.9b, c, g). The other treatment groups including the IR + Veh + VCP746, IR + VCP746 +

VCP746 and IR + Veh + Veh + PERI groups showed a trend towards reduced CD68+ macrophage numbers, although this reduction was not statistically significant (Fig. 6.9b, d-g).

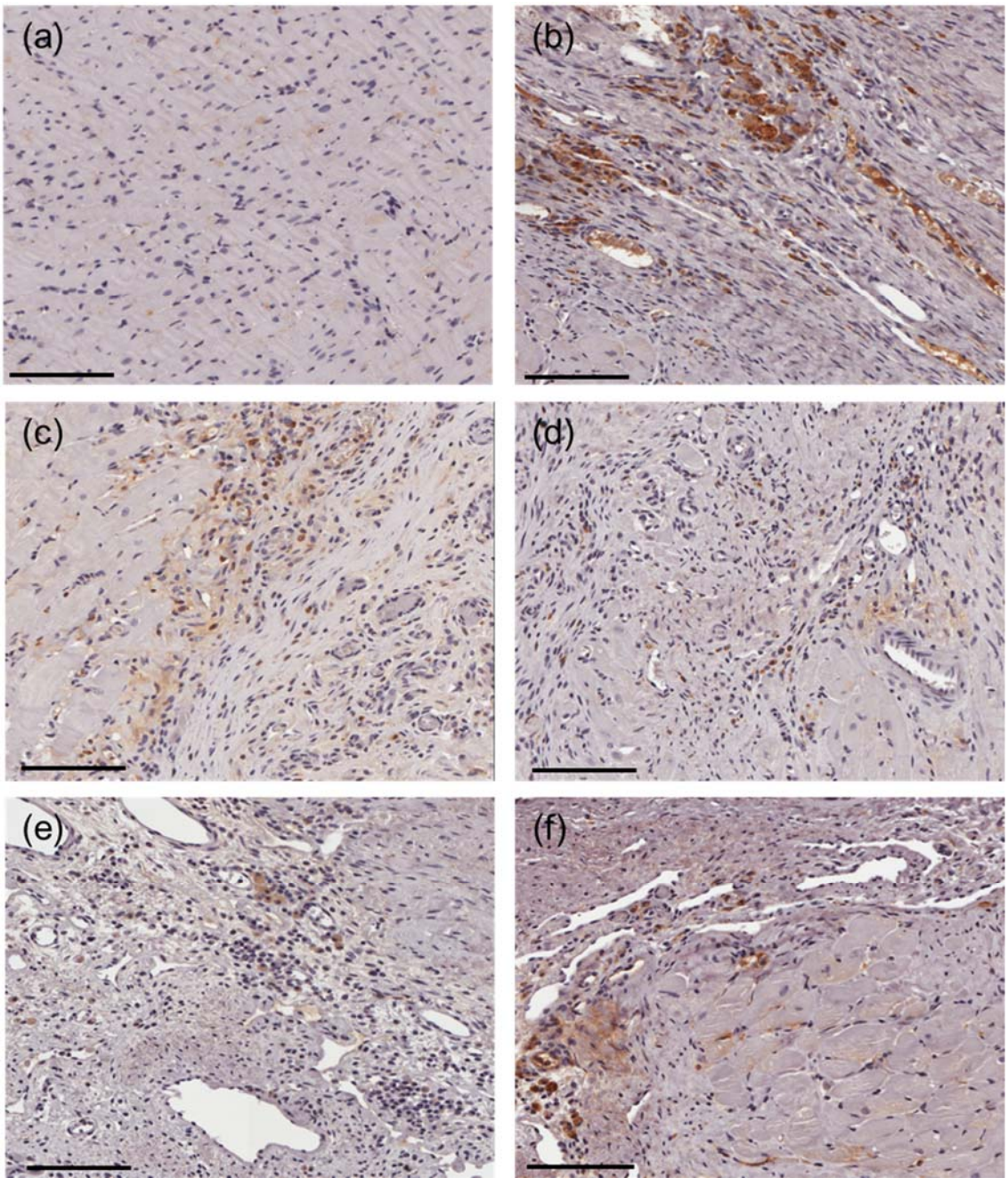

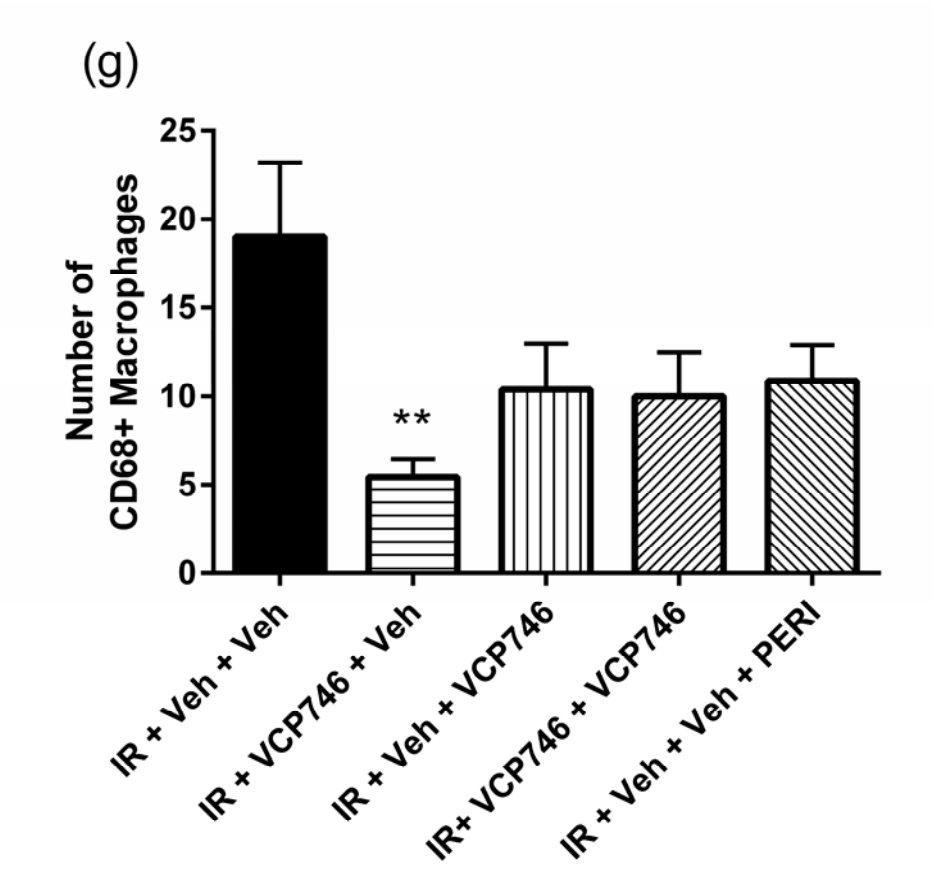

Figure 6.9 Representative images of the LV infarct zone with CD68 immunostaining of macrophage infiltration for the following groups (a) Sham + Veh + Veh (no infarct), (b) IR + Veh + Veh, (c) IR + VCP746 + Veh, (d) IR + Veh + VCP746, (e) IR + VCP746 + VCP746, (f) IR + Veh + Veh + PERI. Scale bar, 100 μm. Quantitation of CD68+ macrophages (g) for all groups (except sham). Data expressed as mean ± SEM. **P<0.01 vs. IR + Veh + Veh.

6.4.10 Western blot analysis

The levels of phospho-NFκB andTIMP2 in cardiac tissue were investigated. As a convergence point for various hypertrophic and fibrotic signalling pathways, the changes in phospho-NFκB levels between groups were of great interest. The protein expression of TIMP2 is also perturbed in post-MI cardiac remodelling especially in the context of fibrosis. No significant differences were observed in the levels of phospho-nuclear factor kappa B (NFκB) among all groups (Fig 6.10a, b). However, a significant

increase in the protein level of tissue inhibitor of metalloproteinases 2 (TIMP2) was found in the IR + Veh + Veh group compared to the sham group (Fig. 6.10c). TIMP2 levels were significantly reduced in all VCP746- and perindopril-treated groups compared to the IR + Veh + Veh group.

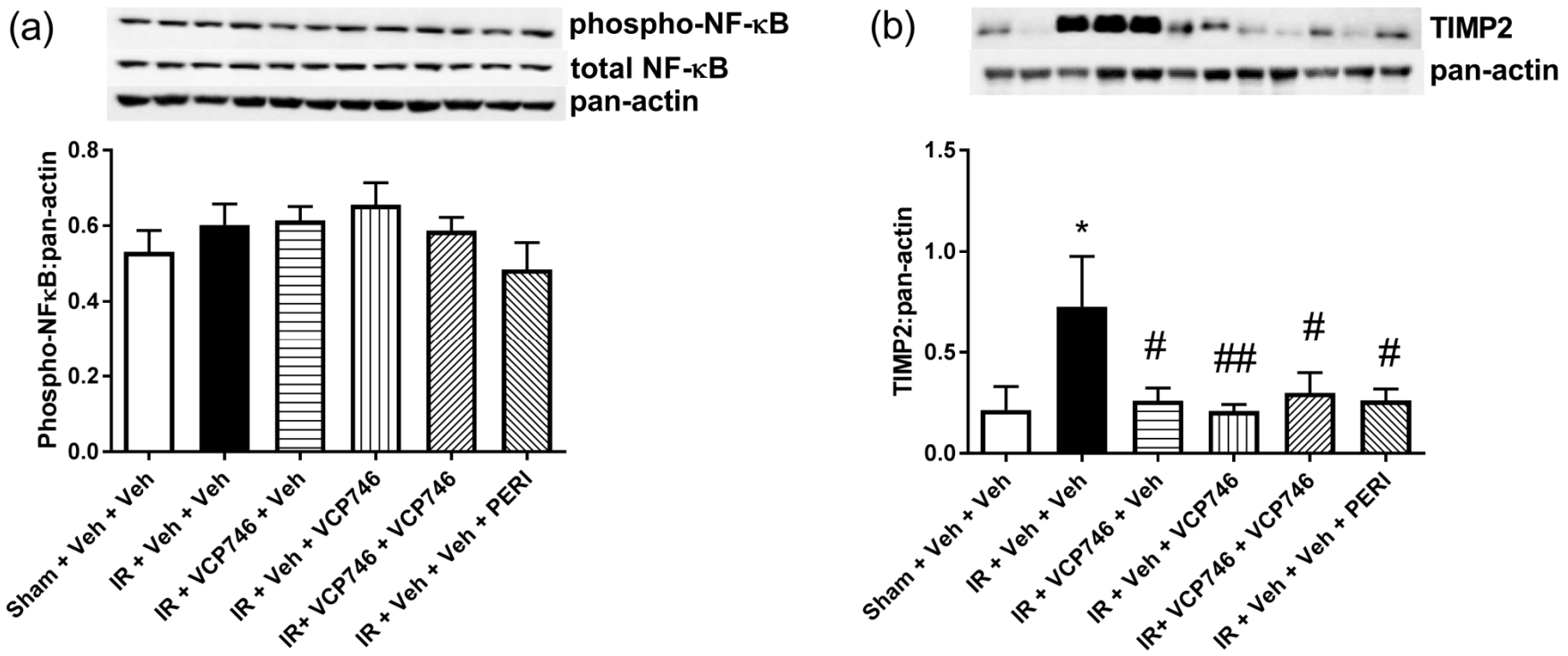

Figure 6.10 Representative blots and quantitation of the protein levels for (a) phospho-NFκB and (b)TIMP2 were normalised with pan-actin. Data expressed as mean ± SEM.

*P<0.05 vs. sham. #P<0.05, ##P<0.01 vs. IR + Veh + Veh

6.4.11 Cardiac mRNA expression

Real time PCR was used to determine gene expression of the pro-fibrotic markers, connective tissue growth factor (CTGF), collagen I (Col I), transforming growth factor-beta 1 (TGF-β1) and tissue inhibitor of metalloproteinase 2 (TIMP2), and the hypertrophic markers beta-myosin heavy chain (β-MHC) and atrial natriuretic peptide (ANP) (Fig. 6.11). The gene expression of all the pro-fibrotic and hypertrophic markers investigated was significantly increased in IR + Veh + Veh rats compared to sham-operated rats. The increased expression of pro-fibrotic genes CTGF, TGF-β1 and TIMP2 was significantly attenuated in all VCP746- and perindopril treated groups (Fig. 6.11a, c, d). Col I expression was also significantly attenuated in all VCP746- and perindopril- treated groups except the IR + VCP746 + Veh group, which only trended towards reduced expression (Fig. 6.11b). The increased expression of the hypertrophic marker ANP was significantly attenuated in all VCP746- and perindopril-treated groups (Fig. 6.11f) while β-MHC expression was significantly reduced in the IR + VCP746 + Veh, IR + VCP746 + VCP746 and IR + Veh + Veh + PERI groups, but not in the IR + Veh + VCP746 group (Fig. 6.11e).

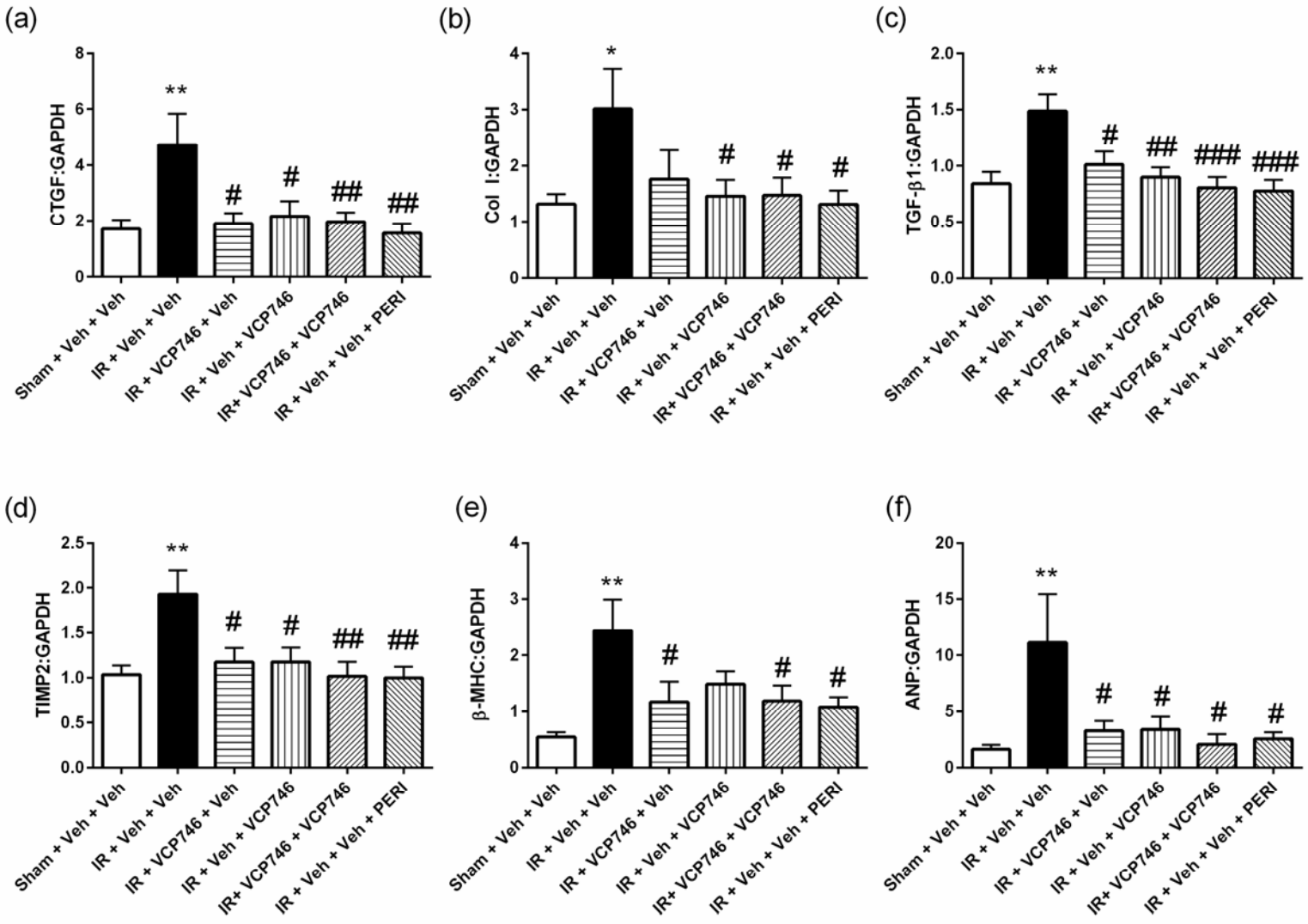

Figure 6.11 Cardiac mRNA expression of pro-fibrotic and hypertrophic markers (a) connective tissue growth factor (CTGF), (b) collagen I (Col I), (c) transforming growth factor-beta 1 (TGF-β1), (d) tissue inhibitor of metalloproteinase 2 (TIMP2), (e) beta-myosin heavy chain (β-MHC), and (f) atrial natriuretic peptide (ANP), expressed as a ratio of GAPDH. Data expressed as mean ± SEM. *P<0.05, **P<0.01 vs. sham. #P<0.05, ##P<0.01, ###P<0.001 vs. IR + Veh + Veh.

6.4.12 Renal function

No significant differences in serum creatinine, creatinine clearance (CrCl) or glomerular filtration rate (GFR) were observed among all groups (Table 6.4). However, rats in the IR + Veh + VCP746, IR + VCP746 + VCP746 and IR + Veh + Veh + PERI groups were found to have significantly reduced proteinuria compared to sham-operated and IR + Veh + Veh rats.

	Sham	IR + Veh + Veh	IR + VCP746 + Veh	IR + Veh + VCP746	IR + VCP746 + VCP746	IR + Veh + Veh + PERI
GFR (mL/min/kg)	7.40 ± 0.49	7.21 ± 0.43	7.13 ± 0.46	6.62 ± 0.34	6.44 ± 0.45	6.95 ± 0.62
CrCl (mL/min)	3.08 ± 0.20	3.11 ± 0.18	3.07 ± 0.20	3.07 ± 0.16	2.87 ± 0.20	2.71 ± 0.24
Serum creatinine (µmol/L)	27.4 ± 1.1	28.3 ± 1.1	29.8 ± 1.3	26.8 ± 1.4	27.5 ± 1.2	32.4 ± 4.4
Proteinuria (mg/day)	15.4 ± 1.1	14.5 ± 1.0	14.8 ± 0.9	9.7 ± 0.8 **, ##	10.1 ± 1.2 *, #	7.3 ± 0.9 ****, ####

Table 6.4 Renal function measured at week 4. No significant differences were found in the serum creatinine, creatinine clearance (CrCl) or glomerular filtration rate (GFR) among all groups. Proteinuria was significantly reduced in the IR + Veh + VCP746, IR + VCP746 + VCP746 and IR + Veh + Veh + PERI groups compared to the sham and IR + V + V groups. Data expressed as mean ± SEM. *P<0.05, **P<0.01, ****P<0.0001 vs. sham. $^{\#}$P<0.05, $^{\#\#}$P<0.01 $^{\#\#\#\#}$P<0.0001 vs. IR + Veh + Veh.

6.5 Discussion

In this chapter, we explored the effect of VCP746 treatment on cardiac remodelling and cardiac function post-MI. An ischaemia and reperfusion injury model was used instead of a permanent ligation model to replicate the clinical scenario where reperfusion therapy is performed and where mitigation of reperfusion injury is possible. The findings reveal that post-MI rats treated with VCP746 had significantly attenuated cardiac hypertrophy and fibrosis, and improved cardiac function compared to post-MI rats treated with only vehicle in the IR + Veh + Veh group, comparable to perindopril treatment.

Rats treated with VCP746 at the start of reperfusion had smaller infarct sizes compared to rats only treated with vehicle at reperfusion, consistent with the findings in Chapter 4. As such, while rats in the IR + VCP746 + Veh group were only treated with a single infarct-sparing bolus dose of VCP746 at reperfusion, this was thought to be sufficient to attenuate cardiac remodelling and preserve cardiac function. Indeed it has previously been demonstrated that infarct size is predictive of later LV remodelling. A study by Orn et al. concluded that there was a linear relationship between scar size and ejection fraction and LV volumes in humans (56). Watzinger and colleagues also observed a similar relationship between infarct size and ejection fraction and LV volumes using magnetic resonance imaging, albeit in rats (55). As such, interventions that reduce reperfusion injury and thus infarct size remain a valid means for mitigating maladaptive post-MI cardiac remodelling.

Consistent with the findings in Chapter 3 and 4, continuous delivery of VCP746 via minipump did not result in any change in blood pressure. This was in contrast to perindopril treatment which led to an expected decrease in blood pressure via the reduction of angiotensin synthesis. Haemodynamic measurements also revealed that continuous administration of VCP746 produced no effect on heart rate. This reinforces the findings of our previous studies where VCP746 was shown to have no effect on heart rate or blood pressure.

Results from echocardiographic and haemodynamic studies demonstrated reduced LV systolic function in rats from the IR + Veh + Veh group, as indicated by reduced ejection fraction, fractional shortening and ESPVR (relationship between pressure and volume in the LV when the myocardium reaches its maximum state of activation, the slope of which represents end-systolic elastance, an index of contractility) (256). Treatment with VCP746 or perindopril led to an improvement in these measures of

systolic function. In this model, diastolic function was largely unaffected as measures such as IVRT, E/A ratios, τ, and EDPVR (relating to the passive filling curve of the LV during diastole, the slope of which is the reciprocal of compliance) (257) were no different in the IR + Veh + Veh group compared to the sham group. This is reflective of the type (ischaemia and reperfusion injury) and duration (4 weeks) of the model used in this study, which is more representative of the clinical scenario but less injurious. As such, a study utilising a model that yields more severe cardiac injury and remodelling (such as an 8-week permanent ligation model) may be warranted to investigate the effects of VCP746 on not just systolic but also diastolic dysfunction.

Assessment of cardiac tissue weights, cardiac myocyte size and hypertrophic marker expression indicate cardiac hypertrophy in the IR + Veh + Veh group as all these measures were significantly elevated. Treatment with VCP746 or perindopril in general led to an improvement in these measures, indicative of an anti-hypertrophic effect. This outcome reinforces the findings of our *in vitro* study in Chapter 5 where VCP746 was shown to reduce ^{3}H-leucine incorporation along with ANP, β-MHC and α-SKA expression in cardiac myocytes. Interestingly, animals treated with only a bolus dose of VCP746 at reperfusion only trended towards reduced HW and LV to BW ratio, suggesting that infarct size reduction alone was not enough to significantly mitigate cardiac hypertrophy. This is in contrast to what was seen in measures of myocyte size and hypertrophic gene expression where bolus VCP746 significantly attenuated increases in both measures. We believe that due to the relatively small therapeutic window between IR + Veh + Veh and sham-operated animals, a significant effect from VCP746 bolus treatment could not be observed. Furthermore, the measurements of cell size and gene expression are inherently more sensitive methods compared to the measurement of tissue weight. As such, it may be premature to conclude that only

chronic VCP746 treatment is effective in reducing cardiac hypertrophy. As discussed above, an MI model generating a larger therapeutic window may be warranted to conclusively determine the role of bolus VCP746 treatment at reperfusion in reducing increases in cardiac tissue weight. Additionally, the increase in lung weight in IR + Veh + Veh animals compared to sham animals is suggestive of pulmonary congestion. Lung weight to body weight ratio was however significantly improved with chronic administration of VCP746, but not bolus VCP746 treatment at reperfusion.

Findings from picrosirius red and collagen I staining revealed significant fibrosis in the LV remote zone of hearts from the IR + Veh + Veh group. RT-PCR studies also show a significant increase in the expression fibrogenic genes such as collagen I, CTGF, TGF-β1 and TIMP2 (also increased TIMP2 protein expression) in the IR + Veh + Veh animals. Rats treated with VCP746 showed a significant improvement in these measures, indicative of an anti-fibrotic effect and again reflective of the findings in our *in vitro* study in Chapter 5.

Adenosine receptor agonists have previously been investigated by others in animal studies. In a study by Liao et al. (177) using a murine model of transverse aortic constriction (TAC), 2-Chloroadenosine (CADO; adenosine analogue) and CPA (A_1AR agonist) – delivered by 4-week minipump infusion – attenuated TAC-induced increases to heart to body weight ratio and myocyte size, and improved fractional shortening and dP/dt_{max}. These effects were blunted by the co-administration of DPCPX (A_1AR antagonist), indicating that CADO-mediated anti-hypertrophic effects and improvement in cardiac function were downstream of A_1AR activation. In a separate report, Wakeno et al. (102) found that post-MI (induced by permanent ligation of the LAD) rats had significantly reduced dP/dt_{max}, dP/dt_{min}, and fractional shortening, and increased cardiac myocyte size, collagen volume fraction in the remote zone, and fibrogenic (TIMP1,

MMP2, Col I, TGF-β1) and hypertrophic (ANP, BNP) gene expression. Treatment with CADO significantly improved cardiac function and reduced myocyte hypertrophy, interstitial fibrosis and fibrogenic/hypertrophic gene expression, suggesting that adenosine receptor activation reduces cardiac remodelling and improves post-MI cardiac function. This was confirmed when co-treatment with MRS1754 (A_{2B}AR antagonist) significantly blunted CADO-mediated improvement in function and reduction in fibrosis and fibrogenic gene expression. Co-treatment with DPCPX (A_1AR antagonist) had no effect on cardiac function but reversed the beneficial effects of CADO on cardiac myoycte hypertrophy and hypertrophic gene expression. The study concluded that the stimulation of the A_1AR and especially the A_{2B}AR attenuates cardiac remodelling and improves cardiac performance in post-MI rats.

The findings in these reports show that the beneficial effects of adenosine receptor agonists on cardiac remodelling and function are not species-dependent, at least in regards to rats and mice. Importantly, our present findings, where VCP746 (a potent agonist at the A_1 and A_{2B}AR) was also shown to improve cardiac function, and attenuate cardiac hypertrophy and fibrosis, are reflective of the outcomes of the studies by Liao et al. and Wakeno et al.. While the exact receptors involved in mediating these effects of VCP746 were not investigated in the present study, findings from our *in vitro* study (refer to Chapter 5) strongly implicate the A_{2B}AR and likely the A_1AR.

A significant concern in the long-term use of A_1AR agonists is kidney function. The A_1AR is known to reduce GFR by constricting afferent arterioles and mediating tubuloglomerular feedback (258, 259). Various clinical trials have also utilised A_1AR antagonists such as SLV320 (197) and rolofylline (198, 260) to increase diuresis and reduce renal impairment, albeit to mixed success. In the present study, VCP746 appears

to have no effect on GFR, CrCl or serum creatinine level, indicating that the compound does not reduce kidney function.

The potential pathways and mechanisms by which ARs reduce hypertrophy and fibrosis are not fully known. Interestingly, while signalling proteins such as ERK1/2 and p38 are involved in cardiac hypertrophy and adenosine-induced cardioprotection, adenosine receptor agonists have been shown to have no effect on these proteins in phenylephrine-stimulated cardiac myocytes (100). Evidence has shown, however, that activation of ARs can reduce Ang II and endothelin-1-stimulated RhoA activation and downstream cofilin phosphorylation, proteins that have previously been associated with cardiac hypertrophy (249). There is also evidence demonstrating that AR-mediated anti-hypertrophic effects are mediated by sarcolemmal (sarc) K_{ATP} and mitoK_{ATP} channels (176). As such, it appears that these channels are not only involved in acute cardioprotection (250, 251), but also in reducing cardiac myocyte hypertrophy. In cardiac fibroblasts, NECA-mediated reduction in Ang II-stimulated collagen production has been shown to involve an A_2AR-G_s-adenylate cyclase (AC)-cAMP-dependent pathway (252). Additionally, it was found that, rather than phosphorylating PKA, this pathway leads to the activation of exchange factor directly activated by cAMP (Epac). This A_2AR-mediated reduction in collagen production was also shown to be dependent on PI3K (a common downstream mediator of Epac) activation as treatment with LY-294002, a PI3K inhibitor, abrogated the effect of NECA on collagen production. Interestingly, ERK1/2 (also a downstream mediator of Epac) inhibition by PD-98059 (MEK-ERK1/2 inhibitor) had no effect on NECA-mediated reduction in collagen production. Findings from a study by Swaney et al. also highlighted the importance of the AC-cAMP-dependent pathway where forskolin (AC activator) was shown to inhibit collagen synthesis and collagen I protein expression in adult rat

cardiac fibroblasts (261). Importantly, they also showed that treatment with forskolin reduces transformation of fibroblasts to myofibroblasts (key contributor to fibrosis), as indicated by reduced α-smooth muscle actin (SMA) protein expression. While currently available data give us a glimpse of how ARs may reduce cardiac remodelling, more studies are required before the full extent of AR-mediated anti-hypertrophic/fibrotic pathways can be unravelled and understood. The present study has thoroughly investigated changes in gene expression mediated by IR and VCP746 intervention. However, the signalling pathways that lead to and result from these gene expression changes have not been investigated. This remains a limitation to the present study and as such, further studies elucidating signalling pathways modulated by VCP746 are warranted.

Overall, the findings of this study suggest that VCP746 reduces cardiac remodelling secondary to myocardial infarction and improves cardiac function. The administration of VCP746 at reperfusion or as a constant infusion appears to be just as effective separately or combined. As such, VCP746-mediated infarct size reduction is as effective as the direct anti-hypertrophic/fibrotic effects of VCP746 (but not synergistic) in reducing LV remodelling and preserving LV function. In addition, VCP746 treatment appears to be similarly effective compared to ACEI treatment, which is the current first-line therapy for post-MI heart failure, and thus warrant further investigation. Future studies using aged (24 months) instead of juvenile rats may be warranted as this would be more reflective of the demographic most affected by post-MI heart failure (262).

Chapter 7 General Discussion

7.1 VCP746 and ischaemia and reperfusion injury

The major finding in this thesis with regards to the infarct-sparing effect of VCP746 is that VCP746 is cardioprotective in isolated hearts and whole animals without causing any disturbance in heart rate or blood pressure. In both the Langendorff-perfused isolated rat heart and acute rat myocardial infarction models, the duration for myocardial ischaemia and reperfusion were selected based on our laboratory's previous work and the work of others (45, 48, 125, 126). We found, in the present thesis, that the 30 min/60 min and 30 min/120 min ischaemic/reperfusion protocol used in the isolated rat heart and rat myocardial infarction studies, respectively, produced an appreciable therapeutic window for VCP746 intervention at reperfusion without causing catastrophic and irreversible injury to the myocardium. The final infarct size of control animals in the acute and long-term myocardial infarction studies were observed to be slightly different at 52.3% and 40%, respectively. This discrepancy seen in the two *in vivo* studies is likely due to differences in infarct size analysis methods; in the acute rat myocardial infarction study, infarct size was visualised using Evans Blue/TTC staining and calculated as a percentage of area at risk while in the long-term rat myocardial infarction study, infarct size was visualised with picrosirius red staining and calculated as an averaged percentage of the endocardial and epicardial scarred circumferences of the left ventricle. In the Langendorff-perfused isolated heart model, the final infarct size was noticeably smaller than in the *in vivo* studies at 32.1%. This is perhaps unsurprising as the protocol used in the isolated heart model to induce ischaemia (global no-flow ischaemia) is vastly different to that in the *in vivo* studies (regional ischaemia). During global no-flow ischaemia, cardiac function measured as LVDP, dP/dt_{max}, and heart rate were not detectable in the isolated hearts. In contrast, hearts in our whole animal studies remain largely functional even during induction of regional

ischaemia via LAD occlusion. As such, the smaller infarct size seen in the isolated hearts could be due to reduced oxygen and ATP demand as a result of the lack of mechanical function. In addition, final infarct size in whole animals is also influenced by the extent of inflammation, a component which is not present in isolated hearts (172). When compared to the findings of others who have used similar protocols in *ex vivo* or *in vivo* studies, infarct sizes in our present studies were comparable (Table 7.1).

Reference	**Model**	**Ischaemia and Reperfusion Duration**	**Infarct size (%)**
***Ex vivo* models**			
Urmaliya et al. (45)	Langendorff-perfused isolated rat heart model	30 min global no-flow ischaemia + 60 min reperfusion	35.0%
Testai et al. (263)	Langendorff-perfused isolatd rat heart model	30 min global no-flow ischaemia + 120 min reperfusion	40.5%
***In vivo* models**			
Lasley et al. (125)	Rat myocardial infarction model	25 min regional ischaemia (left coronary artery occlusion) + 120 min reperfusion	51.0%
Yaoita et al. (264)	Rat myocardial infarction model	30 min regional ischaemia (left coronary artery occlusion) + 24 hr reperfusion	53.9%

Table 7.1 Infarct size comparison between studies with similar ischaemia and reperfusion injury protocol. Infarct sizes in studies using similar protocols were comparable to infarct sizes reported in our *ex vivo* and *in vivo* studies.

Between our present studies, infarct size reduction mediated by VCP746 was greater in the isolated heart model (55% infarct size reduction), compared to the acute and long-term rat myocardial infarction models (34% and 44% infarct size reduction, respectively). This discrepancy between the *ex vivo* and *in vivo* models may again be due to factors present in whole animals but not in isolated hearts that can exacerbate

cardiac injury, such as inflammation (172). However, when compared to prototypical agonists used in the respective studies, no differences in infarct-sparing effect were observed between VCP746 and prototypical agonists, suggesting that VCP746 is as efficacious as the prototypical AR agonists. The magnitude by which VCP746 reduces final infarct size in this thesis is comparable to that reported in other studies also investigating adenosine receptor-mediated cardioprotection. In isolated rat hearts subjected to 30 min/60 min ischaemia/reperfusion injury, Urmaliya et al. observed that CPA (100 nM), infused at reperfusion, reduced infarct size by 50% (45). In whole rats subjected to 25 min of ischaemia induced by left coronary artery occlusion and 120 min of reperfusion, Lasley et al. reported that NECA (10 μg/kg), administered 10 min before ischaemia, reduced infarct size by 36% (125).

In this thesis, VCP746 was shown to have no effects on heart rate or blood pressure at concentrations that confer maximal cardioprotection. We hypothesise that as a biased agonist, VCP746 stabilises receptor conformations that preferentially activates signalling pathways that promote cardioprotection while sparing pathways that promote heart rate reduction, unlike prototypical agonists which would indiscriminately activate both pathways. However, the bias profile that results in VCP746-mediated cardioprotection without bradycardia remains largely undetermined. Previous work in our lab has shown that VCP746 activates the 'Reperfusion Injury Salvage Kinase (RISK) Pathway', which includes pro-survival protein kinases ERK1/2 and Akt (205, 237). Evidence also suggests that VCP746 is biased away from calcium mobilisation pathways in CHO cells (237). Reperfusion injury is hallmarked by changes in calcium handling, often resulting in cytotoxic intracellular concentrations. As such, it is plausible that an agonist, such as VCP746, with a reduced ability to stimulate release of intracellular calcium stores could be used at concentrations that promote cytoprotection

but do not contribute to calcium overload (265). Studies validating the cardioprotective signalling profile of VCP746 in native systems such as isolated cardiac myocytes or isolated hearts are therefore warranted. The mechanism behind the lack of chronotropic effects observed in VCP746 is also undetermined at present. We hypothesise that this may be due to a lack of coupling to G protein-coupled inwardly rectifying K^+ (GIRK) channels which conduct I_{KAdo}. As such, electrophysiological studies on atrial tissue may be warranted to compare and contrast the electrophysiological effects between VCP746 and prototypical agonists on GIRK channels (266).

7.2 VCP746 and cardiac remodelling

An abundance of evidence show that activation of adenosine receptors on cardiac cells confers anti-hypertrophic/fibrotic effects. We hypothesised that as a potent agonist at the A_1 and A_{2B}AR, VCP746 is also anti-hypertrophic and anti-fibrotic in cardiac cells. VCP746 was first screened in an *in vitro* model and found to have potent anti-hypertrophic and anti-fibrotic effects in cardiac myocytes and cardiac fibroblasts, respectively. Having achieved encouraging outcomes in the *in vitro* study, the anti-remodelling effect of VCP746 was further investigated in a long-term rat myocardial infarction model where VCP746 was found to reduce cardiac remodelling and improve cardiac function in post-MI rats. Whether through infarct size reduction alone, direct anti-hypertrophic/fibrotic effects alone or a combination of both, VCP746 was observed to be as effective as perindopril in reducing cardiac remodelling and improving post-MI cardiac function. The A_1 and A_{2B}AR – both targets of VCP746 – play a significant role in mediating these effects. While the majority of animal studies clearly show that A_1AR activation reduces cardiac hypertrophy and preserves function (177, 267), the role of the A_{2B}AR has been subject to much controversy. In this thesis,

we observed that the anti-fibrotic effect of VCP746 was mediated by the activation of A_{2B}AR as only co-treatment with PSB603 (A_{2B}AR antagonist), and not antagonists of other AR subtypes, abolished the inhibitory effect of VCP746 on collagen synthesis and fibrogenic gene expression in isolated cardiac fibroblasts. This strongly suggests that the anti-fibrotic effect seen in our *in vivo* study is also A_{2B}AR-mediated. A study in post-MI rats by Wakeno and colleagues found that 2-Chloroadenosine (CADO) significantly improved cardiac function and attenuated MI-induced increase in collagen volume fraction and expression of fibrogenic genes and proteins. The effects by CADO were blunted by the co-treatment of MRS1754, an A_{2B}AR antagonist, suggesting a beneficial role for A_{2B}AR activation (102). These outcomes are also supported by numerous *in vitro* studies that have shown A_{2B}AR-mediated anti-fibrotic effects in cardiac fibroblasts (102, 121, 128, 179, 268). In contrast to the observations of Wakeno and colleagues, a study by Toldo et al. found that GS-6201 (a selective A_{2B}AR antagonist)-treated MI mice had improved echocardiographic measures of cardiac function and remodelling, and reduced plasma levels of inflammatory markers such as TNF-α and IL-6 (269). In a separate report, the same group observed that GS-6201-treatment in post-MI rats improved EF and reduced ventricular tachycardia inducibility, non-MI fibrosis and plasma levels of IL-6, TGF-β1 and BNP (270). This inconsistency in findings may be a result of the use of different models of myocardial ischaemia/cardiac remodelling, different protocols for agonist/antagonist administration or different selectivity of adenosine receptor ligands for the adenosine receptor subtypes. As such, a study utilising A_{2B}AR knock-out mice may be of value to provide further clarification on the role of A_{2B}AR in post-MI cardiac remodelling and heart failure.

While we were able to clearly show the role of A_{2B}AR in mediating the anti-fibrotic effects of VCP746, we have not been as successful in determining the AR subtype(s) responsible for the anti-hypertrophic effect of VCP746. The bulk of the evidence in the literature strongly implicates a role for A_1AR activation in mediating anti-hypertrophic effects in cardiac myocytes (70, 100, 177). However, using various subtype-selective AR antagonists such as SLV320, DPCPX, KW3902 (A_1AR antagonists), SCH442416 (A_{2A}AR antagonist) and PSB603 (A_{2B}AR antagonist), separately or in combination, we have not been able to significantly attenuate VCP746-mediated inhibition of cardiac myocyte hypertrophy (data not shown). This may be due to the unique bitopic pharmacology of VCP746, or the treatment protocol and assay conditions used in our study. There is also a possibility that the anti-hypertrophic effect of VCP746 is an off-target effect. The use of AR (especially A_1AR) knock-out or knock-down cardiac myocytes to determine the receptor subtype(s) responsible for the effects displayed by VCP746 (assuming VCP746 is not acting via an off-target effect) is therefore warranted.

In the present thesis, the signalling pathways responsible for these anti-hypertrophic/fibrotic effects remain unelucidated. As such, functional assays and Western blot analyses will be of great use in future efforts of understanding the mechanisms by which VCP746 reduces fibrosis and hypertrophy. In addition to mechanistic studies, the long-term myocardial infarction model used in the present study could also be extended to include clinically relevant complications such as age and cardiorenal syndrome. The young rats used in the present study are not representative of the majority of post-MI heart failure patients in the clinical setting who are mostly elderly. The use of aged rats will provide invaluable insight into the effectiveness of VCP746 treatment in the elderly given that previous studies suggest

the possibility of age-dependent changes in adenosine receptor expression in the heart (271, 272). Cardiorenal syndrome is generally described as a disorder of the heart and kidney whereby dysfunction of one organ induces dysfunction of the other. In heart failure patients, renal dysfunction is a common complication that leads to poor clinical outcomes (273). A study investigating the effectiveness of VCP746 in the combined setting of MI and renal dysfunction is therefore also warranted. Experimental models where post-MI animals are subjected to subtotal nephrectomy to induce kidney disease may be of use for this purpose (274).

Overall, the outcomes of this thesis are encouraging and suggest that with further research and development, biased adenosine receptor agonists such as VCP746 may represent a safe and effective therapy in future for the treatment of MI and associated heart failure.

Appendices

Appendix 1: VCP746, a novel A_1 adenosine receptor biased agonist, reduces hypertrophy in a rat neonatal cardiac myocyte model

This peer reviewed article was published in the fourth PhD year in the *Clinical and Experimental Pharmacology and Physiology* 2016; 43: 976-982.

Appendix 2: The hybrid molecule, VCP746, is a potent adenosine A_{2B} receptor agonist that stimulates anti-fibrotic signalling

This peer reviewed article was published in the fourth PhD year in the *Biochemical Pharmacology* 2016; 117; 46-56.

Appendix 3: Pilot pharmacokinetic study for *in vivo* rat myocardial infarction model

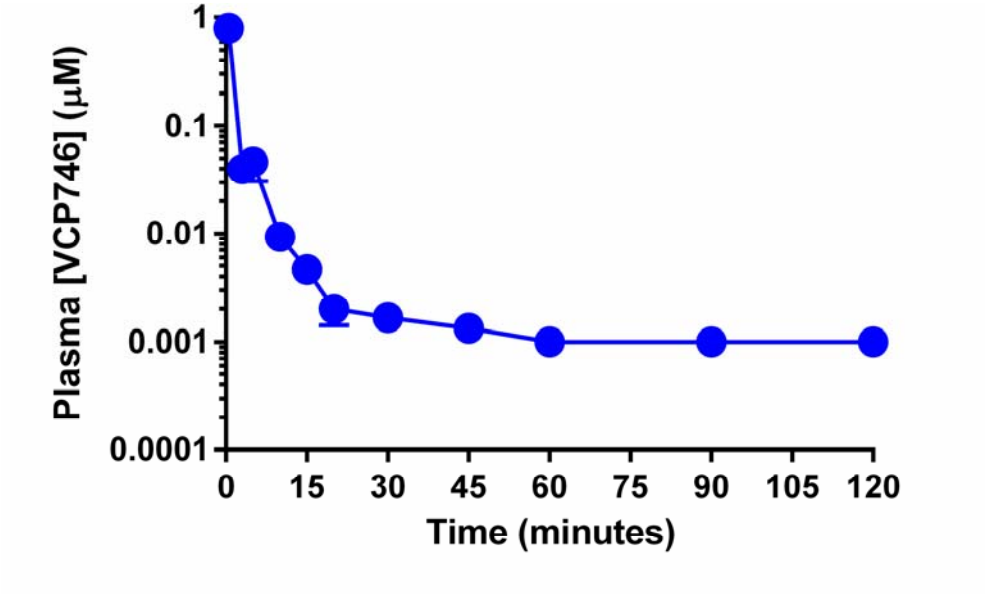

Supp Figure 1 Plasma concentration (μM) over time (min) for VCP746 following a single bolus 100 μg/kg dose administered intravenously. Data expressed as mean ± SEM, n = 3.

Appendix 4: Effect of VCP746 on renal mesangial cell collagen synthesis

Methods

Rat renal mesangial cells (RMC) were cultured and maintained in low glucose (1 g/L) DMEM in the presence of 1% antibiotic/antimycotic and 10% foetal bovine serum. Cells were maintained at 37˚C in a 5% CO_2 humidified incubator. RMC collagen synthesis was determined by ^{3}H-proline incorporation similar as for NCF in Chapter 5. RMC were seeded at a density of 1 x 10^4 cells/well in 12-well plates and incubated overnight prior to serum starvation with 0.1% BSA for 48 h. RMC were pre-treated in the absence or presence of the novel adenosine receptor agonist VCP746 for 1 h. When adenosine receptor antagonists were used, they were added 45 min prior to the addition of VCP746. RMC were then stimulated with TGF-β1 and ^{3}H-proline was added to each well. After 48 h, cells were washed with cold PBS and harvested by trichloroacetic acid (10%) precipitation on ice for 30 min before being solubilised with 1 M NaOH overnight at 4˚C. The samples were then neutralised with 1 M HCl and radioactivity determined using scintillation counting.

Materials

SLV320 (A_1AR selective antagonist) and SCH442416 (A_{2A}AR selective antagonist) were purchased from Sigma-Aldrich, Castle Hills, NSW, Australia. PSB603 (A_{2B}AR selective antagonist) was purchased from Tocris Bioscience, Bristol, UK. The novel A_1/A_{2B}AR agonist VCP746 was synthesised at the Monash Institute of Pharmaceutical Sciences. Stock solutions were prepared in DMSO and kept at – 20ºC until used.

Statistical analysis

Data expressed as mean ± SEM. Statistical significance was defined as P<0.05 as determined by one-way analysis of variance (ANOVA) with Dunnett's multiple comparisons post hoc analysis. All statistical analyses were performed using GraphPad Prism 6.

Results

To determine whether the anti-fibrotic effects of VCP746 were confined to cardiac cells (refer to Chapter 5), we investigated the ability of VCP746 to reduce collagen synthesis in RMC (Supp Fig. 2).

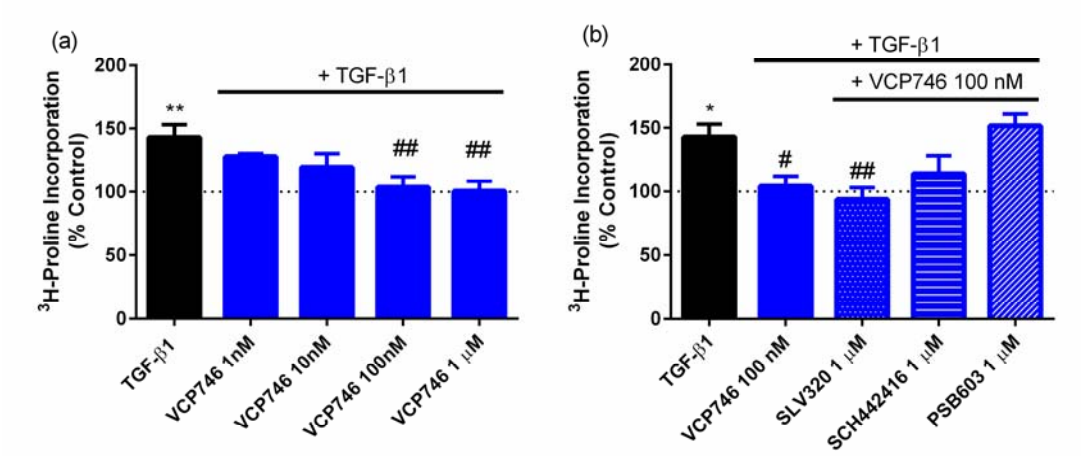

Supp Figure 2 VCP746 stimulated potent inhibition of RMC collagen synthesis. (a) VCP746 mediated inhibited TGF-β1-stimulated collagen synthesis in a concentration-dependent manner as determined by ^{3}H-proline incorporation. (b) The inhibitory effect of VCP746 on TGF-β1-stimulated collagen synthesis was abolished by PSB603, an A_{2B}AR antagonist, but not SLV320 (A_1AR antagonist) and only partially reversed by SCH442416 (A_{2A}AR antagonist). Data expressed as mean ± SEM, n = 3-4. *P<0.05, **P<0.01 vs. control. $^{\#}$P<0.05, $^{\#\#}$P<0.01 vs. TGF-β1.

Similar to NCF, pre-treatment of RMC with VCP746 (1 nM – 1 μM) led to a concentration-dependent reduction in TGF-β1-stimulated ^{3}H-proline incorporation (Supp Fig. 2a). This reduction in ^{3}H-proline incorporation was completely abolished in the presence of PSB603, indicating an A_{2B}AR-mediated effect, but not with SLV320 (A_1AR antagonist) and only partially reversed in the presence of SCH442416 (A_{2A}AR antagonist) (Supp Fig. 2b).

Appendix 5: VCP746 plasma concentration in long-term rat myocardial infarction model

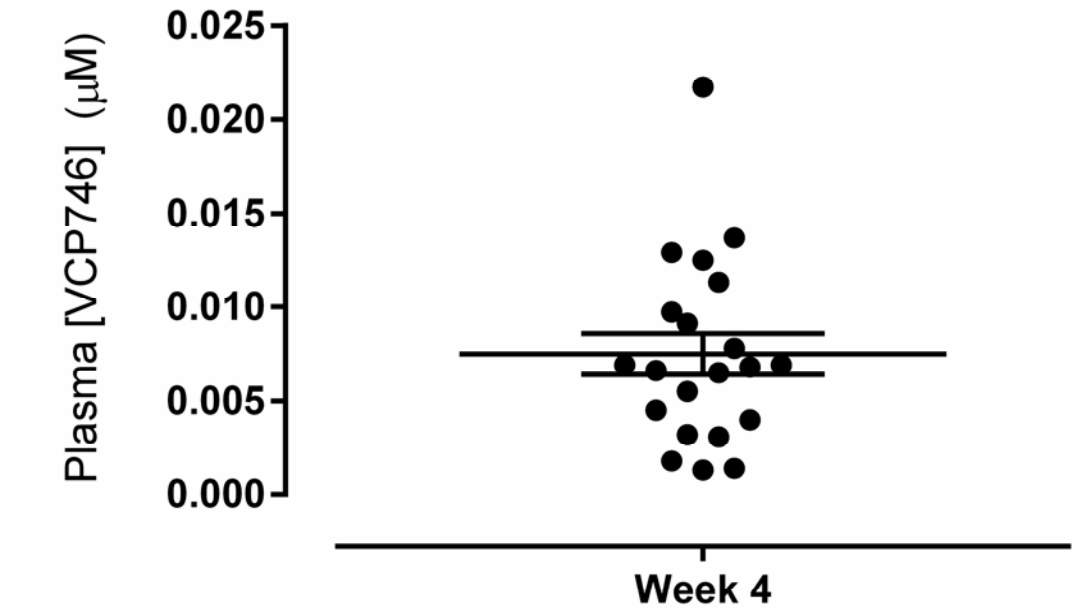

Supp Figure 3 Plasma concentration (μM) of VCP746 in rats receiving chronic infusion of VCP746 via minipump. Mean plasma concentration of VCP746 was 0.0075 ± 0.0011 μM. Data expressed as mean ± SEM, n = 21.

References

1. Montecucco F, Carbone F, Schindler TH. Pathophysiology of ST-segment elevation myocardial infarction: novel mechanisms and treatments. Eur Heart J. 2016;37(16):1268-83.
2. Alpert JS, Thygesen K, Antman E, Bassand JP. Myocardial infarction redefined--a consensus document of The Joint European Society of Cardiology/American College of Cardiology Committee for the redefinition of myocardial infarction. J Am Coll Cardiol. 2000;36(3):959-69.
3. Buja LM, Entman ML. Modes of myocardial cell injury and cell death in ischemic heart disease. Circulation. 1998;98(14):1355-7.
4. James TN. The variable morphological coexistence of apoptosis and necrosis in human myocardial infarction: significance for understanding its pathogenesis, clinical course, diagnosis and prognosis. Coron Artery Dis. 1998;9(5):291-307.
5. Majno G, Joris I. Apoptosis, oncosis, and necrosis. An overview of cell death. Am J Pathol. 1995;146(1):3-15.
6. Kajstura J, Cheng W, Reiss K, Clark WA, Sonnenblick EH, Krajewski S, et al. Apoptotic and necrotic myocyte cell deaths are independent contributing variables of infarct size in rats. Lab Investig. 1996;74(1):86-107.
7. Ohno M, Takemura G, Ohno A, Misao J, Hayakawa Y, Minatoguchi S, et al. "Apoptotic" Myocytes in Infarct Area in Rabbit Hearts May Be Oncotic Myocytes With DNA Fragmentation: Analysis by Immunogold Electron Microscopy Combined With In Situ Nick End-Labeling. Circulation. 1998;98(14):1422-30.
8. O'Gara PT, Kushner FG, Ascheim DD, Casey DE, Jr., Chung MK, de Lemos JA, et al. 2013 ACCF/AHA guideline for the management of ST-elevation myocardial infarction: a report of the American College of Cardiology Foundation/American Heart Association Task Force on Practice Guidelines. Circulation. 2013;127(4):e362-425.
9. Antithrombotic Trialists C. Collaborative meta-analysis of randomised trials of antiplatelet therapy for prevention of death, myocardial infarction, and stroke in high risk patients. BMJ. 2002;324(7329):71-86.
10. Mehta SR, Tanguay JF, Eikelboom JW, Jolly SS, Joyner CD, Granger CB, et al. Double-dose versus standard-dose clopidogrel and high-dose versus low-dose aspirin in individuals undergoing percutaneous coronary intervention for acute coronary syndromes (CURRENT-OASIS 7): a randomised factorial trial. Lancet. 2010;376(9748):1233-43.
11. Nordmann AJ, Hengstler P, Harr T, Young J, Bucher HC. Clinical outcomes of primary stenting versus balloon angioplasty in patients with myocardial infarction: a meta-analysis of randomized controlled trials. Am J Med. 2004;116(4):253-62.
12. Keeley EC, Boura JA, Grines CL. Primary angioplasty versus intravenous thrombolytic therapy for acute myocardial infarction: a quantitative review of 23 randomised trials. Lancet. 2003;361(9351):13-20.
13. Niccoli G, Burzotta F, Galiuto L, Crea F. Myocardial no-reflow in humans. J Am Coll Cardiol. 2009;54(4):281-92.
14. O'Neill WW, Weintraub R, Grines CL, Meany TB, Brodie BR, Friedman HZ, et al. A prospective, placebo-controlled, randomized trial of intravenous streptokinase and angioplasty versus lone angioplasty therapy of acute myocardial infarction. Circulation. 1992;86(6):1710-7.
15. Chen ZM, Pan HC, Chen YP, Peto R, Collins R, Jiang LX, et al. Early intravenous then oral metoprolol in 45,852 patients with acute myocardial infarction: randomised placebo-controlled trial. Lancet. 2005;366(9497):1622-32.
16. Freemantle N, Cleland J, Young P, Mason J, Harrison J. beta Blockade after myocardial infarction: systematic review and meta regression analysis. BMJ. 1999;318(7200):1730-7.
17. GISSI-3: effects of lisinopril and transdermal glyceryl trinitrate singly and together on 6-week mortality and ventricular function after acute myocardial infarction. Gruppo Italiano per lo Studio della Sopravvivenza nell'infarto Miocardico. Lancet. 1994;343(8906):1115-22.

18. ISIS-4: a randomised factorial trial assessing early oral captopril, oral mononitrate, and intravenous magnesium sulphate in 58,050 patients with suspected acute myocardial infarction. ISIS-4 (Fourth International Study of Infarct Survival) Collaborative Group. Lancet. 1995;345(8951):669-85.
19. Cleland JG, Erhardt L, Murray G, Hall AS, Ball SG. Effect of ramipril on morbidity and mode of death among survivors of acute myocardial infarction with clinical evidence of heart failure. A report from the AIRE Study Investigators. Eur Heart J. 1997;18(1):41-51.
20. Pfeffer MA, McMurray JJ, Velazquez EJ, Rouleau JL, Kober L, Maggioni AP, et al. Valsartan, captopril, or both in myocardial infarction complicated by heart failure, left ventricular dysfunction, or both. N Engl J Med. 2003;349(20):1893-906.
21. Randomised trial of cholesterol lowering in 4444 patients with coronary heart disease: the Scandinavian Simvastatin Survival Study (4S). Lancet. 1994;344(8934):1383-9.
22. Sacks FM, Pfeffer MA, Moye LA, Rouleau JL, Rutherford JD, Cole TG, et al. The effect of pravastatin on coronary events after myocardial infarction in patients with average cholesterol levels. Cholesterol and Recurrent Events Trial investigators. N Engl J Med. 1996;335(14):1001-9.
23. Lee KH, Jeong MH, Kim HM, Ahn Y, Kim JH, Chae SC, et al. Benefit of early statin therapy in patients with acute myocardial infarction who have extremely low low-density lipoprotein cholesterol. J Am Coll Cardiol. 2011;58(16):1664-71.
24. Sposito AC, Chapman MJ. Statin therapy in acute coronary syndromes: mechanistic insight into clinical benefit. Arterioscler Thromb Vasc Biol. 2002;22(10):1524-34.
25. Xu Z, Okamoto H, Akino M, Onozuka H, Matsui Y, Tsutsui H. Pravastatin attenuates left ventricular remodeling and diastolic dysfunction in angiotensin II-induced hypertensive mice. J Cardiovasc Pharmacol. 2008;51(1):62-70.
26. Herzog WR, Vogel RA, Schlossberg ML, Edenbaum LR, Scott HJ, Serebruany VL. Short-term low dose intracoronary diltiazem administered at the onset of reperfusion reduces myocardial infarct size. Int JCardiol. 1997;59(1):21-7.
27. Zhao ZQ, Corvera JS, Halkos ME, Kerendi F, Wang NP, Guyton RA, et al. Inhibition of myocardial injury by ischemic postconditioning during reperfusion: comparison with ischemic preconditioning. Am J Physiol Heart Circ Physiol. 2003;285(2):H579-88.
28. Hausenloy DJ, Yellon DM. Myocardial ischemia-reperfusion injury: a neglected therapeutic target. J Clin Invest. 2013;123(1):92-100.
29. Kaminski KA, Bonda TA, Korecki J, Musial WJ. Oxidative stress and neutrophil activation--the two keystones of ischemia/reperfusion injury. Int J Cardiol. 2002;86(1):41-59.
30. Garlick PB, Davies MJ, Hearse DJ, Slater TF. Direct detection of free radicals in the reperfused rat heart using electron spin resonance spectroscopy. Circ Res. 1987;61(5):757-60.
31. Zweier JL, Kuppusamy P, Williams R, Rayburn BK, Smith D, Weisfeldt ML, et al. Measurement and characterization of postischemic free radical generation in the isolated perfused heart. J Biol Chem. 1989;264(32):18890-5.
32. Duilio C, Ambrosio G, Kuppusamy P, DiPaula A, Becker LC, Zweier JL. Neutrophils are primary source of O2 radicals during reperfusion after prolonged myocardial ischemia. Am J Physiol Heart Circ Physiol. 2001;280(6):H2649-57.
33. Ambrosio G, Zweier JL, Duilio C, Kuppusamy P, Santoro G, Elia PP, et al. Evidence that mitochondrial respiration is a source of potentially toxic oxygen free radicals in intact rabbit hearts subjected to ischemia and reflow. J Biol Chem. 1993;268(25):18532-41.
34. Hardy L, Clark JB, Darley-Usmar VM, Smith DR, Stone D. Reoxygenation-dependent decrease in mitochondrial NADH:CoQ reductase (Complex I) activity in the hypoxic/reoxygenated rat heart. Biochem J. 1991;274 (Pt 1):133-7.
35. Paradies G, Petrosillo G, Pistolese M, Di Venosa N, Serena D, Ruggiero FM. Lipid peroxidation and alterations to oxidative metabolism in mitochondria isolated from rat heart subjected to ischemia and reperfusion. Free Radic Biol Med. 1999;27(1-2):42-50.
36. Suzuki S, Kaneko M, Chapman DC, Dhalla NS. Alterations in cardiac contractile proteins due to oxygen free radicals. Biochim Biophys Acta. 1991;1074(1):95-100.

37. Miyamae M, Camacho SA, Weiner MW, Figueredo VM. Attenuation of postischemic reperfusion injury is related to prevention of [Ca2+]m overload in rat hearts. Am J Physiol. 1996;271(5 Pt 2):H2145-53.
38. Bar FW, Tzivoni D, Dirksen MT, Fernandez-Ortiz A, Heyndrickx GR, Brachmann J, et al. Results of the first clinical study of adjunctive CAldaret (MCC-135) in patients undergoing primary percutaneous coronary intervention for ST-Elevation Myocardial Infarction: the randomized multicentre CASTEMI study. Eur Heart J. 2006;27(21):2516-23.
39. Griffiths EJ, Halestrap AP. Mitochondrial non-specific pores remain closed during cardiac ischaemia, but open upon reperfusion. Biochem J. 1995;307 (Pt 1):93-8.
40. Argaud L, Gateau-Roesch O, Muntean D, Chalabreysse L, Loufouat J, Robert D, et al. Specific inhibition of the mitochondrial permeability transition prevents lethal reperfusion injury. J Mol Cell Cardiol. 2005;38(2):367-74.
41. Hausenloy DJ, Duchen MR, Yellon DM. Inhibiting mitochondrial permeability transition pore opening at reperfusion protects against ischaemia-reperfusion injury. Cardiovasc Res. 2003;60(3):617-25.
42. Skyschally A, Schulz R, Heusch G. Cyclosporine A at reperfusion reduces infarct size in pigs. Cardiovasc Drugs Ther. 2010;24(1):85-7.
43. Piot C, Croisille P, Staat P, Thibault H, Rioufol G, Mewton N, et al. Effect of cyclosporine on reperfusion injury in acute myocardial infarction. N Engl J Med. 2008;359(5):473-81.
44. Germack R, Dickenson JM. Adenosine triggers preconditioning through MEK/ERK1/2 signalling pathway during hypoxia/reoxygenation in neonatal rat cardiomyocytes. J Mol Cell Cardiol. 2005;39(3):429-42.
45. Urmaliya VB, Pouton CW, Devine SM, Haynes JM, Warfe L, Scammells PJ, et al. A novel highly selective adenosine A1 receptor agonist VCP28 reduces ischemia injury in a cardiac cell line and ischemia-reperfusion injury in isolated rat hearts at concentrations that do not affect heart rate. J Cardiovasc Pharmacol. 2010;56(3):282-92.
46. O'Brien JD, Ferguson JH, Howlett SE. Effects of ischemia and reperfusion on isolated ventricular myocytes from young adult and aged Fischer 344 rat hearts. Am J Physiol Heart Circ Physiol. 2008;294(5):H2174-83.
47. Hausenloy DJ, Whittington HJ, Wynne AM, Begum SS, Theodorou L, Riksen N, et al. Dipeptidyl peptidase-4 inhibitors and GLP-1 reduce myocardial infarct size in a glucose-dependent manner. Cardiovasc Diabetol. 2013;12:154.
48. Urmaliya VB, Pouton CW, Ledent C, Short JL, White PJ. Cooperative cardioprotection through adenosine A1 and A2A receptor agonism in ischemia-reperfused isolated mouse heart. J Cardiovasc Pharmacol. 2010;56(4):379-88.
49. Lasley RD, Jahania MS, Mentzer RM, Jr. Beneficial effects of adenosine A(2a) agonist CGS-21680 in infarcted and stunned porcine myocardium. Am J Physiol Heart Circ Physiol. 2001;280(4):H1660-6.
50. Lankford AR, Yang JN, Rose'Meyer R, French BA, Matherne GP, Fredholm BB, et al. Effect of modulating cardiac A1 adenosine receptor expression on protection with ischemic preconditioning. Am J Physiol Heart Circ Physiol. 2006;290(4):H1469-73.
51. Morel S, Braunersreuther V, Chanson M, Bouis D, Rochemont V, Foglia B, et al. Endothelial Cx40 limits myocardial ischaemia/reperfusion injury in mice. Cardiovasc Res. 2014;102(2):329-37.
52. French BA, Kramer CM. Mechanisms of Post-Infarct Left Ventricular Remodeling. Drug Discov Today Dis Mech. 2007;4(3):185-96.
53. Kuch B, Bolte HD, Hoermann A, Meisinger C, Loewel H. What is the real hospital mortality from acute myocardial infarction? Epidemiological vs clinical view. Eur Hear J. 2002;23(9):714-20.
54. Sutton MG, Sharpe N. Left ventricular remodeling after myocardial infarction: pathophysiology and therapy. Circulation. 2000;101(25):2981-8.
55. Watzinger N, Lund GK, Higgins CB, Wendland MF, Weinmann HJ, Saeed M. The potential of contrast-enhanced magnetic resonance imaging for predicting left ventricular remodeling. J Magn Reson Imaging. 2002;16(6):633-40.

56. Orn S, Manhenke C, Anand IS, Squire I, Nagel E, Edvardsen T, et al. Effect of left ventricular scar size, location, and transmurality on left ventricular remodeling with healed myocardial infarction. Am J Cardiol. 2007;99(8):1109-14.
57. Cleutjens JP, Kandala JC, Guarda E, Guntaka RV, Weber KT. Regulation of collagen degradation in the rat myocardium after infarction. J Mol Cell Cardiol. 1995;27(6):1281-92.
58. Maillet M, van Berlo JH, Molkentin JD. Molecular basis of physiological heart growth: fundamental concepts and new players. Nat Rev Mol Cell Biol. 2013;14(1):38-48.
59. Desmouliere A, Geinoz A, Gabbiani F, Gabbiani G. Transforming growth factor-beta 1 induces alpha-smooth muscle actin expression in granulation tissue myofibroblasts and in quiescent and growing cultured fibroblasts. J Cell Biol. 1993;122(1):103-11.
60. Cleutjens JP, Verluyten MJ, Smiths JF, Daemen MJ. Collagen remodeling after myocardial infarction in the rat heart. Am J Pathol. 1995;147(2):325-38.
61. Colucci WS. The effects of norepinephrine on myocardial biology: implications for the therapy of heart failure. Clin Cardiol. 1998;21(12 Suppl 1):I20-4.
62. Bertel O, Buhler FR, Baitsch G, Ritz R, Burkart F. Plasma adrenaline and noradrenaline in patients with acute myocardial infarction. Relationship to ventricular arrhythmias of varying severity. Chest. 1982;82(1):64-8.
63. Gray MO, Long CS, Kalinyak JE, Li HT, Karliner JS. Angiotensin II stimulates cardiac myocyte hypertrophy via paracrine release of TGF-beta 1 and endothelin-1 from fibroblasts. Cardiovasc Res. 1998;40(2):352-63.
64. Liu Y, Leri A, Li B, Wang X, Cheng W, Kajstura J, et al. Angiotensin II stimulation in vitro induces hypertrophy of normal and postinfarcted ventricular myocytes. Circ Res. 1998;82(11):1145-59.
65. Huang CY, Kuo WW, Chueh PJ, Tseng CT, Chou MY, Yang JJ. Transforming growth factor-beta induces the expression of ANF and hypertrophic growth in cultured cardiomyoblast cells through ZAK. Biochem Biophys Res Commun. 2004;324(1):424-31.
66. Lim JY, Park SJ, Hwang HY, Park EJ, Nam JH, Kim J, et al. TGF-beta1 induces cardiac hypertrophic responses via PKC-dependent ATF-2 activation. J Mol Cell Cardiol. 2005;39(4):627-36.
67. See F, Kompa A, Martin J, Lewis DA, Krum H. Fibrosis as a therapeutic target post-myocardial infarction. Curr Pharm Des. 2005;11(4):477-87.
68. Guillen I, Blanes M, Gomez-Lechon MJ, Castell JV. Cytokine signaling during myocardial infarction: sequential appearance of IL-1 beta and IL-6. Am J Physiol. 1995;269(2 Pt 2):R229-35.
69. Bozkurt B, Kribbs SB, Clubb FJ, Jr., Michael LH, Didenko VV, Hornsby PJ, et al. Pathophysiologically relevant concentrations of tumor necrosis factor-alpha promote progressive left ventricular dysfunction and remodeling in rats. Circulation. 1998;97(14):1382-91.
70. Liao Y, Lin L, Lu D, Fu Y, Bin J, Xu D, et al. Activation of adenosine A1 receptor attenuates tumor necrosis factor-alpha induced hypertrophy of cardiomyocytes. Biomed Pharmacother. 2011;65(7):491-5.
71. Du XJ. Divergence of hypertrophic growth and fetal gene profile: the influence of beta-blockers. Brit J Pharmacol. 2007;152(2):169-71.
72. Dirkx E, da Costa Martins PA, De Windt LJ. Regulation of fetal gene expression in heart failure. Biochim Biophys Acta. 2013;1832(12):2414-24.
73. Cleutjens JP, Blankesteijn WM, Daemen MJ, Smits JF. The infarcted myocardium: simply dead tissue, or a lively target for therapeutic interventions. Cardiovasc Res. 1999;44(2):232-41.
74. Weber KT, Brilla CG. Factors associated with reactive and reparative fibrosis of the myocardium. Basic Res Cardiol. 1992;87 Suppl 1:291-301.
75. Weber KT, Sun Y, Tyagi SC, Cleutjens JP. Collagen network of the myocardium: function, structural remodeling and regulatory mechanisms. J Mol Cell Cardiol. 1994;26(3):279-92.
76. See F, Kompa A, Martin J, Lewis DA, Krum H. Fibrosis as a Therapeutic Target Post-Myocardial Infarction. Curr Pharm Des. 2005;11(4):477-87.

77. Santiago JJ, Dangerfield AL, Rattan SG, Bathe KL, Cunnington RH, Raizman JE, et al. Cardiac fibroblast to myofibroblast differentiation in vivo and in vitro: expression of focal adhesion components in neonatal and adult rat ventricular myofibroblasts. Dev Dynam 2010;239(6):1573-84.
78. Norton GR, Tsotetsi J, Trifunovic B, Hartford C, Candy GP, Woodiwiss AJ. Myocardial stiffness is attributed to alterations in cross-linked collagen rather than total collagen or phenotypes in spontaneously hypertensive rats. Circulation. 1997;96(6):1991-8.
79. Pauschinger M, Knopf D, Petschauer S, Doerner A, Poller W, Schwimmbeck PL, et al. Dilated cardiomyopathy is associated with significant changes in collagen type I/III ratio. Circulation. 1999;99(21):2750-6.
80. Sun Y, Zhang JQ, Zhang J, Ramires FJ. Angiotensin II, transforming growth factor-beta1 and repair in the infarcted heart. J Mol Cell Cardiol. 1998;30(8):1559-69.
81. Dean RG, Balding LC, Candido R, Burns WC, Cao Z, Twigg SM, et al. Connective tissue growth factor and cardiac fibrosis after myocardial infarction. J Histochem Cytochem. 2005;53(10):1245-56.
82. Pfeffer JM, Pfeffer MA, Braunwald E. Influence of chronic captopril therapy on the infarcted left ventricle of the rat. Circ Res. 1985;57(1):84-95.
83. Pfeffer MA, Braunwald E, Moye LA, Basta L, Brown EJ, Jr., Cuddy TE, et al. Effect of captopril on mortality and morbidity in patients with left ventricular dysfunction after myocardial infarction. Results of the survival and ventricular enlargement trial. The SAVE Investigators. N Engl J Med. 1992;327(10):669-77.
84. Harada K, Sugaya T, Murakami K, Yazaki Y, Komuro I. Angiotensin II type 1A receptor knockout mice display less left ventricular remodeling and improved survival after myocardial infarction. Circulation. 1999;100(20):2093-9.
85. Dickstein K, Kjekshus J, Group OSCotOS. Effects of losartan and captopril on mortality and morbidity in high-risk patients after acute myocardial infarction: the OPTIMAAL randomised trial. Optimal Trial in Myocardial Infarction with Angiotensin II Antagonist Losartan. Lancet. 2002;360(9335):752-60.
86. Kim S, Yoshiyama M, Izumi Y, Kawano H, Kimoto M, Zhan Y, et al. Effects of combination of ACE inhibitor and angiotensin receptor blocker on cardiac remodeling, cardiac function, and survival in rat heart failure. Circulation. 2001;103(1):148-54.
87. Mankad S, d'Amato TA, Reichek N, McGregor WE, Lin J, Singh D, et al. Combined angiotensin II receptor antagonism and angiotensin-converting enzyme inhibition further attenuates postinfarction left ventricular remodeling. Circulation. 2001;103(23):2845-50.
88. Silvestre JS, Heymes C, Oubenaissa A, Robert V, Aupetit-Faisant B, Carayon A, et al. Activation of cardiac aldosterone production in rat myocardial infarction: effect of angiotensin II receptor blockade and role in cardiac fibrosis. Circulation. 1999;99(20):2694-701.
89. Lal A, Veinot JP, Leenen FH. Prevention of high salt diet-induced cardiac hypertrophy and fibrosis by spironolactone. Am J Hypertens. 2003;16(4):319-23.
90. Pitt B, Zannad F, Remme WJ, Cody R, Castaigne A, Perez A, et al. The effect of spironolactone on morbidity and mortality in patients with severe heart failure. Randomized Aldactone Evaluation Study Investigators. N Engl J Med. 1999;341(10):709-17.
91. Zannad F, Alla F, Dousset B, Perez A, Pitt B. Limitation of excessive extracellular matrix turnover may contribute to survival benefit of spironolactone therapy in patients with congestive heart failure: insights from the randomized aldactone evaluation study (RALES). Rales Investigators. Circulation. 2000;102(22):2700-6.
92. Pitt B, Remme W, Zannad F, Neaton J, Martinez F, Roniker B, et al. Eplerenone, a selective aldosterone blocker, in patients with left ventricular dysfunction after myocardial infarction. N Engl J Med. 2003;348(14):1309-21.
93. The Cardiac Insufficiency Bisoprolol Study II (CIBIS-II): a randomised trial. Lancet. 1999;353(9146):9-13.
94. Effect of metoprolol CR/XL in chronic heart failure: Metoprolol CR/XL Randomised Intervention Trial in Congestive Heart Failure (MERIT-HF). Lancet. 1999;353(9169):2001-7.

95. Dargie HJ. Effect of carvedilol on outcome after myocardial infarction in patients with left-ventricular dysfunction: the CAPRICORN randomised trial. Lancet. 2001;357(9266):1385-90.
96. Pratt CM. Three decades of clinical trials with beta-blockers: the contribution of the CAPRICORN trial and the effect of carvedilol on serious arrhythmias. J Am Coll Cardiol. 2005;45(4):531-2.
97. Packer M, Coats AJS, Fowler MB, Katus HA, Krum H, Mohacsi P, et al. Effect of Carvedilol on Survival in Severe Chronic Heart Failure. N Engl J Med. 2001;344(22):1651-8.
98. Beta-Blocker Evaluation of Survival Trial I. A trial of the beta-blocker bucindolol in patients with advanced chronic heart failure. N Engl J Med. 2001;344(22):1659-67.
99. Wang BH, Bertucci MC, Ma JY, Adrahtas A, Cheung RY, Krum H. Celecoxib, but not rofecoxib or naproxen, attenuates cardiac hypertrophy and fibrosis induced in vitro by angiotensin and aldosterone. Clin Exp Pharmacol Physiol. 2010;37(9):912-8.
100. Gan XT, Rajapurohitam V, Haist JV, Chidiac P, Cook MA, Karmazyn M. Inhibition of phenylephrine-induced cardiomyocyte hypertrophy by activation of multiple adenosine receptor subtypes. J Pharmacol Exp Ther. 2005;312(1):27-34.
101. Tanaka K, Honda M, Takabatake T. Redox regulation of MAPK pathways and cardiac hypertrophy in adult rat cardiac myocyte. J Am Coll Cardiol. 2001;37(2):676-85.
102. Wakeno M, Minamino T, Seguchi O, Okazaki H, Tsukamoto O, Okada K, et al. Long-term stimulation of adenosine A2b receptors begun after myocardial infarction prevents cardiac remodeling in rats. Circulation. 2006;114(18):1923-32.
103. Lu Z, Fassett J, Xu X, Hu X, Zhu G, French J, et al. Adenosine A3 receptor deficiency exerts unanticipated protective effects on the pressure-overloaded left ventricle. Circulation. 2008;118(17):1713-21.
104. George I, Morrow B, Xu K, Yi GH, Holmes J, Wu EX, et al. Prolonged effects of B-type natriuretic peptide infusion on cardiac remodeling after sustained myocardial injury. Am J Physiol Heart Circ Physiol. 2009;297(2):H708-17.
105. Fredholm BB. Adenosine, an endogenous distress signal, modulates tissue damage and repair. Cell Death Differ. 2007;14(7):1315-23.
106. Noji T, Karasawa A, Kusaka H. Adenosine uptake inhibitors. Eur J Pharmacol. 2004;495(1):1-16.
107. Fredholm BB. Adenosine receptors as drug targets. Exp Cell Res. 2010;316(8):1284-8.
108. Fredholm BB, AP IJ, Jacobson KA, Klotz KN, Linden J. International Union of Pharmacology. XXV. Nomenclature and classification of adenosine receptors. Pharmacol Rev. 2001;53(4):527-52.
109. Jacobson KA, Gao ZG. Adenosine receptors as therapeutic targets. Nat Rev Drug Dis. 2006;5(3):247-64.
110. Jin X, Shepherd RK, Duling BR, Linden J. Inosine binds to A3 adenosine receptors and stimulates mast cell degranulation. J Clin Invest. 1997;100(11):2849-57.
111. Shen H, Chen GJ, Harvey BK, Bickford PC, Wang Y. Inosine reduces ischemic brain injury in rats. Stroke. 2005;36(3):654-9.
112. Rittiner JE, Korboukh I, Hull-Ryde EA, Jin J, Janzen WP, Frye SV, et al. AMP Is an Adenosine A1 Receptor Agonist. J Biol Chem. 2012;287(8):5301-9.
113. Fredholm BB, Arslan G, Halldner L, Kull B, Schulte G, Wasserman W. Structure and function of adenosine receptors and their genes. Naunyn Schmiedebergs Arch Pharmacol. 2000;362(4-5):364-74.
114. Dixon AK, Gubitz AK, Sirinathsinghji DJ, Richardson PJ, Freeman TC. Tissue distribution of adenosine receptor mRNAs in the rat. Brit J Pharmacol. 1996;118(6):1461-8.
115. Bohm M, Pieske B, Ungerer M, Erdmann E. Characterization of A1 adenosine receptors in atrial and ventricular myocardium from diseased human hearts. Circ Res. 1989;65(5):1201-11.
116. Musser B, Morgan ME, Leid M, Murray TF, Linden J, Vestal RE. Species comparison of adenosine and beta-adrenoceptors in mammalian atrial and ventricular myocardium. Eur J Pharmacol. 1993;246(2):105-11.

117. Hussain T, Mustafa SJ. Binding of A1 adenosine receptor ligand [3H]8-cyclopentyl-1,3-dipropylxanthine in coronary smooth muscle. Circ Res. 1995;77(1):194-8.
118. Teng B, Qin W, Ansari HR, Mustafa SJ. Involvement of p38-mitogen-activated protein kinase in adenosine receptor-mediated relaxation of coronary artery. Am J Physiol Heart Circ Physiol. 2005;288(6):H2574-80.
119. Zahler S, Becker BF, Raschke P, Gerlach E. Stimulation of endothelial adenosine A1 receptors enhances adhesion of neutrophils in the intact guinea pig coronary system. Cardiovasc Res. 1994;28(9):1366-72.
120. Marala RB, Mustafa SJ. Immunological Characterization of Adenosine A2AReceptors in Human and Porcine Cardiovascular Tissues. J Pharmacol Exp Ther. 1998;286(2):1051-7.
121. Sassi Y, Ahles A, Truong D-JJ, Baqi Y, Lee S-Y, Husse B, et al. Cardiac myocyte–secreted cAMP exerts paracrine action via adenosine receptor activation. J Clin Invest. 2014;124(12):0-.
122. Sanjani MS, Teng B, Krahn T, Tilley S, Ledent C, Mustafa SJ. Contributions of A2A and A2B adenosine receptors in coronary flow responses in relation to the KATP channel using A2B and A2A/2B double-knockout mice. Am J Physiol Heart Circ Physiol. 2011;301(6):H2322-33.
123. Teng B, Ledent C, Mustafa SJ. Up-regulation of A 2B adenosine receptor in A 2A adenosine receptor knockout mouse coronary artery. J Mol Cell Cardiol. 2008;44(5):905-14.
124. Liang BT, Haltiwanger B. Adenosine A2a and A2b receptors in cultured fetal chick heart cells. High- and low-affinity coupling to stimulation of myocyte contractility and cAMP accumulation. Circ Res. 1995;76(2):242-51.
125. Lasley RD, Kristo G, Keith BJ, Mentzer RM, Jr. The A2a/A2b receptor antagonist ZM-241385 blocks the cardioprotective effect of adenosine agonist pretreatment in in vivo rat myocardium. Am J Physiol Heart Circ Physiol. 2007;292(1):H426-31.
126. Zhan E, McIntosh VJ, Lasley RD. Adenosine A2A and A2B receptors are both required for adenosine A1 receptor-mediated cardioprotection. Am J Physiol Heart Circ Physiol. 2011;301(3):H1183-H9.
127. Epperson SA, Brunton LL, Ramirez-Sanchez I, Villarreal F. Adenosine receptors and second messenger signaling pathways in rat cardiac fibroblasts. Am J Physiol Cell Physiol. 2009;296(5):C1171-7.
128. Dubey RK, Gillespie DG, Jackson EK. Adenosine inhibits collagen and protein synthesis in cardiac fibroblasts: role of A2B receptors. Hypertension. 1998;31(4):943-8.
129. Hinschen AK, Rose'Meyer RB, Headrick JP. Adenosine receptor subtypes mediating coronary vasodilation in rat hearts. J Cardiovasc Pharmacol. 2003;41(1):73-80.
130. Feoktistov I, Goldstein AE, Ryzhov S, Zeng D, Belardinelli L, Voyno-Yasenetskaya T, et al. Differential expression of adenosine receptors in human endothelial cells: role of A2B receptors in angiogenic factor regulation. Circ Res. 2002;90(5):531-8.
131. Martin PL. Relative agonist potencies of C2-substituted analogues of adenosine: evidence for adenosine A2B receptors in the guinea pig aorta. Eur J Pharmacol. 1992;216(2):235-42.
132. Headrick JP, Ashton KJ, Rose'meyer RB, Peart JN. Cardiovascular adenosine receptors: expression, actions and interactions. Pharmacol Ther. 2013;140(1):92-111.
133. Carr CS, Hill RJ, Masamune H, Kennedy SP, Knight DR, Tracey WR, et al. Evidence for a role for both the adenosine A1 and A3 receptors in protection of isolated human atrial muscle against simulated ischaemia. Cardiovasc Res. 1997;36(1):52-9.
134. Park SS, Zhao H, Jang Y, Mueller RA, Xu Z. N6-(3-iodobenzyl)-adenosine-5'-N-methylcarboxamide confers cardioprotection at reperfusion by inhibiting mitochondrial permeability transition pore opening via glycogen synthase kinase 3 beta. J Pharmacol Exp Ther. 2006;318(1):124-31.
135. Zhao Z, Francis CE, Ravid K. An A3-subtype adenosine receptor is highly expressed in rat vascular smooth muscle cells: its role in attenuating adenosine-induced increase in cAMP. Microvasc Res. 1997;54(3):243-52.

136. Son YK, Park WS, Ko JH, Han J, Kim N, Earm YE. Protein kinase A-dependent activation of inward rectifier potassium channels by adenosine in rabbit coronary smooth muscle cells. Biochem Biophys Res Commun. 2005;337(4):1145-52.
137. Kristo G, Yoshimura Y, Keith BJ, Mentzer RM, Jr., Lasley RD. Aged rat myocardium exhibits normal adenosine receptor-mediated bradycardia and coronary vasodilation but increased adenosine agonist-mediated cardioprotection. J Gerontol A Biol Sci Med Sci. 2005;60(11):1399-404.
138. Yang JN, Tiselius C, Dare E, Johansson B, Valen G, Fredholm BB. Sex differences in mouse heart rate and body temperature and in their regulation by adenosine A1 receptors. Acta Physiol. 2007;190(1):63-75.
139. Belardinelli L, Shryock JC, Song Y, Wang D, Srinivas M. Ionic basis of the electrophysiological actions of adenosine on cardiomyocytes. FASEB J. 1995;9(5):359-65.
140. Koeppen M, Eckle T, Eltzschig HK. Selective deletion of the A1 adenosine receptor abolishes heart-rate slowing effects of intravascular adenosine in vivo. PLoS ONE. 2009;4(8):e6784.
141. Biel M, Schneider A, Wahl C. Cardiac HCN channels: structure, function, and modulation. Trends Cardiovasc Med. 2002;12(5):206-12.
142. DiFrancesco D, Ducouret P, Robinson RB. Muscarinic modulation of cardiac rate at low acetylcholine concentrations. Science. 1989;243(4891):669-71.
143. Headrick JP, Gauthier NS, Morrison RR, Matherne GP. Chronotropic and vasodilatory responses to adenosine and isoproterenol in mouse heart: effects of adenosine A1 receptor overexpression. Clin Exp Pharmacol Physiol. 2000;27(3):185-90.
144. Rankin AC, Martynyuk AE, Workman AJ, Kane KA. Ionic mechanisms of the effect of adenosine on single rabbit atrioventricular node myocytes. Can J Cardiol. 1997;13(12):1183-7.
145. Rubio R, Ceballos G, Balcells E. Intravascular adenosine: the endothelial mediators of its negative dromotropic effects. Eur J Pharmacol. 1999;370(1):27-37.
146. Dobson JG, Jr. Mechanism of adenosine inhibition of catecholamine-induced responses in heart. Circ Res. 1983;52(2):151-60.
147. Fenton RA, Komatsu S, Ikebe M, Shea LG, Dobson JG, Jr. Adenoprotection of the heart involves phospholipase C-induced activation and translocation of PKC-epsilon to RACK2 in adult rat and mouse. Am J Physiol Heart Circ Physiol. 2009;297(2):H718-25.
148. Lorbar M, Chung ES, Nabi A, Skalova K, Fenton RA, Dobson JG, Jr., et al. Receptors subtypes involved in adenosine-mediated modulation of norepinephrine release from cardiac nerve terminals. Can J Physiol Pharmacol. 2004;82(11):1026-31.
149. Dobson JG, Jr., Fenton RA. Adenosine A2 receptor function in rat ventricular myocytes. Cardiovasc Res. 1997;34(2):337-47.
150. Dobson JG, Jr., Shea LG, Fenton RA. Adenosine A2A and beta-adrenergic calcium transient and contractile responses in rat ventricular myocytes. Am J Physiol Heart Circ Physiol. 2008;295(6):H2364-72.
151. Chandrasekera PC, McIntosh VJ, Cao FX, Lasley RD. Differential effects of adenosine A2a and A2b receptors on cardiac contractility. Am J Physiol Heart Circ Physiol. 2010;299(6):H2082-9.
152. Flood A, Headrick JP. Functional characterization of coronary vascular adenosine receptors in the mouse. Brit Journal Pharmacol. 2001;133(7):1063-72.
153. Gurden MF, Coates J, Ellis F, Evans B, Foster M, Hornby E, et al. Functional characterization of three adenosine receptor types. Brit J Pharmacol. 1993;109(3):693-8.
154. Sato A, Terata K, Miura H, Toyama K, Loberiza FR, Jr., Hatoum OA, et al. Mechanism of vasodilation to adenosine in coronary arterioles from patients with heart disease. Am J Physiol Heart Circ Physiol. 2005;288(4):H1633-40.
155. Shepherd RK, Linden J, Duling BR. Adenosine-induced vasoconstriction in vivo. Role of the mast cell and A3 adenosine receptor. Circ Res. 1996;78(4):627-34.
156. Gerczuk PZ, Kloner RA. An update on cardioprotection: a review of the latest adjunctive therapies to limit myocardial infarction size in clinical trials. J Am Coll Cardiol. 2012;59(11):969-78.

157. Hausenloy DJ, Tsang A, Mocanu MM, Yellon DM. Ischemic preconditioning protects by activating prosurvival kinases at reperfusion. Am J Physiol Heart Circ Physiol. 2005;288(2):H971-6.
158. Liu GS, Thornton J, Van Winkle DM, Stanley AW, Olsson RA, Downey JM. Protection against infarction afforded by preconditioning is mediated by A1 adenosine receptors in rabbit heart. Circulation. 1991;84(1):350-6.
159. Huang K, Lu SJ, Zhong JH, Xiang Q, Wang L, Wu M. Comparative analysis of different cyclosporine A doses on protection after myocardial ischemia/reperfusion injury in rat. Asian Pac J Trop Med. 2014;7(2):144-8.
160. Nazareth W, Yafei N, Crompton M. Inhibition of anoxia-induced injury in heart myocytes by cyclosporin A. J Mol Cell Cardiol. 1991;23(12):1351-4.
161. Lasley RD, Rhee JW, Van Wylen DGL, Mentzer Jr RM. Adenosine A1 receptor mediated protection of the globally ischemic isolated rat heart. J Mol Cell Cardiol. 1990;22(1):39-47.
162. Norton ED, Jackson EK, Turner MB, Virmani R, Forman MB. The effects of intravenous infusions of selective adenosine A1-receptor and A2-receptor agonists on myocardial reperfusion injury. Am Heart J. 1992;123(2):332-8.
163. Thornton JD, Liu GS, Olsson RA, Downey JM. Intravenous pretreatment with A1-selective adenosine analogues protects the heart against infarction. Circulation. 1992;85(2):659-65.
164. Stambaugh K, Jacobson KA, Jiang JL, Liang BT. A novel cardioprotective function of adenosine A1 and A3 receptors during prolonged simulated ischemia. Am J Physiol. 1997;273(1 Pt 2):H501-5.
165. Germack R, Dickenson JM. Adenosine triggers preconditioning through MEK/ERK1/2 signalling pathway during hypoxia/reoxygenation in neonatal rat cardiomyocytes. J Mol Cell Cardiol. 2005;39(3):429-42.
166. Solenkova NV, Solodushko V, Cohen MV, Downey JM. Endogenous adenosine protects preconditioned heart during early minutes of reperfusion by activating Akt. Am J Physiol Heart Circ Physiol. 2006;290(1):H441-9.
167. Sato T, Sasaki N, O'Rourke B, Marban E. Adenosine primes the opening of mitochondrial ATP-sensitive potassium channels: a key step in ischemic preconditioning? Circulation. 2000;102(7):800-5.
168. Peart JN, Gross GJ. Adenosine and opioid receptor-mediated cardioprotection in the rat: evidence for cross-talk between receptors. Am J Physiol Heart Circ Physiol. 2003;285(1):H81-H9.
169. Lopes LV, Cunha RA, Ribeiro JA. Cross Talk Between A1 and A2A Adenosine Receptors in the Hippocampus and Cortex of Young Adult and Old Rats. J Neurophysiol. 1999;82(6):3196-203.
170. Lasley RD, Kristo G, Keith BJ, Mentzer RM. The A2a/A2b receptor antagonist ZM-241385 blocks the cardioprotective effect of adenosine agonist pretreatment in in vivo rat myocardium. Am J Physiol Heart Circ Physiol. 2007;292(1):H426-H31.
171. Jordan JE, Zhao ZQ, Sato H, Taft S, Vinten-Johansen J. Adenosine A2 receptor activation attenuates reperfusion injury by inhibiting neutrophil accumulation, superoxide generation and coronary endothelial adherence. J Pharmacol Exp Ther. 1997;280(1):301-9.
172. Koeppen M, Harter PN, Bonney S, Bonney M, Reithel S, Zachskorn C, et al. Adora2b signaling on bone marrow derived cells dampens myocardial ischemia-reperfusion injury. Anesthesiology. 2012;116(6):1245-57.
173. Black RG, Jr., Guo Y, Ge ZD, Murphree SS, Prabhu SD, Jones WK, et al. Gene dosage-dependent effects of cardiac-specific overexpression of the A3 adenosine receptor. Circ Res. 2002;91(2):165-72.
174. Safran N, Shneyvays V, Balas N, Jacobson KA, Nawrath H, Shainberg A. Cardioprotective effects of adenosine A1 and A3 receptor activation during hypoxia in isolated rat cardiac myocytes. Mol Cell Biochem. 2001;217(1-2):143-52.

175. Ge ZD, van der Hoeven D, Maas JE, Wan TC, Auchampach JA. A(3) adenosine receptor activation during reperfusion reduces infarct size through actions on bone marrow-derived cells. J Mol Cell Cardiol. 2010;49(2):280-6.
176. Xia Y, Javadov S, Gan TX, Pang T, Cook MA, Karmazyn M. Distinct KATP channels mediate the antihypertrophic effects of adenosine receptor activation in neonatal rat ventricular myocytes. J Pharmacol Exp Ther. 2007;320(1):14-21.
177. Liao Y, Takashima S, Asano Y, Asakura M, Ogai A, Shintani Y, et al. Activation of adenosine A1 receptor attenuates cardiac hypertrophy and prevents heart failure in murine left ventricular pressure-overload model. Circ Res. 2003;93(8):759-66.
178. Lu Z, Fassett J, Xu X, Hu X, Zhu G, French J, et al. Adenosine A3 Receptor Deficiency Exerts Unanticipated Protective Effects on the Pressure-Overloaded Left Ventricle. Circulation. 2008;118(17):1713-21.
179. Chen Y, Epperson S, Makhsudova L, Ito B, Suarez J, Dillmann W, et al. Functional effects of enhancing or silencing adenosine A2b receptors in cardiac fibroblasts. Am J Physiol Heart Circ Physiol. 2004 Dec;287(6):H2478-86.
180. Dubey RK, Gillespie DG, Mi Z, Jackson EK. Adenosine Inhibits PDGF-Induced Growth of Human Glomerular Mesangial Cells Via A2B Receptors. Hypertension. 2005;46(3):628-34.
181. Przyklenk K. Efficacy of cardioprotective 'conditioning' strategies in aging and diabetic cohorts: the co-morbidity conundrum. Drugs Aging. 2011;28(5):331-43.
182. Peart JN, Pepe S, Reichelt ME, Beckett N, See Hoe L, Ozberk V, et al. Dysfunctional survival-signaling and stress-intolerance in aged murine and human myocardium. Exp Gerontol. 2014;50:72-81.
183. Marso SP, Miller T, Rutherford BD, Gibbons RJ, Qureshi M, Kalynych A, et al. Comparison of myocardial reperfusion in patients undergoing percutaneous coronary intervention in ST-segment elevation acute myocardial infarction with versus without diabetes mellitus (from the EMERALD Trial). Am J Cardiol. 2007;100(2):206-10.
184. Schulman D, Latchman DS, Yellon DM. Effect of aging on the ability of preconditioning to protect rat hearts from ischemia-reperfusion injury. Am J Physiol Heart Circ Physiol. 2001 Oct;281(4):H1630-6.
185. Dobson JG, Jr., Fenton RA, Romano FD. Increased myocardial adenosine production and reduction of beta-adrenergic contractile response in aged hearts. Circ Res. 1990;66(5):1381-90.
186. Ethier MF, Hickler RB, Dobson JG, Jr. Aging increases adenosine and inosine release by human fibroblast cultures. Mech Ageing Development. 1989;50(2):159-68.
187. Korzick DH, Holiman DA, Boluyt MO, Laughlin MH, Lakatta EG. Diminished alpha1-adrenergic-mediated contraction and translocation of PKC in senescent rat heart. Am J Physiol Heart Circ Physiol. 2001;281(2):H581-9.
188. Takayama M, Ebihara Y, Tani M. Differences in the expression of protein kinase C isoforms and its translocation after stimulation with phorbol ester between young-adult and middle-aged ventricular cardiomyocytes isolated from Fischer 344 rats. Circ J. 2001;65(12):1071-6.
189. Przyklenk K, Li G, Simkhovich BZ, Kloner RA. Mechanisms of myocardial ischemic preconditioning are age related: PKC-epsilon does not play a requisite role in old rabbits. J Appl Physiol. 2003;95(6):2563-9.
190. Ueda Y, Kitakaze M, Komamura K, Minamino T, Asanuma H, Sato H, et al. Pravastatin restored the infarct size-limiting effect of ischemic preconditioning blunted by hypercholesterolemia in the rabbit model of myocardial infarction. J Am Coll Cardiol. 1999;34(7):2120-5.
191. Sharma NK, Mahadevan N, Balakumar P. Adenosine transport blockade restores attenuated cardioprotective effects of adenosine preconditioning in the isolated diabetic rat heart: potential crosstalk with opioid receptors. Cardiovasc Toxicol. 2013;13(1):22-32.
192. Podgorska M, Kocbuch K, Grden M, Szutowicz A, Pawelczyk T. Reduced ability to release adenosine by diabetic rat cardiac fibroblasts due to altered expression of nucleoside transporters. J Physiol. 2006;576(Pt 1):179-89.

193. Mahaffey KW, Puma JA, Barbagelata NA, DiCarli MF, Leesar MA, Browne KF, et al. Adenosine as an adjunct to thrombolytic therapy for acute myocardial infarction: Results of a multicenter, randomized, placebo-controlled trial: the Acute Myocardial Infarction STudy of ADenosine (AMISTAD) Trial. J Am Coll Cardiol. 1999;34(6):1711-20.
194. Ross AM, Gibbons RJ, Stone GW, Kloner RA, Alexander RW. A Randomized, Double-Blinded, Placebo-Controlled Multicenter Trial of Adenosine as an Adjunct to Reperfusion in the Treatment of Acute Myocardial Infarction (AMISTAD-II). J Am Coll Cardiol. 2005;45(11):1775-80.
195. Kloner RA, Forman MB, Gibbons RJ, Ross AM, Alexander RW, Stone GW. Impact of time to therapy and reperfusion modality on the efficacy of adenosine in acute myocardial infarction: the AMISTAD-2 trial. Eur Heart J. 2006;27(20):2400-5.
196. Kopecky SL, Aviles RJ, Bell MR, Lobl JK, Tipping D, Frommell G, et al. A randomized, double-blinded, placebo-controlled, dose-ranging study measuring the effect of an adenosine agonist on infarct size reduction in patients undergoing primary percutaneous transluminal coronary angioplasty: the ADMIRE (AmP579 Delivery for Myocardial Infarction REduction) study. Am Heart J. 2003;146(1):146-52.
197. Mitrovic V, Seferovic P, Dodic S, Krotin M, Neskovic A, Dickstein K, et al. Cardio-renal effects of the A1 adenosine receptor antagonist SLV320 in patients with heart failure. Circ Heart Fail. 2009;2(6):523-31.
198. Massie BM, O'Connor CM, Metra M, Ponikowski P, Teerlink JR, Cotter G, et al. Rolofylline, an adenosine A1-receptor antagonist, in acute heart failure. N Engl J Med. 2010;363(15):1419-28.
199. Urban JD, Clarke WP, von Zastrow M, Nichols DE, Kobilka B, Weinstein H, et al. Functional selectivity and classical concepts of quantitative pharmacology. J Pharmacol Exp Ther. 2007;320(1):1-13.
200. Stallaert W, Christopoulos A, Bouvier M. Ligand functional selectivity and quantitative pharmacology at G protein-coupled receptors. Expert Opin Drug Discov. 2011;6(8):811-25.
201. DeWire SM, Violin JD. Biased ligands for better cardiovascular drugs: dissecting G-protein-coupled receptor pharmacology. Circ Res. 2011;109(2):205-16.
202. Berg KA, Maayani S, Goldfarb J, Scaramellini C, Leff P, Clarke WP. Effector pathway-dependent relative efficacy at serotonin type 2A and 2C receptors: evidence for agonist-directed trafficking of receptor stimulus. Mol Pharmacol. 1998;54(1):94-104.
203. Nickolls SA, Fleck B, Hoare SR, Maki RA. Functional selectivity of melanocortin 4 receptor peptide and nonpeptide agonists: evidence for ligand-specific conformational states. J Pharmacol Exp Ther. 2005;313(3):1281-8.
204. Walters RW, Shukla AK, Kovacs JJ, Violin JD, DeWire SM, Lam CM, et al. beta-Arrestin1 mediates nicotinic acid-induced flushing, but not its antilipolytic effect, in mice. J Clin Invest. 2009;119(5):1312-21.
205. Valant C, May LT, Aurelio L, Chuo CH, White PJ, Baltos JA, et al. Separation of on-target efficacy from adverse effects through rational design of a bitopic adenosine receptor agonist.Proc Natl Acad Sci USA. 2014;111(12):4614-9.
206. Simpson P. Stimulation of hypertrophy of cultured neonatal rat heart cells through an alpha 1-adrenergic receptor and induction of beating through an alpha 1- and beta 1-adrenergic receptor interaction. Evidence for independent regulation of growth and beating. Circ Res. 1985;56(6):884-94.
207. Woodcock EA, Wang BH, Arthur JF, Lennard A, Matkovich SJ, Du XJ, et al. Inositol polyphosphate 1-phosphatase is a novel antihypertrophic factor. The Journal of biological chemistry. 2002 Jun 21;277(25):22734-42. PubMed PMID: 11932254. Epub 2002/04/05. eng.
208. Woodcock EA, Wang BH, Arthur JF, Lennard A, Matkovich SJ, Du X-J, et al. Inositol Polyphosphate 1-Phosphatase Is a Novel Antihypertrophic Factor. J Biol Chem. 2002;277(25):22734-42.
209. Tzanidis A, Hannan RD, Thomas WG, Onan D, Autelitano DJ, See F, et al. Direct Actions of Urotensin II on the Heart: Implications for Cardiac Fibrosis and Hypertrophy. Circ Res. 2003;93(3):246-53.

210. Hannan RD, Rothblum LI. Regulation of ribosomal DNA transcription during neonatal cardiomyocyte hypertrophy. Cardiovasc Res. 1995;30(4):501-10.
211. Thomas WG, Brandenburger Y, Autelitano DJ, Pham T, Qian H, Hannan RD. Adenoviral-Directed Expression of the Type 1A Angiotensin Receptor Promotes Cardiomyocyte Hypertrophy via Transactivation of the Epidermal Growth Factor Receptor. Circ Res. 2002;90(2):135-42.
212. See F, Thomas W, Way K, Tzanidis A, Kompa A, Lewis D, et al. P38 mitogen-activated protein kinase inhibition improves cardiac function and attenuates left ventricular remodeling following myocardial infarction in the rat. J Am Coll Cardiol. 2004;44(8):1679-89.
213. Lekawanvijit S, Adrahtas A, Kelly DJ, Kompa AR, Wang BH, Krum H. Does indoxyl sulfate, a uraemic toxin, have direct effects on cardiac fibroblasts and myocytes? Eur Heart J. 2010;31(14):1771-9.
214. Tran L, Kompa AR, Kemp W, Phrommintikul A, Wang BH, Krum H. Chronic urotensin-II infusion induces diastolic dysfunction and enhances collagen production in rats. Am J Physiol Heart Circ Physiol. 2010;298(2):H608-H13.
215. Schiller N, Shah P, Crawford M, DeMaria A, Devereux R, Feigenbaum H, et al. Recommendations for quantitation of the left ventricle by two-dimensional echocardiography. American Society of Echocardiography Committee on Standards, Subcommittee on Quantitation of Two-Dimensional Echocardiograms. J Am Soc Echocardiogr. 1989;2(5):358-67.
216. Connelly KA, Prior DL, Kelly DJ, Feneley MP, Krum H, Gilbert RE. Load-sensitive measures may overestimate global systolic function in the presence of left ventricular hypertrophy: a comparison with load-insensitive measures. Am J Physiol Heart Circ Physiol. 2006;290(4):H1699-705.
217. Ito H, Takaki M, Yamaguchi H, Tachibana H, Suga H. Left ventricular volumetric conductance catheter for rats. Am J Physiol Heart Circ Physiol. 1996;270(4):H1509-H14.
218. Georgakopoulos D, Kass DA. Estimation of parallel conductance by dual-frequency conductance catheter in mice. Am J Physiol Heart Circ Physiol. 2000;279(1):H443-H50.
219. Kelly JD, Wilkinson-Berka JL, Allen TJ, Cooper ME, Skinner SL. A new model of diabetic nephropathy with progressive renal impairment in the transgenic (mRen-2)27 rat (TGR). Kidney Int. 1998;54(2):343-52.
220. Kelly DJ, Zhang Y, Gow R, Gilbert RE. Tranilast attenuates structural and functional aspects of renal injury in the remnant kidney model. J Am Soc Nephrol. 2004;15:2619-29.
221. Lekawanvijit S, Kompa AR, Manabe M, Wang BH, Langham RG, Nishijima F, et al. Chronic kidney disease-induced cardiac fibrosis is ameliorated by reducing circulating levels of a non-dialysable uremic toxin, indoxyl sulfate. PLoS ONE. 2012;7(7):e41281.
222. Loennechen JP, Stoylen A, Beisvag V, Wisloff U, Ellingsen O. Regional expression of endothelin-1, ANP, IGF-1, and LV wall stress in the infarcted rat heart. Am J Physiol Heart Circ Physiol. 2001;280(6):H2902-10.
223. Imamura T, Takase M, Nishihara A, Oeda E, Hanai J-i, Kawabata M, et al. Smad6 inhibits signalling by the TGF-β superfamily. Nature. 1997;389:622-6.
224. Nayebpour M, Billette J, Amellal F, Nattel S. Effects of adenosine on rate-dependent atrioventricular nodal function. Potential roles in tachycardia termination and physiological regulation. Circulation. 1993;88(6):2632-45.
225. Nieri P, Martinotti E, Calderone V, Breschi MC. Adenosine-mediated hypotension in in vivo guinea-pig: receptors involved and role of NO. Brit J Pharmacol. 2001;134(4):745-52.
226. Hein TW, Belardinelli L, Kuo L. Adenosine A(2A) receptors mediate coronary microvascular dilation to adenosine: role of nitric oxide and ATP-sensitive potassium channels. J Pharmacol Exp Ther. 1999;291(2):655-64.
227. Kemp BK, Cocks TM. Adenosine mediates relaxation of human small resistance-like coronary arteries via A2B receptors. Brit J Pharmacol. 1999;126(8):1796-800.
228. Shin HK, Shin YW, Hong KW. Role of adenosine A(2B) receptors in vasodilation of rat pial artery and cerebral blood flow autoregulation. Am J Physiol Heart Circ Physiol. 2000;278(2):H339-44.

229. Hofman PL, Hiatt K, Yoder MC, Rivkees SA. A1 adenosine receptors potently regulate heart rate in mammalian embryos. Am J Physiol. 1997;273(4 Pt 2):R1374-80.
230. Anderson NH, Devlin AM, Graham D, Morton JJ, Hamilton CA, Reid JL, et al. Telemetry for cardiovascular monitoring in a pharmacological study: new approaches to data analysis. Hypertension. 1999;33(1 Pt 2):248-55.
231. Lang XE, Wang X, Zhang KR, Lv JY, Jin JH, Li QS. Isoflurane preconditioning confers cardioprotection by activation of ALDH2. PLoS ONE. 2013;8(2):e52469.
232. Peart JN, Gross GJ. Adenosine and opioid receptor-mediated cardioprotection in the rat: evidence for cross-talk between receptors. Am J Physiol Heart Circ Physiol. 2003;285(1):H81-9.
233. Schulz R, Rose J, Skyschally A, Heusch G. Bradycardic agent UL-FS 49 attenuates ischemic regional myocardial dysfunction and reduces infarct size in swine: comparison with the beta-blocker atenolol. J Cardiovasc Pharmacol. 1995;25(2):216-28.
234. Dewald O, Ren G, Duerr GD, Zoerlein M, Klemm C, Gersch C, et al. Of mice and dogs: species-specific differences in the inflammatory response following myocardial infarction. Am J Pathol. 2004;164(2):665-77.
235. Frangogiannis NG, Lindsey ML, Michael LH, Youker KA, Bressler RB, Mendoza LH, et al. Resident cardiac mast cells degranulate and release preformed TNF-alpha, initiating the cytokine cascade in experimental canine myocardial ischemia/reperfusion. Circulation. 1998;98(7):699-710.
236. Neri M, Fineschi V, Di Paolo M, Pomara C, Riezzo I, Turillazzi E, et al. Cardiac oxidative stress and inflammatory cytokines response after myocardial infarction. Curr Vasc Pharmacol. 2015;13(1):26-36.
237. Baltos JA, Gregory KJ, White PJ, Sexton PM, Christopoulos A, May LT. Quantification of adenosine A(1) receptor biased agonism: Implications for drug discovery. Biochem Pharmacol. 2016;99:101-12.
238. Zhang RL, Christensen LP, Tomanek RJ. Chronic heart rate reduction facilitates cardiomyocyte survival after myocardial infarction. Anat Rec. 2010;293(5):839-48.
239. Davidson SM, Hausenloy D, Duchen MR, Yellon DM. Signalling via the reperfusion injury signalling kinase (RISK) pathway links closure of the mitochondrial permeability transition pore to cardioprotection. Int J Biochem Cell Biol. 2006;38(3):414-9.
240. Qiao S, Olson JM, Paterson M, Yan Y, Zaja I, Liu Y, et al. MicroRNA-21 Mediates Isoflurane-induced Cardioprotection against Ischemia-Reperfusion Injury via Akt/Nitric Oxide Synthase/Mitochondrial Permeability Transition Pore Pathway. Anesthesiology. 2015;123(4):786-98.
241. Zhang JY, Chen ZW, Yao H. Protective effect of urantide against ischemia-reperfusion injury via protein kinase C and phosphtidylinositol 3'-kinase - Akt pathway. Can J Physiol Pharmacol. 2012;90(5):637-45.
242. Sumi S, Kobayashi H, Yasuda S, Iwasa M, Yamaki T, Yamada Y, et al. Postconditioning effect of granulocyte colony-stimulating factor is mediated through activation of risk pathway and opening of the mitochondrial KATP channels. Am J Physiol Heart Circ Physiol. 2010;299(4):H1174-82.
243. Xi J, McIntosh R, Shen X, Lee S, Chanoit G, Criswell H, et al. Adenosine A2A and A2B receptors work in concert to induce a strong protection against reperfusion injury in rat hearts. J Mol Cell Cardiol. 2009 Nov;47(5):684-90.
244. Taegtmeyer H, Sen S, Vela D. Return to the fetal gene program: a suggested metabolic link to gene expression in the heart. An N Y Acad Sci. 2010;1188:191-8.
245. Tsuchimochi H, Kurimoto F, Ieki K, Koyama H, Takaku F, Kawana M, et al. Atrial natriuretic peptide distribution in fetal and failed adult human hearts. Circulation. 1988;78(4):920-7.
246. Sigel AV, Centrella M, Eghbali-Webb M. Regulation of Proliferative Response of Cardiac Fibroblasts by Transforming Growth Factor-β1. J Mol Cell Cardiol. 1996;28(9):1921-9.

247. Griffin SA, Brown WC, MacPherson F, McGrath JC, Wilson VG, Korsgaard N, et al. Angiotensin II causes vascular hypertrophy in part by a non-pressor mechanism. Hypertension. 1991;17(5):626-35.
248. Pan X, Chen Z, Huang R, Yao Y, Ma G. Transforming growth factor beta1 induces the expression of collagen type I by DNA methylation in cardiac fibroblasts. PLoS ONE. 2013;8(4):e60335.
249. Zeidan A, Gan XT, Thomas A, Karmazyn M. Prevention of RhoA activation and cofilin-mediated actin polymerization mediates the antihypertrophic effect of adenosine receptor agonists in angiotensin II- and endothelin-1-treated cardiomyocytes. Mol Cell Biochem. 2014;385(1-2):239-48.
250. Miura T, Liu Y, Goto M, Tsuchida A, Miki T, Nakano A, et al. Mitochondrial ATP-sensitive K+ channels play a role in cardioprotection by Na+-H+ exchange inhibition against ischemia/reperfusion injury. J Am Coll Cardiol. 2001;37(3):957-63.
251. Suzuki M, Sasaki N, Miki T, Sakamoto N, Ohmoto-Sekine Y, Tamagawa M, et al. Role of sarcolemmal K(ATP) channels in cardioprotection against ischemia/reperfusion injury in mice. J Clin Invest. 2002;109(4):509-16.
252. Villarreal F, Epperson SA, Ramirez-Sanchez I, Yamazaki KG, Brunton LL. Regulation of cardiac fibroblast collagen synthesis by adenosine: roles for Epac and PI3K. Am J Physiol Cell Physiol. 2009;296(5):C1178-84.
253. Sigel AV, Centrella M, Eghbali-Webb M. Regulation of proliferative response of cardiac fibroblasts by transforming growth factor-beta 1. J Mol Cell Cardiol. 1996;28(9):1921-9.
254. Patrizio M, Musumeci M, Stati T, Fasanaro P, Palazzesi S, Catalano L, et al. Propranolol causes a paradoxical enhancement of cardiomyocyte foetal gene response to hypertrophic stimuli. Brit J Pharmacol. 2007;152(2):216-22.
255. Driesen RB, Verheyen FK, Debie W, Blaauw E, Babiker FA, Cornelussen RN, et al. Re-expression of alpha skeletal actin as a marker for dedifferentiation in cardiac pathologies. J Cell Mol Med. 2009;13(5):896-908.
256. Shoucri RM. Clinical applications of the areas under ESPVR. Cardiovasc Diagn Ther. 2013;3(2):60-3.
257. Farias S, Powers FM, Law WR. End-diastolic pressure-volume relationship in sepsis: relative contributions of compliance and equilibrium chamber volume differ. J Surg Res. 1999;82(2):172-9.
258. Modlinger PS, Welch WJ. Adenosine A1 receptor antagonists and the kidney. Current opinion in nephrology and hypertension. 2003 Sep;12(5):497-502. PubMed PMID: 12920396.
259. Vallon V, Muhlbauer B, Osswald H. Adenosine and kidney function. Physiol Rev. 2006;86(3):901-40.
260. Cotter G, Dittrich HC, Weatherley BD, Bloomfield DM, O'Connor CM, Metra M, et al. The PROTECT pilot study: a randomized, placebo-controlled, dose-finding study of the adenosine A1 receptor antagonist rolofylline in patients with acute heart failure and renal impairment. J Card Fail. 2008;14(8):631-40.
261. Swaney JS, Roth DM, Olson ER, Naugle JE, Meszaros JG, Insel PA. Inhibition of cardiac myofibroblast formation and collagen synthesis by activation and overexpression of adenylyl cyclase. Proc Natl Acd Sci USA. 2005;102(2):437-42.
262. Liang CS, Delehanty JD. Increasing post-myocardial infarction heart failure incidence in elderly patients a call for action. J Am Coll Cardiol. 2009;53(1):21-3.
263. Testai L, Martelli A, Cristofaro M, Breschi MC, Calderone V. Cardioprotective effects of different flavonoids against myocardial ischaemia/reperfusion injury in Langendorff-perfused rat hearts. J Pharm Pharmacol. 2013;65(5):750-6.
264. Yaoita H, Ogawa K, Maehara K, Maruyama Y. Attenuation of ischemia/reperfusion injury in rats by a caspase inhibitor. Circulation. 1998;97(3):276-81.
265. Verma S, Fedak PW, Weisel RD, Butany J, Rao V, Maitland A, et al. Fundamentals of reperfusion injury for the clinical cardiologist. Circulation. 2002;105(20):2332-6.

266. Wang X, Liang B, Skibsbye L, Olesen SP, Grunnet M, Jespersen T. GIRK channel activation via adenosine or muscarinic receptors has similar effects on rat atrial electrophysiology. J Cardiovasc Pharmacol. 2013;62(2):192-8.
267. Sabbah HN, Gupta RC, Kohli S, Wang M, Rastogi S, Zhang K, et al. Chronic therapy with a partial adenosine A1-receptor agonist improves left ventricular function and remodeling in dogs with advanced heart failure. Circ Heart Fail. 2013;6(3):563-71.
268. Vecchio EA, Chuo CH, Baltos JA, Ford L, Scammells PJ, Wang BH, et al. The hybrid molecule, VCP746, is a potent adenosine A2B receptor agonist that stimulates anti-fibrotic signalling. Biochem Pharmacol. 2016;117:46-56.
269. Toldo S, Zhong H, Mezzaroma E, Van Tassell BW, Kannan H, Zeng D, et al. GS-6201, a selective blocker of the A2B adenosine receptor, attenuates cardiac remodeling after acute myocardial infarction in the mouse. J Pharmacol Exp Ther. 2012;343(3):587-95.
270. Zhang H, Zhong H, Everett THt, Wilson E, Chang R, Zeng D, et al. Blockade of A2B adenosine receptor reduces left ventricular dysfunction and ventricular arrhythmias 1 week after myocardial infarction in the rat model. Heart Rhythm. 2014;11(1):101-9.
271. Jenner TL, Mellick AS, Harrison GJ, Griffiths LR, Rose'Meyer RB. Age-related changes in cardiac adenosine receptor expression. Mech Ageing Dev. 2004;125(3):211-7.
272. Ashton KJ, Nilsson U, Willems L, Holmgren K, Headrick JP. Effects of aging and ischemia on adenosine receptor transcription in mouse myocardium. Biochem Biophys Res Commun. 2003;312(2):367-72.
273. Liu S, Lekawanvijit S, Kompa AR, Wang BH, Kelly DJ, Krum H. Cardiorenal syndrome: pathophysiology, preclinical models, management and potential role of uraemic toxins. Clin Exp Pharmacol Physiol. 2012;39(8):692-700.
274. Liu S, Kompa AR, Kumfu S, Nishijima F, Kelly DJ, Krum H, et al. Subtotal nephrectomy accelerates pathological cardiac remodeling post-myocardial infarction: implications for cardiorenal syndrome. Int J Cardiol. 2013;168(3):1866-80.